7-8-2016

Semi-automated Ultrasensitive Electrochemical Microfluidic Immunoarray for On-line Capture and Detection of Cancer Protein Biomarkers

Brunah Akinyi Otieno
University of Connecticut - Storrs, brunah.otieno@uconn.edu

Semi-automated Ultrasensitive Electrochemical Microfluidic Immunoarray for On-line Capture and Detection of Cancer Protein Biomarkers

Brunah Akinyi Otieno, Ph.D.

University of Connecticut, 2016

Early cancer diagnoses promise to improve treatment outcomes and patient survival rates. However, current cancer diagnostics often rely on finding a tumor, making early detection difficult and possibly compromising therapy outcomes. Screening for cancer without tumor detection can be based on assays of body fluids such as serum or plasma for cancer biomarker proteins to provide an instantaneous record of a patient's disease status. Measurement of these biomarker proteins should be accurate, sensitive, cheap and preferably at point-of-care (POC) for translation to the clinic. In addition, due to low predictive power of some biomarker proteins and their over-expression by multiple cancer types, it is essential to measure panels of biomarker proteins as opposed to a single biomarker for reliable diagnosis of cancer. Simultaneous measurement of the levels of a panel of biomarker proteins can lead to more accurate diagnoses and offer clarity about disease characteristics and progression that may help guide treatment strategies.

The long-term goal of this thesis research is to provide multiple biomarker-based diagnostics to enable accurate early detection of cancer and therapy

monitoring. A simple, low-cost, 8-electrode semi-automated modular microfluidic system for on-line capture and electrochemical detection of panels of cancer protein biomarkers was designed and validated. Proteins that were validated include oral cancer biomarkers (IL-6 & IL-8) and oral mucositis biomarkers (IL-6, TNF-α, IL-1β and CRP). This thesis also describes our first electrochemical assay for parathyroid hormone related peptide (PTHrP); a paraneoplastic peptide responsible for hypercalcemia in cancer patients and also implicated in cancer metastasis. Also described in the dissertation, is a novel 16-electrode electrochemical set up for simultaneous detection of upto 8-prostate cancer biomarkers, many of which are thought to be specific for aggressive prostate cancer. Measurement of these small panels of selective biomarkers holds remarkable promise for future cancer diagnostics and personalized cancer therapies and most importantly in identifying aggressive vs indolent forms of prostate cancer.

Semi-automated Ultrasensitive Electrochemical Microfluidic Immunoarray for On-line Capture and Detection of Cancer Protein Biomarkers

Brunah Akinyi Otieno

B.S. Industrial Chemistry, University of Nairobi, 2009

A Dissertation Submitted in Partial Fulfilment of the Requirements for the Degree of Doctoral of Philosophy at the University of Connecticut

2016

Approval Page

Doctor of Philosophy Dissertation

Semi-automated Ultrasensitive Electrochemical Microfluidic Immunoarray for On-line Capture and Detection of Cancer Protein Biomarkers

Presented by

Brunah Akinyi Otieno, BSc

Major Advisor……..

Dr. James F. Rusling

Associate Advisor……..

Dr. Douglas Adamson

Associate Advisor……..

Dr. Alfredo-Angeles M. Boza

University of Connecticut

2016

Dedicated to

My Parents

Consolata and Paul Otieno

&

My Husband

Stephen M. Opimbi

2016

Acknowledgement

Though only my name appears on the cover of this dissertation, many people have contributed and extended their valuable assistance to its production. I owe my gratitude to all those people who have made this dissertation possible and because of whom my graduate experience has been one that I will cherish forever.

My deepest gratitude is to my advisor, Dr. James F. Rusling for his patience, motivation, enthusiasm, and immense knowledge. His guidance helped me in all the time of research and writing of this thesis. I could not have imagined having a better advisor and mentor for my PhD program. Jim taught me how to question thoughts and express ideas. I am grateful to him for holding me to a high research standard and enforcing strict validations for each research result, and thus teaching me how to do research. His patience and support helped me overcome many crisis situations and finish this dissertation. His insightful comments and constructive criticisms at different stages of my research were thought-provoking and they helped me focus my ideas. I am also thankful to him for reading my reports, commenting on my views and helping me understand and enrich my ideas. I am deeply grateful to him for the long discussions that helped me sort out the technical details of my work. I hope that one day I would become a good mentor as Jim has been to me. Besides my advisor, I would like to thank the rest of my thesis committee: Prof. Douglas Adamson, Dr. Alfredo M. Boza,

and Dr. Edward Neth, for their encouragement, insightful comments, and hard questions.

My sincere thanks also goes to Prof. Donal Leech for facilitating my stay in National University of Ireland, Galway (NUIG) for the US-Ireland collaborative project. Thanks for offering me a conducive environment to perform research for 3 months. I also thank his students Conan, Dr. Peter, Cindy and Richard for the warm welcome to NUIG and being supportive throughout my stay in Ireland. I would also like to thank our visiting researchers Dr. Ronaldo Faria and Dr. Alina Latus for their guidance and support in completing the project in chapter two of this thesis.

I would like to thank Dr. Dan Eustace for his professional development class that enlightened me on career development and enabled me secure a position at my dream company. Many thanks to Charlene Fuller and Daniel Delab for their assistance with placing orders and designing microfluidic devices respectively.

I thank former and present labmates in JFR Lab: Dr. Colleen Krause, Dr Dhanuka, Abby, Amit, Mohammed, Min, Itti, Gayatri, Jen, Karteek, Spundana, Boya, Di, Snehasis, Islam, Dr. Bishop, Dr. Kiran and Dr. Chandra for the stimulating discussions, and for all the fun we have had in the last five years. In particular, I am grateful to Dr. Colleen Krause for enlightening me the first glance of research, for the sleepless nights we were working together before deadlines, and for being my best friend to date.

Last but not the least, I would like to thank my family: my parents Consolata and Paul Otieno, for giving birth to me at the first place and supporting me spiritually throughout my life. My siblings Milly, Zephan, Juve and Antonia, thank you for your unending support and prayers. I also would like to thank my husband, Stephen Opimbi for his immense love and support throughout my PhD program. Glory be to the Almighty God.

Table of Contents

List of Schemes

List of figures

List of Tables

CHAPTER ONE

Introduction

1.1 Goal and Significance

Despite tremendous efforts to develop strategies against cancer-related mortality, cancer still remains a major public health problem in the United States and throughout the world. It is the second leading cause of death in the United States after heart disease.[1] Cancer arises in 1 out of 3 individuals and affect people of all ages and certain types of cancer arises more according to the gender, age or geo-graphical location globally.[2] According to the National Cancer Institute one out of every four deaths occurring daily in the US is due to cancer. In 2016 alone, 1,685,210 new cancer cases are projected to occur in the US which translates to 4,600 new cancer diagnoses each day.[1] The lifetime probability of being diagnosed with an invasive cancer is 42% in men and 38% in women. It is also estimated that 595,690 Americans are expected to die in 2016, corresponding to about 1,600 deaths per day.[1] These deaths arise mostly from cancers of the lung and bronchus, prostate, breast and colorectal cancer which accounts for 46% of all cancer deaths.[1]

Cancer is a multi-gene, multi-step disease originating from a single abnormal cell of clonal origin with an altered DNA sequence (mutation).[3] Uncontrolled proliferation of these abnormal cells leads to successive rounds of mutation and natural selection resulting in formation of tumors (Figure 1.1).

Subsequent mutation leads to malignant tumor which breaks through the basal membrane and spread to distant locations.[3-5]

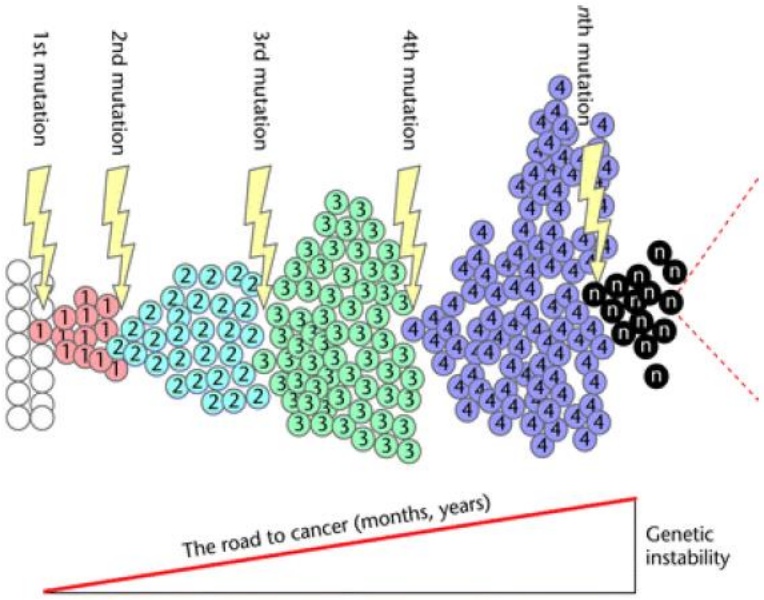

Figure 1.1: Clonal expansion of mutation leading to formation of tumors (*Adapted from reference 3*).

Initiation and progression of cancer depends on both external factors/ environmental factors (diet, lifestyle and exposure to ultraviolet radiation or carcinogenic pollutants) and internal factors within the cells (inherited mutations, hormones, immune conditions, and mutations that occur from metabolism).[1,3] These factors act together or in sequence, resulting in abnormal cell behavior and excessive proliferation. As the causes of cancer are so diverse, there are many types of cancer. There are more than 200 types and sub-types of cancer affecting more than 60 human organs.[4] The dysregulation in normal signaling pathway in cancer patients leads to inactivation of tumor suppressor genes and

activation of oncogenes.[6] However, in terms of diagnosis, no single gene is universally altered during this process, and the patterns of change differ in tumors from different organs, as well within tumors from the same location. In addition, approximately 90% of all cancer-related deaths occur from metastasis and not directly from the primary tumor site.[7] Therefore, there is urgent need to develop tools for early diagnosis of cancer to improve treatment outcomes and patients' survival rate.

Existing methods of screening for cancer often rely heavily on finding and imaging a tumor. Imaging modalities such as magnetic resonance imaging (MRI), positron emission tomography (PET), and computed tomography (CT), use contrast materials to distinguish between different anatomical features of tumor.[2, 8-10] These techniques determine the precise location of tumor thereby aiding in directing treatment options, monitoring cancer therapy and recurrence of the disease. Unfortunately, some tumors fail to show a marked difference from surrounding healthy tissue due to uptake of the contrast agent. In addition, some of the techniques lack the sensitivity to detect small (<1 cm) and low grade tumors leading to false negative results. Furthermore, most of these techniques are also expensive and hence might not be available or affordable in low resource settings.[11-13] Other techniques employed for screening of cancer rely on traditional methods based on cell morphology using staining and microscopy.[6] These are invasive techniques based on taking a biopsy and then examining the tissue using cell fixation and morphology approaches to identify and detect

cancer cells. These tests, however, are not individually conclusive as tissue removal can miss cancer cells at the earlier onset of the disease and further research is needed to develop tests to identify the malignancy without the need for invasive examinations.[6]

The goal of this dissertation was to develop and validate a simple, low-cost technique that allows patients to be screened for cancer without undergoing any invasive procedure. The methodology is based on assaying bodily fluids such as serum or plasma to measure the levels of biomolecules that are over- or under-expressed during early cancer stages.[14,15] These biomolecules also known as cancer biomarkers can deliver a "snapshot" of disease status in patients. The technique addressed in this thesis for detection of these cancer biomarkers, employs different aspects of automation, microfluidics, nanotechnology and novel labeling methods in conjunction with electrochemical detection. First, the semi-automated microfluidic device was first optimized and validated with experimental samples consisting of conditioned media from human oral cancer cells, followed by real-time monitoring of small biomarker proteins panel for oral cancer and prostate cancer in human serum and plasma. The clinical data obtained from the semi-automated device along with the low cost of the assay holds excellent promise for cancer diagnosis and therapy monitoring.

1.2 Cancer Biomarkers

According to National Health Institute (NIH), a biomarker is defined as “a characteristic that is objectively measured and evaluated as an indicator of normal biologic processes, pathogenic processes, or pharmacologic responses to a therapeutic intervention.”[16] According to the definition, a cancer biomarker is a biological molecule found in blood, other body fluids or tissues that is indicative of the presence of cancer in body. It might be a molecule secreted by a malignancy itself, or it can be a specific response of the body to presence of cancer. Cancer biomarkers typically differentiate an affected patient from a person without a disease. The alterations could be due to a number of factors, including germline or somatic mutations, transcriptional changes and post translational modifications.

There is tremendous variety of biomarkers, including DNA, DNA modifications, RNA, proteins, hormones and related molecules, molecules of the immune system, oncogenes and other modified molecules.[6,17] Cancer biomarkers can also be a collection of alterations, such as gene expression, proteomic and metabolomics signatures. Biomarkers can be detected in circulation (whole blood, serum or plasma), or excretions or secretions (stool, urine, sputum or nipple, discharge) and thus easily assessed non-invasively, or can be tissue driven and require either biopsy or special imaging for evaluation. Genetic biomarkers can be inherited and detected as sequence variations in

germ line DNA isolated from whole blood, sputum, or buccal cells or can be somatic and identified as mutations in DNA derived from tumor tissue.[18]

Cancer biomarkers have many potential applications in oncology, including risk assessment, screening, differential diagnosis, determination of prognosis, prediction of response to treatment, and monitoring status of the disease, either to detect recurrence or determine response or progression to therapy. In addition, biomarkers can be used in combination with imaging techniques to detect cancer *in vivo* and assess response to therapy.[17] Because of the critical role that biomarkers play at all stages of disease, it is important that they undergo rigorous evaluation, including analytical validation, clinical validation, and assessment of clinical utility, prior to incorporation into routine clinical care.[18]

1.2.1 Cancer Protein Biomarkers

One most important class of cancer biomarkers include proteins that are elevated or depressed in serum or plasma patients and their levels indicate the presence of cancer in the body.[19] These proteins are often specific to one or several types of cancer and the levels of such proteins can give clear indication of the patient's status.[20] Cancer biomarker proteins have been identified for almost every major type of cancer, however only a few of the biomarkers have been approved by FDA (Table 1.1).

Table 1.1: List of FDA approved protein markers currently used in clinical practice

Protein Biomarkers	Clinical use	Cancer	Specimen	Year Approved
Cancer antigen-125 (CA-125) + Human epididymis protein 4 (HE4)	Prediction of malignancy, monitoring disease progression, response to therapy	Ovarian cancer	Serum, Plasma	2011
HE4	Monitoring recurrence or progression of disease	Ovarian	Serum	2008
Alpha-Fetoprotein (AFP)	Staging of non-seminomatous testicular cancer Risk assessment for development of disease	Hepatocellular Testicular	Serum, plasma, amniotic fluid	2005
CA19-9	Monitoring disease status	Pancreatic	Serum, Plasma	2002
CA15-3	Monitoring of disease response to therapy/assessment of therapy	Breast cancer	Serum, Plasma	1997
CA27.29	Monitoring disease response to therapy	Breast cancer	Serum	1997
Free PSA	Discriminating cancer from benign disease	Prostate cancer	Serum	1997
Thyroglobulin (Tg)	Aid in monitoring	Thyroid	Serum,	1997
Total PSA	Screening & monitoring disease	Prostate	Serum	1986
Carcinogenic embryonic antigen (CEA)	Aid in management and prognosis	Pancreatic cancer	Serum, Plasma	1985

Many of these proteins are secreted into the blood at higher than normal levels when cancers begin to develop and are useful for diagnosis even before the onset of tumours.[14] For example prostate specific antigen (PSA) is a serum protein biomarker recommended by the American cancer society as an early screening tool for prostate cancer. PSA is produced by the cells of the prostate

gland and is typically elevated in the presence of prostate cancer. A PSA serum concentration of 4−10 ng mL^{-1} suggests the possibility of early stage prostate cancer, while normal levels are typically 0.5−2 ng mL^{-1} and late stage prostate cancer is characterized by values above 100 ng mL^{-1}.[14,19] Interleukin-6 (IL-6) on the other hand is a multifunctional cytokine associated with several different cancers, including head and neck squamous cell carcinoma (HNSCC). Mean serum IL-6 levels in healthy individuals are typically less than 6 pg mL^{-1}, whereas in patients with HNSCC, the levels are 20 pg mL^{-1} or greater. Serum IL-6 is also elevated in colorectal, gastrointestinal, and prostate cancers.[21] Protein biomarkers are also used to monitor response to therapy and recurrence of disease in ovarian, pancreatic and colon cancer, through measuring the proteins cancer antigen (CA125), CA19-9 and carcinoembryonic antigen (CEA), respectively.[17]

However, single biomarker proteins typically have insufficient positive predictive value e.g about 70% for PSA which is one of the better single biomarkers.[22] PSA has low specificity to prostate cancer as the levels can also be elevated above the threshold in benign prostate hyperplasia (BPH), a condition in which the prostate enlarges, prostatitis (prostate inflammation) and urinary infection. In addition, PSA fails to discriminate between aggressive tumors from low-risk ones and between malignant disease and other benign prostate conditions, and as such, over-diagnosis and over-treatment represent critical consequences of PSA-based screening. Failure to distinguish between

indolent and more aggressive forms of cancer is also a common problem with other clinically used single biomarkers, including CA 125 for ovarian cancer, CA 19-9 for pancreatic cancer and CEA for colon cancer.[20] Owing to low inherent predictive ability of some biomarkers and their overexpression by multiple cancer types, highly reliable prediction for a specific cancer ultimately require measuring a number of relevant biomarker proteins for each cancer. Multiple protein measurements have been shown to improve both the specificity and sensitivity of the diagnostic tests.[15,20]

For example, detecting 5 or more biomarkers for a given cancer by liquid chromatography-mass spectrometry (LC-MS) has provided >99% reliable diagnostics.[6,23] Lumachi and his co-workers used simple multianalyte immunoassay for measurement of five protein biomarkers CEA, CA 19-9 and 72-4, cytokeratin-19 fragment (CYFRA 21-1), and osteopontin, comparing their expressions in patients with colorectal cancer and age- and sex-matched patients suffering from confirmed benign colorectal diseases (controls). Single marker measurements showed low specificity and sensitivity; however, simultaneous measurements of all five markers achieved 74.1% sensitivity and 94.3% specificity in patients with colorectal cancer.[24] Karl and colleagues evaluated expression of known markers hemoglobin (iFOBT), hemoglobin-haptoglobin, calprotectin, carcinoembryogenic antigen, and the novel fecal markers tissue inhibitor of metalloproteinase-1 (TIMP-1) and S100A12. The combination of S100A12, immune-FOBT, and TIMP-1 reached sensitivity greater

than 80% at a high specificity (98%), giving a novel noninvasive colorectal cancer screening tool.[25] Also, when human Kallikrein 6 **(**hK6) is combined with CA-125, at 90% specificity, sensitivity increases to 72% (for all patients) and to 42% in stage I or II of ovarian cancer.[26] The diagnostic sensitivity of serum hK6 alone at 90% and 95% specificity is 52% and 47%, respectively, in the whole patient population (n=238). For early stage disease (stage I or II), sensitivity is approximately 21% to 26%. However, measurements of the multiple biomarker proteins need to be done at high accuracy and cheaply at point-of-care, *e.g.* in a physician's office or clinic, to reduce costs, minimize sample decomposition, facilitate-on the-spot diagnosis, and alleviate patient stress.[15]

1.3 Platforms for Cancer Biomarker Detection

1.3.1 Enzyme-Linked Immunosorbent Assay (ELISA)

Currently, most clinical protein biomarker detection is done using an enzyme-linked immunosorbent assay (ELISA). Since its introduction in 1971, ELISA has remained the gold standard method for protein measurements.[27] In ELISA, primary antibodies are attached onto a 96-well plate to selectively capture the analyte protein from the sample. After washing, a secondary antibody with a label attached is added, and binds selectively to the protein on the surface. A substrate that reacts with enzyme label is then added to produce a colored complex detected optically (Scheme 1.1). Success of ELISA stems from enzyme-based amplification mode and ease of use, along with the specificity and

sensitivity of antibody-antigen interactions common to all immunoassays.[28] ELISA-type approaches have been quite useful in assays utilizing immunoarrays. However, with the demand for multiplexing capability, shorter analysis time, smaller sample volume and higher sensitivity, other techniques are being explored for protein determinations.[29,30]

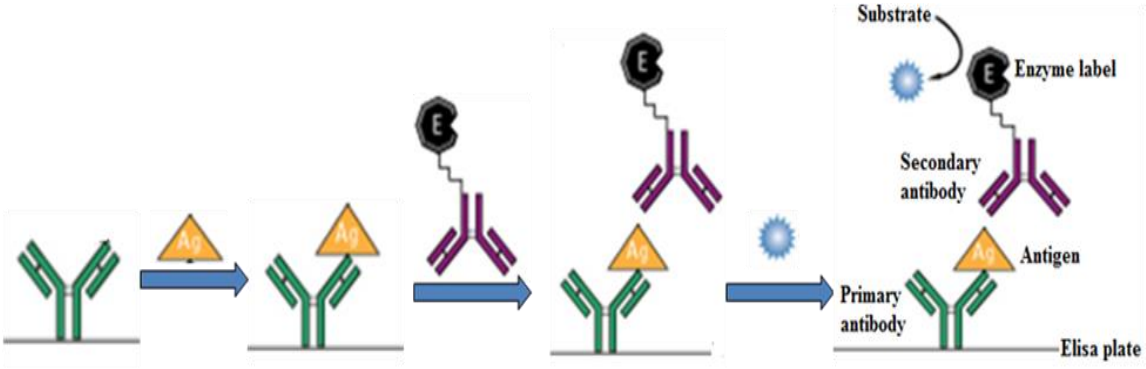

Scheme 1.1: ELISA Scheme; Antigen is added to ELISA plate coated with primary antibody, followed by addition of secondary antibody conjugate by enzyme label. Generation of signal is by addition of a substrate that forms a colored product that can be measured by an optical plate reader.

1.3.2 LC-MS based Proteomics & Commercial Assays

Liquid chromatography coupled with mass spectrometry (LC-MS)-based proteomics can achieve multiple biomarker measurements approaching acceptable sensitivity. However, the current analysis technology is too expensive, time consuming and technically complex for routine clinical diagnostics.[17,31] At present, LC-MS-based proteomics is more suited for biomarker discovery research. Alternatively, analyzers based on antibody-coated

microarrays are being developed in 96- or 384-well plate format (Quansys Biosciences, SA Biosciences). Analyte proteins are captured by primary antibody or aptamers on each spot on the array and after washing with buffer designed to minimize non-specific binding, a labeled secondary antibody dispersion is added to bind to the analyte proteins. A substrate is then added to react with enzyme label to generate optical or electrical signal. These arrays are highly selective and sensitive, easy to use, less costly and have multiplexing capabilities.

Currently, there are several commercially available automated and semi-automated analyzers for multiplexed protein measurements of upto 10 selected target proteins per sample with detection limits ranging from 1-100 pg mL^{-1} in serum.[15] These analyzers are based on surface plasmon resonance (Horiba Inc, BIO-RAD), fluorescence (Luminex, Myriad RBM), electrochemiluminiscence (Roche Diagnostics, Mesoscale Discovery) measurement technologies. However, these commercial instruments are not suitable for point of care applications in resource limited settings as they require specialized consumables including sample well plates, chips, and reagent kits which are very costly. Fluorescence-based detection strategies on the other hand require laser sources and precise alignment of optical components.[19] Therefore, there is still a need for a simple, low-cost device for multiple protein measurements that could be employed in resource limited settings.

1.3.3 Electrochemical Methods

Electrochemical methods have recently attracted considerable interest because of their sensitivity, low cost and inherent minitiarization. In 1980s, Heineman and Halsall pioneered enzyme-linked electrochemical immunoassays for small molecules and proteins.[32] In their approach, antibody-antigen binding events and enzyme substrate reactions were separated in space and time from detection of electroactive products. Electroactive products formed from the enzyme label alkaline phosphatase are transported by a chromatographic or fluidic system to the detecting electrode. Advances have included interdigitated electrodes to achieve high sensitivity and incorporation into microfluidic devices. Excellent detection limits in the pg mL^{-1} to ng mL^{-1} range have been obtained for proteins and small molecules depending on the design and nature of the electrochemical detector.[33-35]

Since the introduction of enzyme-linked electrochemical immunoassays by Heineman, various electrochemical methods such as voltammetry (linear sweep, differential pulse, square wave) and amperometry have been widely applied for sensitive detection of cancer protein biomarkers.[19] These methods employ a detection antibody (Ab_2) labeled with an electroactive species that is allowed to bind with the analyte (Figure 1.2). The analyte bound on the labeled-Ab_2 is then introduced onto primary antibody (Ab_1)-modified electrode surface to complete the sandwich assay. The concentration of the targeted protein biomarker is quantified by applying a potential and measuring the resulting current at the

electrode. The applied potential drives the redox reaction of the labeled electroactive species and provides a current signal that is proportional to the concentration of the protein analyte.[19,33]

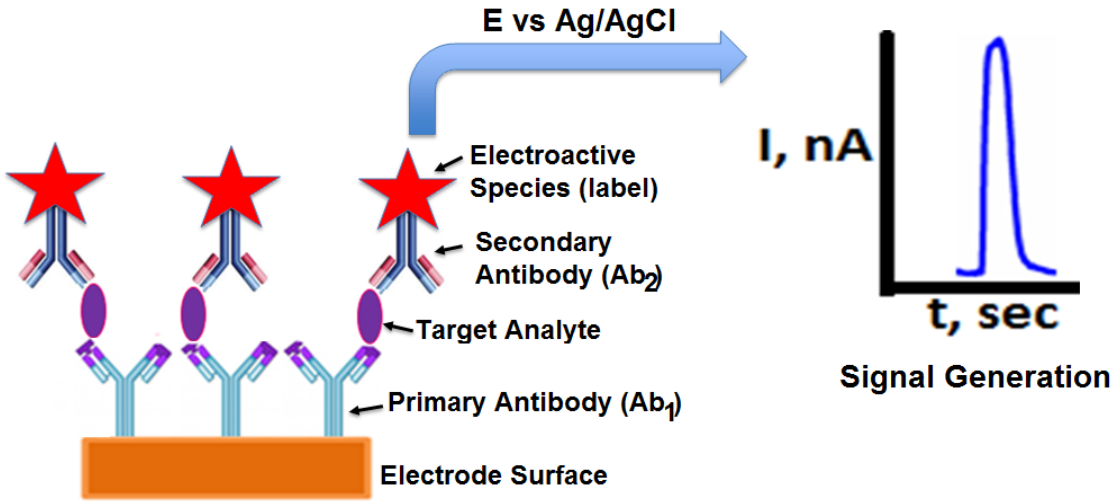

Figure 1.2: Illustration of electrochemical method for protein biomarker detection. Signal generated is proportional to the concentration of the target analyte. Labels commonly employed include horseradish peroxidase (HRP) and alkaline phosphatase.

In order to increase the sensitivity of the electrochemical immunoassays, nanomaterials such as gold nanoparticles, carbon nanotubes (CNTs), magnetic beads and quantum dots have been incorporated into the assays as substrates for the capture antibodies or for target antigens.[14,15,19,33] Signal amplification for target protein detection can be achieved by loading greater numbers of biomolecules or multi-enzymes onto nanomaterials. These approaches greatly

enhance sensitivity by providing a large number of labels for each protein bound on the sensor surface. Nanostructured sensor surfaces can also provide additional increases in sensitivity by providing high surface areas enabling attachment of a large number of capture antibodies, and by facilitating better access of protein analytes to these antibodies.[19,33]

Our laboratory has employed enzyme-coated magnetic beads along with sensors nanostructured with gold nanoparticles and CNTs to achieve high sensitivity. Gold nanoparticle immunosensor was fabricated by depositing a dense 5 nm layer of glutathione-decorated gold nanoparticles onto a 0.5 nm polycation layer, on a pyrolytic graphite.[36] Detection limit of 0.5 pg mL^{-1} was achieved using 1 μm magnetic bead-Ab_2-horseradish peroxidase (HRP) bioconjugates, coated with 7500 HRPs per bead. Good correlation was found between the immunosensor level of PSA in patient samples with the standard ELISA. Immunosensor responses were measured by rotating disk amperometry, using H_2O_2 to activate HRP to ferryloxyHRP species and hydroquinone as an electron mediator, which resulted in a steady state current proportional to protein concentration (Scheme 1.2).

Immunosensor for PSA in serum using multi-labeled CNT-HRP-Ab_2 particles using this approach gave detection limits of 4 pg mL^{-1}.[37] SWCNT immunosensors were also used to measure PSA levels in 1000 prostate cancer cells laser dissected from prostate tissue. These immunosensors achieved a detection limit of 0.5 pg mL^{-1} for IL-6 released from a variety of oral cancer cells

into cell growth media.[38] SWCNT forests provided 5 to 10-fold better sensitivity than immunosensors without nanotubes because of a large increase in density of Ab_1 compared to that on a flat immunosensor.[33]

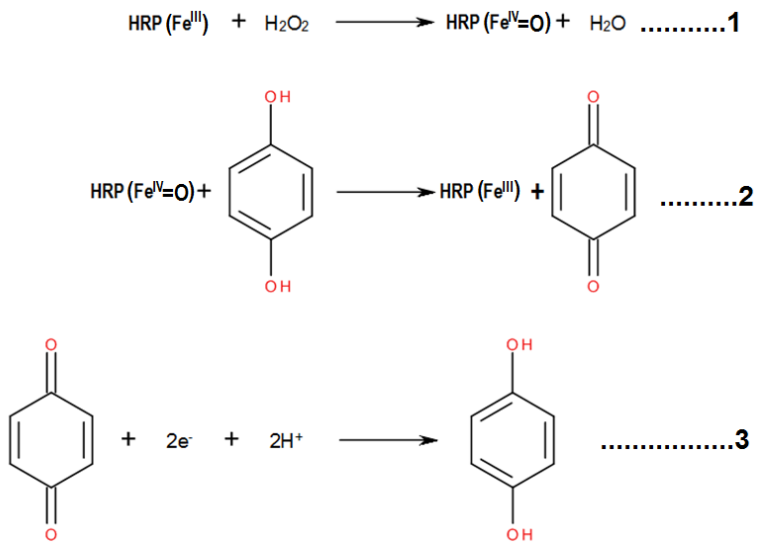

Scheme 1.2: Generation of signal from HRP. H_2O_2 activates HRP to ferryloxyHRP (1) form which further oxidizes hydroquinone to benzoquinone (2). Signal is generated via a two electron transfer reaction regenerating hydroquinone (3).

We recently employed AuNPs immunosensors for amperometric detection of PSA and IL-6 with magnetic bead conjugates labeled with 90,000 Ab_2 and ~200,000 HRPs. With this method, PSA and IL-6 were analysed down to 0.1 pg mL^{-1} and 0.25 pg mL^{-1} respectively, in 5000-fold diluted calf serum.[39] Increasing the number of labels on the magnetic bead surfaces to 400,000 HRPs, increase the sensitivity of the assay further (Figure 1.3). Limits of detection of 10 fg mL^{-1},

15 fg mL^{-1}, 8 fg mL^{-1}, and 60 fg mL^{-1} were reached for IL-6, IL-8, vascular endothelial growth factor (VEGF) and VEGF-C respectively in 5000-fold diluted calf serum.[40] In collaboration with Munge et al, an unprecedented DL of 1.0 fg mL^{-1} for IL-8 using magnetic bead bioconjugates with a half-million HRP units each was achieved. An added advantage is that tens of thousands of antibodies can be included on 1 µm beads, promoting binding of analyte proteins to the beads at concentrations well below what can be achieved with a single antibody.[41]

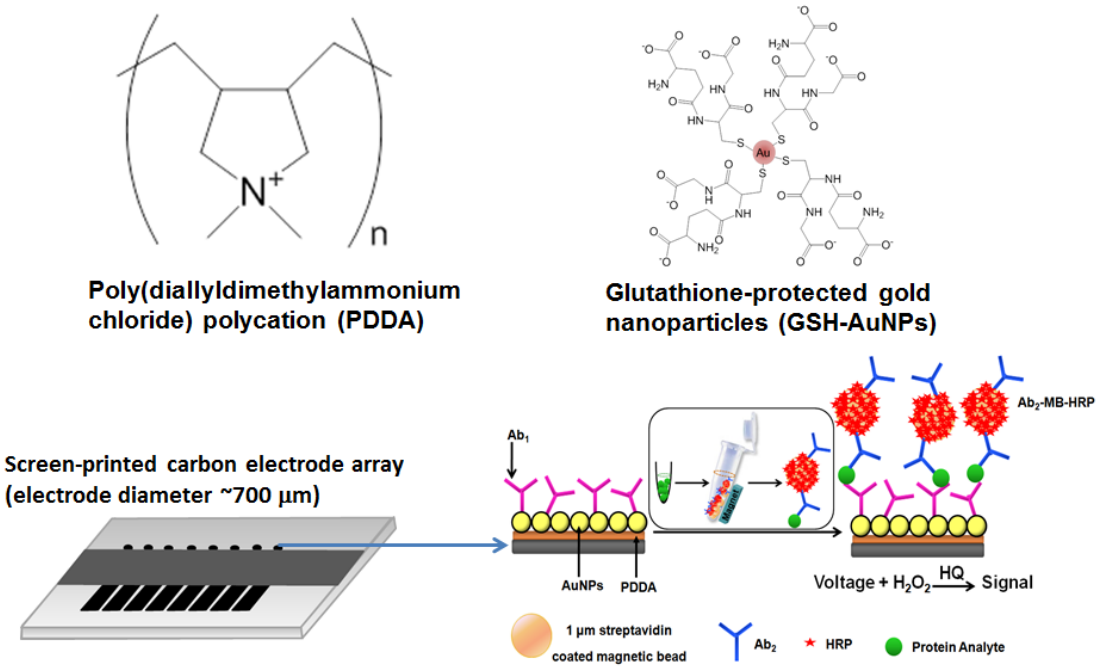

Figure 1.3: AuNPs Immunosensor for amperometric detection of cancer protein biomarkers using magnetic bead conjugates labeled with thousands of Ab_2 and HRPs.

1.4 Microfluidics for Biomarker Detection

Since its introduction in 1990[42], microfluidics also known as lab-on-chip (LOB) or micro total analysis (mTAS), has attracted a lot of interest and grown explosively. Microfluidic technology possesses remarkable features for simple, low-cost and rapid disease diagnosis, such as; (1) increased surface-to-volume ratio for efficient mass transport in immunoreactions leading to fast analysis; (2) a miniaturized microchannel dimension to reduce sample and reagent consumption; (3) high portability along with automated integration with other functions such as valves, pumps, mixtures and detectors; and (4) analysis of complex biological fluids with high sensitivity for health care applications.[43,44] An enormous number of microfluidic devices have been developed for biomedical applications. These devices enable on-chip POC diagnosis and real-time monitoring of diseases from a small volume of body fluids. These microfluidic devices may act as a bridge to improve the global health care system with high efficiency and sensitivity, especially for remote areas with low-resource settings, such as the underdeveloped and developing countries, in home health care setting, and in emergency situations. Because of all these significant features, numerous microfluidic devices have been developed for biomarker detection in cancer diagnosis.[43]

Microfluidic chips for immunoassays are commonly fabricated from silicon, glass, and polymer materials.[44] The first generation of microfluidic devices were made from silicon and glass by photolithography and wet-etching. However,

polymers such as polymethylmethacrylate (PMMA), cyclic olefin copolymer, polystyrene, and polydimethylsiloxane (PDMS) and paper-based microfluidic devices have emerged as alternative materials to silicon and glass due to the simple fabrication process (e.g., molding, printing) and low cost.[45-47] Among the polymers, PDMS is the most popular material used for microfluidic immunoassays because of its flexibility, optical transparency, biocompatibility and low-autofluorescence properties. Furthermore, PDMS can be easily bonded to silicon, glass or another piece of PDMS through treatment with oxygen plasma.[43,44]

In recent years, great efforts have been devoted for the development of electrochemical detection-based microfluidic devices for detection of cancer biomarkers. For example, Li et al. developed an electrochemical ELISA on paper-based microfluidic devices.[48] Paper-based microfluidic devices were fabricated by patterning chromatography paper using the photolithography technique. Working and counter electrodes were screen printed from graphite ink, and a reference electrode from silver/silver chloride ink. The electrochemical ELISA of IgG based on cyclic voltammetry (CV) was demonstrated with the LOD of 3.9 fM. Liu et al. developed a PMMA microfluidic chip coupled with a three-electrode electrochemical detection system to detect the trace level of AFP.[49] For covalent immobilization of the AFP monoclonal antibody, PMMA microchannels were first modified with poly(ethyleneimine). The captured analyte, AFP, was finally bound to the HRP-conjugated AFP antibody for electrochemical detection.

When the substrate mixture of 2-amino hydroxybenzene and hydrogen peroxide was pumped into the PMMA microchannel, the HRP enzyme labeled on the AFP antibody within microchannels instantaneously catalyzed the substrate, and the generated electroactive 3-amino phenoxazine was detected using DPV. The immunochip had the LOD of 1 pg mL^{-1} for AFP with a detectable linear concentration range of 1–500 pg mL^{-1}.

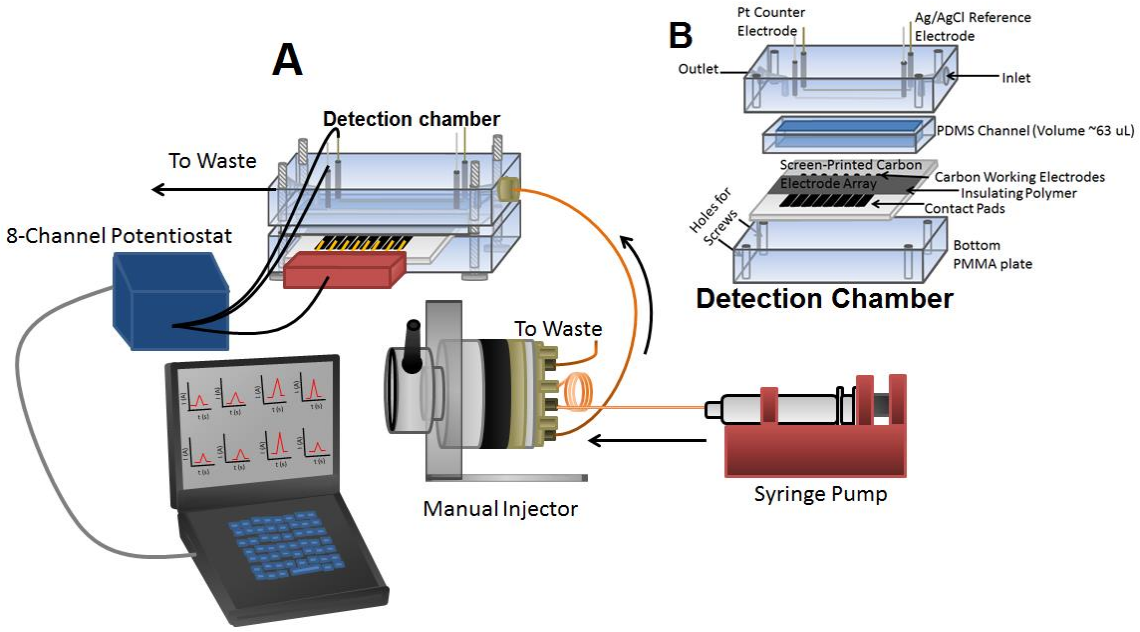

Figure 1.4: (A) Electrochemical microfluidic set up for off-line detection of cancer protein biomarkers. (B) Detection chamber housing the Ab1-modified 8-electrode array.

Our first microfluidic electrochemical immunoassay for multiplexed detection of cancer biomarkers was made up of a molded PDMS channel sandwiched between two PMMA plate and interfaced with a pump and sample

injector (Figure 1.4). The detection chamber was 63 µL volume in size and easily housed the 8-electrode array. Prior to incorporation of the array onto the detection chamber, the array was coated sequentially with a layer of PDDA, AuNPs and Ab_1 as described in Figure 1.3. Protein analyte were captured off-line by magnetic bead conjugate and then introduced into the detection chamber to be captured by the primary antibody on the surface of the array. Detection of the target analyte was performed amperometrically by injecting a mixture of hydroquinone and hydrogen peroxide. This microfluidic device was employed for detection of oral cancer and prostate cancer biomarkers.[38,39] For POC applications, the assays needs to be automated such that it only requires loading of reagents and samples.

1.5 On-line Protein Analyte Capture

Point-of-care devices require simple, low cost, adequately sensitive and technically undemanding automated methodology for personalized cancer diagnostics and therapy.[14,15,19] However, most immunoassay techniques employ manual off-line protein analyte capture. Protein analytes are captured from serum by magnetic bioconjugates in small vials, outside microfluidic device, prior to being introduced to the Ab_1-modified array (Figure 1.3). In addition, most immunoassay steps are performed manually limiting their applications for POC applications.

This thesis addresses for the first time, development and validation of a simple, low-cost, semi-automated microfluidic device for cancer biomarker

protein detection.[50] The microfluidic immunoassay system incorporates an on-line protein capture chamber into the previously reported modular device by Chikkaveeraiah et al. (Figure 1.4).[39] This chamber feature layer of molded, flexible PDMS sandwiched in between two flat, machined PMMA plates. The assembly is bolted together tightly to form an oval cylinder channel 1.5 mm wide and 100 ± 2 µL in volume housing a tiny magnetic stir bar (Figure 1.5). Flow out of the channel is directed to waste or to the detection chamber by a switch valve. Protein analytes are captured from biomedical samples by magnetic bead conjugates in the on-line capture chamber. The protein-magnetic bead conjugate is then magnetically separated, washed and introduced into the detection chamber housing an 8-electrode screen printed carbon arrays coated with glutathione protected gold nanoparticles (GSH-AuNPs).

Inclusion of the on-line protein capture module provides a more automated strategy compared to the earlier device that required off-line capture since capture and washing are done in the microfluidic system, not manually as previously (Figure 1.4). In addition, most immunoassay steps are incorporated into the microfluidic device, requiring only loading of reagents, samples and wash solutions by the operator. The assay requires relatively short time of 30 min, which is less than 50 min for the off-line capture assay and much less than standard ELISA (>2 hrs) and other commercial detection methods. Thus, assay time and level of automation begin to approach the needs of POC applications.

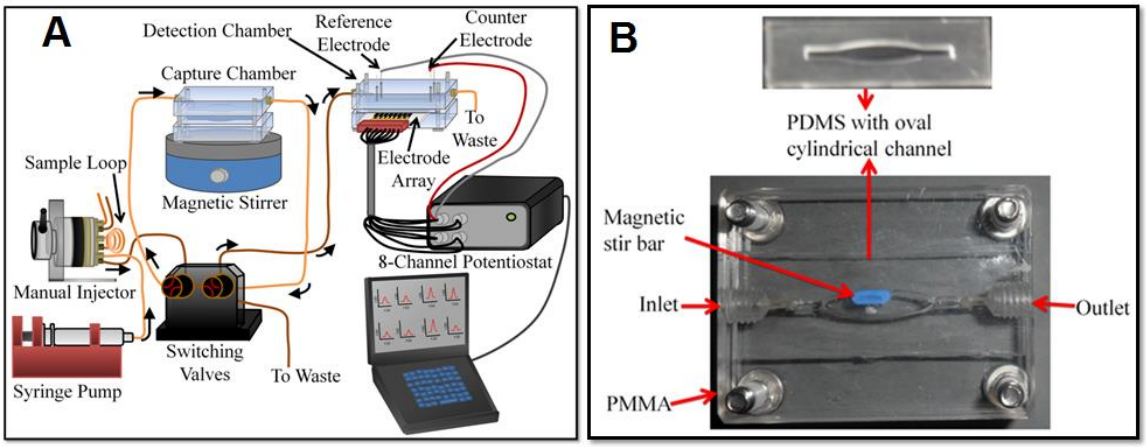

Figure 1.5: (A) Conceptual instrumentation and strategy for ultrasensitive amperometric detection by microfluidic immunoarray and (B) photograph of capture chamber in which target proteins will be captured on-line from the sample by heavily labeled HRP-antibody-magnetic beads to form protein-bead bioconjugates.

1.6 Summary/Overview of dissertation

In this Ph.D. research thesis, the main goal was to develop a low-cost semi-automated point-of-care diagnostic devices that can be used for rapid and sensitive measurement of protein biomarkers for various types of cancer. The immunoassay devices should ideally be affordable to use in any biomedical laboratory for mass screening of patient population especially in resource limited settings. This thesis is composed of 5 chapters.

Chapter 1 provides introduction to protein cancer biomarkers and various platforms employed for detection of the cancer protein biomarkers. This chapter also highlights electrochemical based protein detection strategies that are

currently implemented in the sensitive detection of biomolecules & biomarker proteins and also the importance of integration of microfluidics into immunoassay devices. The chapter also includes a summary of the goals of various projects in the thesis and the research background which served as a concrete foundation to the work presented in this thesis.

Chapter 2 describes a novel simple, low-cost semi-automated modular microfluidic device for on-line capture and detection of oral cancer protein biomarkers and oral mucositis biomarkers. This system incorporates an on-line capture chamber where protein analytes are captured from biomedical samples by magnetic bead conjugates. Ultralow detection limits of 5 fg mL^{-1} and 10 fg mL^{-1} were achieved for simultaneous detection of two oral cancer biomarkers and four oral mucositis biomarkers respectively. Accuracy and diagnostic utility of these microfluidic arrays were demonstrated by measuring the levels of the oral cancer biomarkers in conditioned media of oral cancer cell lines. The levels of oral mucositis biomarkers were also measured in serum of head and neck cancer patients undergoing radiotherapy and compared with standard ELISA to demonstrate the accuracy of the immunoarray. The use of microfluidic immunosensors to measure concentrations of elevated biomarkers holds promise for accurate, low cost, and rapid determination of oral cancer and also determination of projected risk of oral mucositis that can be used by dentists and oncologists for patient management.

Chapter 3 describes the first application of the on-line modular microfluidic device for detection of a peptide, parathyroid hormone-related peptide (PTHrP). PTHrP is recognized as the major a causative agent of humoral hypercalcemia of malignancy (HHM) and it has also been implicated in tumor progression and metastasis of many human cancers. The first ultrasensitive multiplexed assay to measure intact PTHrP 1-173 as well as circulating N-terminal and C-terminal peptide fragments is described in this chapter. Using, ink-jet printed gold nanoparticles immunoarray, limits of detection (LOD) of 3 fg/mL (~1000 fold lower than IRMA) were achieved for simultaneous detection of PTHrP isoforms and fragments in 30 min. Good correlation for patient samples was found with immunoradiometric assay (IRMA) (n=57); r^2=0.99 assaying PTHrP 1-173 and 1-86 fragment. Analysis by ROC gave area under the curve of 0.96, 80-83% clinical sensitivity and 96-100% clinical specificity. This new ultrasensitive, multiplexed assay for PTHrP and fragments is promising for clinical diagnosis, prognosis and therapeutic monitoring from early to advanced stage cancer patients and to examine underlying mechanisms of PTHrP overproduction.

Chapter 4 describes a novel 16-electrode immunoarray set-up for simultaneous detection of upto 8 cancer protein biomarkers to aid in identifying aggressive from indolent forms of prostate cancer. The system consists of a two-channel reaction chamber and a two-channel detection chamber for detection of 4 protein biomarkers on each channel. The protein panel includes; PSA, vascular endothelial growth factor-D (VEGF-D), pigment epithelial derived factor (PEDF),

insulin growth factor-1 (IGF-1), insulin growth factor binding protein-3 (IGFBP-3), monocyte differentiation antigen CD-14 (CD14), V-Ets avian erythroblastosis virus E26 oncogene homolog ETS-related gene (ERG), and Golgi membrane protein 1 (GOLM-1); many of which are thought to be specific for aggressive prostate cancer. Detection limit in the pM range was achieved for multiplexed detection of the cancer biomarker proteins from as little as 5 µL. Measurements of this panel of selected biomarkers will be tested with prostate cancer patient samples in future to assess its diagnostic capability in discriminating aggressive from indolent forms of prostate cancer.

Chapter 5 describes the importance of incorporating nanomaterials in immunoassay. It also gives detailed description of the methods used in our laboratory to functionalize magnetic beads with antibodies and enzyme labels for ultrasensitive detection of protein analytes. In addition, it describes strategies for characterizing the magnetic bead bioconjugates employed in chapters 2, 3 and 4.

1.7 References

1. Siegel, R. L.; Miller, K. D.; Jemal, A., Cancer statistics, 2016. *CA. Cancer J. Clin.* **2016,** *66*, 7-30.
2. Altintas, Z.; Tothill, I., Biomarkers and biosensors for the early diagnosis of lung cancer. *Sens Actuators B Chem.* **2013,** *188*, 988-998.
3. Hejmadi, M.V; Introduction to cancer biology ISBN: 978-87-7681-478-6 2 edition Pg1-48
4. Rasooly, A.; Jacobson, J., Development of biosensors for cancer clinical testing. *Biosens. Bioelectron.* **2006,** *21*, 1851-1858.
5. Hanahan, D.; Weinberg, R. A., The hallmarks of cancer. *Cell* **2000,** *100* (1), 57-70.
6. Tothill, I. E., Biosensors for cancer markers diagnosis. *Semin. Cell Dev. Biol.* **2009,** *20*, 55-62.
7. Soper, S. A.; Brown, K.; Ellington, A.; Frazier, B.; Garcia-Manero, G.; Gau, V.; Gutman, S. I.; Hayes, D. F.; Korte, B.; Landers, J. L.; Larson, D.; Ligler, F.; Majumdar, A.; Mascini, M.; Nolte, D.; Rosenzweig, Z.; Wang, J.; Wilson, D., Point-of-care biosensor systems for cancer diagnostics/prognostics. *Biosens. Bioelectron.* **2006,** *21*, 1932-1942.
8. Adams, S.; Baum, R. P.; Stuckensen, T.; Bitter, K.; Hor, G., Prospective comparison of 18F-FDG PET with conventional imaging modalities (CT, MRI, US) in lymph node staging of head and neck cancer. *Eur J. Nucl Med.* **1998,** *25*, 1255-60.

9. Schmidt, G. P.; Haug, A. R.; Schoenberg, S. O.; Reiser, M. F., Whole-body MRI and PET-CT in the management of cancer patients. *Eur. Radiol.* **2006,** *16*, 1216-25.
10. Blodgett, T. M.; Meltzer, C. C.; Townsend, D. W., PET/CT: form and function. *Radiology* **2007,** *242*, 360-85.
11. Kovacs, A. F., Remarks on sentinel node biopsy in head and neck cancer. *Br. J. Cancer* **2005,** *92*, 206-7.
12. Jodlowska, E.; Czepczynski, R.; Wyszomirska, A.; Jarzabek, G.; Kedzia, W.; Ruchala, M., Application of positron emission tomography (PET/CT) in diagnosis of breast cancer. Part I. Diagnosis of breast cancer prior to treatment. *Contemp Oncol (Pozn)* **2016,** *20*, 8-12.
13. Cooper, K. L.; Meng, Y.; Harnan, S.; Ward, S. E.; Fitzgerald, P.; Papaioannou, D.; Wyld, L.; Ingram, C.; Wilkinson, I. D.; Lorenz, E., Positron emission tomography (PET) and magnetic resonance imaging (MRI) for the assessment of axillary lymph node metastases in early breast cancer: systematic review and economic evaluation. *Health Technol Assess.* **2011,** *15*, 1-134.
14. Rusling, J. F., Multiplexed electrochemical protein detection and translation to personalized cancer diagnostics. *Anal Chem.* **2013,** *85*, 5304-10.
15. Rusling, J. F.; Kumar, C. V.; Gutkind, J. S.; Patel, V., Measurement of biomarker proteins for point-of-care early detection and monitoring of cancer. *Analyst* **2010,** *135*, 2496-511.

16. Atkinson, A. J.; Colburn, W.A.; DeGruttola, V. G.; DeMets, D.L.; Downing, G.J.; Hoth, D. F.; Oates, J. A.; Peck, C. C.; Schooley, R. T.; Spilker, B. A.; et al. Biomarkers and SurrogateEndpoints: Preferred Definitions and Conceptual Framework. *Clin Pharmacol Ther.* **2001**, *69*, 89–95.
17. Hanash, S. M.; Pitteri, S. J.; Faca, V. M., Mining the plasma proteome for cancer biomarkers. *Nature* **2008,** *452*, 571-579.
18. Henry, N. L.; Hayes, D. F., Cancer biomarkers. *Mol Oncol.* **2012,** *6*, 140-146.
19. Chikkaveeraiah, B. V.; Bhirde, A. A.; Morgan, N. Y.; Eden, H. S.; Chen, X., Electrochemical immunosensors for detection of cancer protein biomarkers. *ACS nano* **2012,** *6*, 6546-61.
20. Mani, V.; Chikkaveeraiah, B. V.; Rusling, J. F., Magnetic particles in ultrasensitive biomarker protein measurements for cancer detection and monitoring. *Expert Opin. Med. Diagn.* **2011,** *5*, 381-391.
21. Riedel, F.; Zaiss, I.; Herzog, D.; Gotte, K.; Naim, R.; Hormann, K., Serum levels of interleukin-6 in patients with primary head and neck squamous cell carcinoma. *Anticancer Res.* **2005,** *25*, 2761-5.
22. Ward, A. M.; Catto, J. W.; Hamdy, F. C., Prostate specific antigen: biology, biochemistry and available commercial assays. *Ann. Clin. Biochem.* **2001,** *38*, 633-51.
23. Li, J.; Zhang, Z.; Rosenzweig, J.; Wang, Y. Y.; Chan, D. W., Proteomics and bioinformatics approaches for identification of serum biomarkers to detect breast cancer. *Clin Chem.* **2002,** *48*, 1296-304.

24. Lumachi, F.; Marino, F.; Orlando, R.; Chiara, G. B.; Basso, S. M., Simultaneous multianalyte immunoassay measurement of five serum tumor markers in the detection of colorectal cancer. *Anticancer Res.* **2012,** *32*, 985 8.

25. Karl, J.; Wild, N.; Tacke, M.; Andres, H.; Garczarek, U.; Rollinger, W.; Zolg, W., Improved diagnosis of colorectal cancer using a combination of fecal occult blood and novel fecal protein markers. *Clin. Gastroenterol. Hepatol.* **2008,** *6*, 1122-8.

26. Diamandis, E. P.; Scorilas, A.; Fracchioli, S.; Van Gramberen, M.; De Bruijn, H.; Henrik, A.; Soosaipillai, A.; Grass, L.; Yousef, G. M.; Stenman, U. H.; Massobrio, M.; Van Der Zee, A. G.; Vergote, I.; Katsaros, D., Human kallikrein 6 (hK6): a new potential serum biomarker for diagnosis and prognosis of ovarian carcinoma. *J Clin Oncol.* **2003,** *21*, 1035-43.

27. Engvall, E.; Jonsson, K.; Perlmann, P., Enzyme-linked immunosorbent assay. II. Quantitative assay of protein antigen, immunoglobulin G, by means of enzyme-labelled antigen and antibody-coated tubes. *Biochim. Biophys. Acta.* **1971,** *251*, 427-34.

28. Fowler, J. M.; Wong, D. K. Y.; Halsall, H. B.; Heineman, W. R., CHAPTER 5 - Recent developments in electrochemical immunoassays and immunosensors A2 - Zhang, Xueji. In *Electrochemical Sensors, Biosensors and their Biomedical Applications*, Ju, H.; Wang, J., Eds. Academic Press: San Diego, 2008; pp 115- 143.

29. Lim, C. T.; Zhang, Y., Bead-based microfluidic immunoassays: The next generation. *Biosens. Bioelectron.* **2007,** *22*, 1197-1204.
30. Aytur, T.; Foley, J.; Anwar, M.; Boser, B.; Harris, E.; Beatty, P. R., A novel magnetic bead bioassay platform using a microchip-based sensor for infectious disease diagnosis. *J. Immunol. Methods* **2006,** *314*, 21-9.
31. Hawkridge, A. M.; Muddiman, D. C., Mass Spectrometry–Based Biomarker Discovery: Toward a Global Proteome Index of Individuality. *Annu. Rev. Anal. Chem.* **2009,** *2*, 265-277.
32. Heineman, W. R.; Halsall, H. B., Strategies for electrochemical immunoassay. *Anal. Chem.* **1985,** *57*, 1321A-1331A.
33. Rusling, J. F., Nanomaterials-based electrochemical immunosensors for proteins. *Chem. Rec.* **2012,** *12*, 164-176.
34. Bange, A.; Halsall, H. B.; Heineman, W. R., Microfluidic immunosensor systems. *Biosens. Bioelectron.* **2005,** *20*, 2488-2503.
35. Ronkainen, N. J.; Halsall, H. B.; Heineman, W. R., Electrochemical biosensors. *Chem. Soc. Rev.* **2010,** *39*, 1747-63
36. Mani, V.; Chikkaveeraiah, B. V.; Patel, V.; Gutkind, J. S.; Rusling, J. F., Ultrasensitive immunosensor for cancer biomarker proteins using gold nanoparticle film electrodes and multienzyme-particle amplification. *ACS nano* **2009,** *3*, 585-94.

37. Yu, X.; Kim, S. N.; Papadimitrakopoulos, F.; Rusling, J. F., Protein immunosensor using single-wall carbon nanotube forests with electrochemical detection of enzyme labels. *Mol. BioSyst.* **2005,** *1*, 70-8.
38. Malhotra, R.; Patel, V.; Vaque, J. P.; Gutkind, J. S.; Rusling, J. F., Ultrasensitive electrochemical immunosensor for oral cancer biomarker IL-6 using carbon nanotube forest electrodes and multilabel amplification. *Anal. Chem.* **2010,** *82*, 3118-23.
39. Chikkaveeraiah, B. V.; Mani, V.; Patel, V.; Gutkind, J. S.; Rusling, J. F., Microfluidic electrochemical immunoarray for ultrasensitive detection of two cancer biomarker proteins in serum. *Biosens. Bioelectron.* **2011,** *26*, 4477 83.
40. Malhotra, R.; Patel, V.; Chikkaveeraiah, B. V.; Munge, B. S.; Cheong, S. C.; Zain, R. B.; Abraham, M. T.; Dey, D. K.; Gutkind, J. S.; Rusling, J. F., Ultrasensitive detection of cancer biomarkers in the clinic by use of a nanostructured microfluidic array. *Anal. Chem.* **2012,** *84*, 6249-55.
41. Munge, B. S.; Coffey, A. L.; Doucette, J. M.; Somba, B. K.; Malhotra, R.; Patel, V.; Gutkind, J. S.; Rusling, J. F., Nanostructured immunosensor for attomolar detection of cancer biomarker interleukin-8 using massively labeled superparamagnetic particles. *Angew. Chem. Int. Ed. Engl***. 2011,** *50*, 7915-8.

42. Manz, A.; Graber, N.; Widmer, H. M., Miniaturized total chemical analysis systems: A novel concept for chemical sensing. *Sens Actuators B Chem.* **1990,** *1*, 244-248.
43. Sanjay, S. T.; Fu, G.; Dou, M.; Xu, F.; Liu, R.; Qi, H.; Li, X., Biomarker detection for disease diagnosis using cost-effective microfluidic platforms. *Analyst* **2015,** *140*, 7062-7081.
44. Han, K. N.; Li, C. A.; Seong, G. H., Microfluidic chips for immunoassays. *Annu. Rev. Anal. Chem.* **2013,** *6*, 119-41.
45. Becker, H.; Gartner, C., Polymer microfabrication technologies for microfluidic systems. *Anal. Bioanal. Chem.* **2008,** *390*, 89-111.
46. McDonald, J. C.; Whitesides, G. M., Poly(dimethylsiloxane) as a Material for Fabricating Microfluidic Devices. *Acc. Chem. Res.* **2002,** *35*, 491-499.
47. Martinez, A. W.; Phillips, S. T.; Whitesides, G. M.; Carrilho, E., Diagnostics for the Developing World: Microfluidic Paper-Based Analytical Devices. *Anal. Chem.* **2010,** *82*, 3-10.
48. Li, X.J.; Nie, Z.H.; Cheng, C.M.; Goodale, A.B.; Whitesides, G.M. Paperbased electrochemical ELISA. *Proc. Micro. Total Anal. Syst.* **2010**, *14*, 1487– 489.
49. Liu, Y.; Wang, H.; Huang, J.; Yang, J.; Liu, B.; Yang, P., Microchip-based ELISA strategy for the detection of low-level disease biomarker in serum. *Anal. Chim. Acta* **2009,** *650*, 77-82.

50. Otieno, B. A.; Krause, C. E.; Latus, A.; Chikkaveeraiah, B. V.; Faria, R. C.; Rusling, J. F., On-line protein capture on magnetic beads for ultrasensitive microfluidic immunoassays of cancer biomarkers. *Biosens. Bioelectron.* **2014,** *53*, 268-274.

CHAPTER TWO

On-line Protein Capture on Magnetic Beads for Ultrasensitive Microfluidic Immunoassays of Cancer Biomarkers

2.1 Abstract

Accurate, sensitive, multiplexed detection of biomarker proteins holds significant promise for personalized cancer diagnostics. Here we describe the incorporation of a novel on-line chamber to capture cancer biomarker proteins on magnetic beads derivatized with 300,000 enzyme labels and 40,000 antibodies into a modular microfluidic immunoarray. Capture and detection chambers are produced from PDMS on machined molds and do not require lithography. Protein analytes are captured from serum or other biological samples in the stirred capture chamber on the beads held in place magnetically. The beads are subsequently washed free of sample components, and wash solutions sent to waste. Removal of the magnet and valve switching sends the magnetic bead–protein bioconjugates into a detection chamber where they are captured on 8 antibody-decorated gold nanoparticle-film sensors and detected amperometrically. Most steps in the immunoassay including protein capture, washing and measurement are incorporated into the device. In simultaneous assays, the microfluidic system gave ultralow detection limits of 5 fg mL^{-1} for interleukin-6 (IL-6) and 7 fg mL^{-1} for IL-8 in serum. Accuracy was demonstrated by measuring IL-6 and IL-8 in conditioned media from oral cancer cell lines and

showing good correlations with standard ELISAs. We also adapted this analyte capture strategy to detect a panel of biomarkers associated with oral mucositis; an inflammatory lesion of oral mucosa caused by high-dose chemotherapy and/or radiation that is especially prevalent during oral cancer treatment. The target proteins involved in the pathobiology of oral mucositis include IL-6, IL1-β, tumor necrosis factor (TNF-α) and C-reactive protein (CRP). Ultralow detection limits of 10-40 fg mL^{-1} were achieved for multiplexed detection of these proteins in 5 μL serum (2.5–10 zmol). Accuracy was verified by agreement of immunoassay results with ELISA values in oral cancer patients undergoing radiation therapy. This approach may lead to rapid, low-cost estimates of projected risk for severity of oral mucositis in cancer patients to enable improved therapeutic management. The on-line capture chamber facilitates rapid, sensitive, repetitive protein separation and measurement in 30 min in a semi-automated system adaptable to multiplexed detection of virtually any protein.

2.2 Introduction

Molecule-based early cancer diagnoses promise to improve treatment outcomes and patient survival rates.[1,2] Current cancer diagnostics often rely on biopsies, observing symptoms or lesions, or in vivo imaging. These approaches depend on finding a tumor, making early detection difficult and possibly compromising therapy outcomes. Screening for cancer without detecting tumors can be based on assays of body fluids for cancer biomarker proteins to provide an instantaneous record of a patient's disease status.[2-5] For translation to the

clinic, measurement devices for biomarker proteins should be accurate, sensitive, cheap and preferably capable of point-of-care (POC) use. For reliable diagnoses of cancers, it will be essential to measure panels of biomarker proteins rather than single proteins for the best prediction efficiency.[2, 6]

Existing methods for measuring protein biomarkers including enzyme linked immunosorbent assay (ELISA),[7] magnetic bead-based assays[2,8] and liquid chromatography-mass spectrometry (LC-MS)[9] are currently too expensive, time consuming, and technically complex for multiplexed POC protein determinations in clinical samples. Arrays based on optical,[10,11] electrochemical[12-16] or nanotransistor[17] detection have been developed to overcome some of these limitations.[6, 18] In reality, selected detection approaches can already achieve the high sensitivity and accuracy necessary for clinical applications, but complexity, cost and to a lesser extent multiplexing issues hold back clinical applications.

Microfluidics can improve immunoassay speed, cost and multiplexing.[18, 19-23] For example, an integrated microfluidic system recently reported for clinical diagnosis of HIV and syphilis detects antibodies to the disease vectors at clinical levels.[10] This chip used optical detection to analyze 1 µL of whole blood within 20 min in clinics in the developing world. However, improvements in integrated microfluidic systems still need to address multiplexing and other complexity issues.

We have developed modular microfluidic systems to facilitate fast multiplexed detection of proteins in biomedical samples.[12,24,25] These devices

feature a sensor array coated with gold nanoparticle (AuNP)-antibody conjugates in a poly(dimethylsiloxane) (PDMS) microchannel interfaced to a syringe pump and sample injector. Paramagnetic beads loaded with multiple detection antibodies and horseradish peroxidase (HRP) enzyme labels are used to capture protein analytes from sample solutions in small vials to provide detection of biomarker proteins in serum down into the low fg mL^{-1} range.[25] Accuracy and diagnostic utility of these microfluidic arrays was demonstrated by measuring four biomarker proteins in oral cancer patient serum samples.

While useful for diagnostics, the above system would benefit from simpler operation for clinical and POC screening. Herein we report incorporation of an on-line protein capture chamber in the modular microfluidic system. We used magnetic beads coated with ~40,000 antibodies and ~300,000 HRP labels, and validated the new system for simultaneous immunoassays of two proteins. The capture chamber features an oval PDMS channel equipped with a tiny stir bar sandwiched between two transparent poly(methyl methacrylate) (PMMA) plates (Figure 2.1A). The bioconjugated magnetic beads and protein samples are incubated in the chamber for on-line protein capture. After washing the beads and sending the wash to waste, the protein-magnetic beads are directed into the microfluidic detection chamber housing the 8-sensor AuNP array. This new design allows semi-automated ultrasensitive assays to be completed in the microfluidic device within 30 min. Nanostructured sensors combined with massively labeled magnetic detection beads provided simultaneous assays with

detection limits (DLs) of 5 fg mL^{-1} for IL-6 and 7 fg mL^{-1} for IL-8 in serum, similar to DLs for off-line manual protein capture. In a four-protein multiplexed measurement of IL-6, IL-1β, TNF-α and CRP, detection limits of 10-40 fg mL^{-1} were achieved in 5 μL serum. Accuracy and diagnostic utility of the arrays was demonstrated by correlating the levels of these proteins in conditioned media for oral cancer cell lines and serum from head and neck cancer patients with standard ELISA.

2.3 Experimental Section

2.3.1 Chemicals and Materials

Screen-printed carbon arrays with 8 700 μm dia. sensors were from Kanichi Research (UK). L -glutathione reduced (GSH, 99%), gold (III) chloride trihydrate ($HAuCl_4 \cdot 3H_2O$, 99.9%), sodium borohydride (99%), poly(diallyldimethylammonium chloride) (PDDA, MW 100,00-200,000, 20%), bovine serum albumin (BSA), 1-(3-(Dimethylamino)propyl)-3-ethylcarbodiimide hydrochloride (EDC) and N-hydroxysulfosuccinimide (NHSS) were from Sigma. Hydrogen peroxide (H_2O_2, 30%) was from Fisher. The poly(dimethoxy)silane (PDMS) kit was from Dow Corning. Buffer pH 7.4 phosphate saline (PBS) was 0.01 M in phosphate, 0.14 M NaCl, 2.7 mM KCl. Tween-20 and hydroquinone (HQ, ≥ 99%) were from Sigma-Aldrich. Streptavidin-coupled superparamagnetic beads (1 μm, Dynabeads) and biotinylated horseradish peroxidase (HRP) were from Invitrogen. All solutions were prepared with water purified by a Hydro water purification system to 18 MΩ•cm.

2.3.2 Antibodies and Proteins

Tumor Necrosis Factor (TNF-α) Duoset (catalog # DY210), Human CReactive Protein (CRP) Duoset (catalog # DY1707), Interleukin-1β (IL-1β) Duoset (catalog # DY201), monoclonal Human IL-6 Antibody (Ab_1, clone no. 6708), human IL-6 biotinylated polyclonal antibody (Ab_2, goat IgG), monoclonal human CXCL8/IL-8 antibody (Ab_1, clone no. 6217), human CXCL8/IL-8 biotinylated polyclonal Antibody (Ab_2, goat IgG), protein standards, and ELISA kits were from R&D systems.

2.3.3 Human Serum Samples and Conditioned media

Human serum samples were collected from patients undergoing high-dose radiation therapy for H&N cancer at the Neag Comprehensive Cancer Center, University of Connecticut Health Center (UCHC), USA. The study protocol was IRB approved and written Informed Consent of participants was obtained prior to sample collection. All samples were stored at or below -80 ^{o}C until use. Serum samples were assayed directly and in selected cases spiked with biomarker proteins for validation tests. Conditioned media from known oral cancer and control cell lines[26,27] were supplied by the National Institute of Dental and Craniofacial Research (NIDCR), NIH, Bethesda, MD.

2.3.4 Instrumentation

Amperometric measurements were done at ambient temperature with a CHI 1040 electrochemical workstation. The modular microfluidic immunoarray

system (Figure 2.2) incorporates an on-line protein capture chamber (Figure 2.1A) upstream of an 8-sensor detection device (Figure 2.1B) that we reported previously.[12] The capture chamber features an internal layer of flexible PDMS prepared on a machined template to have an oval hole sandwiched in between two flat, machined PMMA plates (Figure 2.1A). When bolted tightly together, this assembly forms an oval cylindrical channel 1.5 mm wide and 100 ± 2 µL in volume housing a tiny magnetic stir bar (Figure 2.2A). Flow out of this channel can be directed to waste or to the detection chamber by a switch valve system.

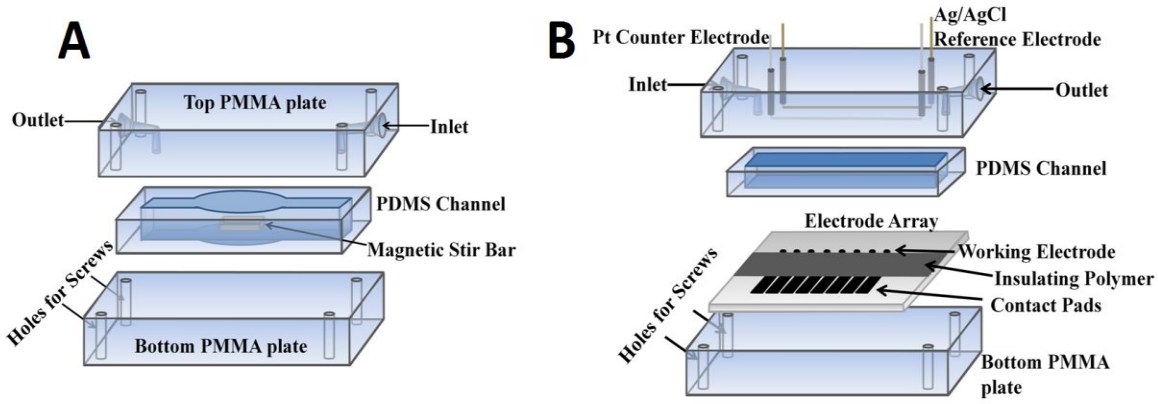

Figure 2.1: Components of (A) capture chamber in which target proteins are captured on-line from the sample and (B) detection chamber that houses the 8-electrode array.

The detection chamber is a PMMA-supported PDMS slab, with rectangular channel 1.5 mm wide, 2.8 cm long and 63 ± 2 µL volume placed on top of an 8-sensor gold nanoparticle-antibody coated screen-printed carbon array (Figure 2.1B).[12] The top PMMA plate features ports to connect 0.2 mm i.d. PEEK

tubing at inlet and outlet. The detection chamber has a 0.6 mm dia. hole for inserting a Ag/AgCl reference wire and 0.2 mm dia. hole for a Pt wire counter electrode that both run along the entire length of the detection channel (Figure 2.1B). A syringe pump (Harvard, no. 70 4504) was connected to 2 switch valves via sample injector (Rheodyne, 9725i) using 0.2 mm i.d. tubing (Figure 2.2). These 2 valves enable changing the direction of flow from reaction chamber to waste or to the detection chamber.

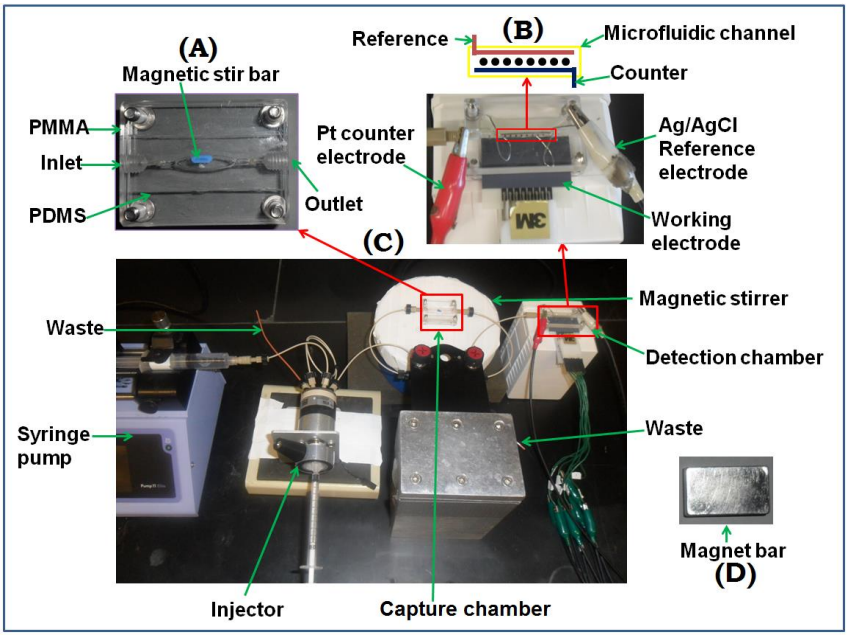

Figure 2.2: Photographs of microfluidic system for on-line protein capture and detection using magnetic beads. (A) Capture chamber in which target proteins are captured on-line from the sample by heavily labeled HRP-antibody-magnetic beads to form protein-bead bioconjugates. These are washed, and then flowed into the detection chamber (B) in the modular microfluidic system (C). The magnet (D) traps bioconjugate beads in the channel during injection of sample and washing, and is removed for transfer of beads to the detection chamber.

2.3.5 Preparation of Ab_2-magnetic particle -HRP (Ab_2-MP-HRP)

Biotinylated secondary antibodies (Ab_2) and biotinylated HRP labels were attached onto the 1 µm diameter streptavidin-coated superparamagnetic beads (MPs) as previously described.[25] Briefly, 20 µL of MP (10 mg mL^{-1}) were washed three times with 0.1% BSA in PBS pH 7.4 and then reconstituted with 80 µL of 0.1% BSA in PBS pH 7.4. 40 µL of biotinylated-Ab_2 (20 µg mL^{-1}) and 80 µL of biotinylated-HRP (2.5 mg mL^{-1}) were then simultaneously added to the MP dispersion to link biotin to streptavidin. The reaction was done at 37°C for 25 min with slow tilt rotation in 1.5 mL microcentrifuge tubes. Ab_2-MP-HRP conjugates were separated magnetically, using an Invitrogen DynaMag-spin magnet, washed three times with 0.1% BSA in PBS pH 7.4 to remove unbound Ab_2 and HRP, reconstituted with 200 µL of 0.1 % BSA in PBS and stored at 4°C until use.

From enzyme activity assays, the number of horseradish peroxidase labels per MP was estimated to be 321,000 (± 23,000) using 2,2'-Azino-bis(3-Ethylbenzthiazoline-6-Sulfonic acid) as a reactant.[12,28] The average number of Ab_2 per MP was estimated by difference, from the amount left in solution, to be 38,000 (±7,000) using the bicinchoninic acid assay **(**BCA**)** kit.[12,29,30]

2.3.6 Array Preparation and Characterization

Glutathione-decorated gold nanoparticles (GSH-AuNPs) with diameter 5.0 ± 2 nm were prepared by reduction of gold (III) chloride trihydrate salt using sodium borohydride as reported previously.[31] The screen-printed carbon electrode was modified by electrostatic layer-by-layer deposition. Briefly,

poly(diallyldimethylammonium chloride) (PDDA), a polycation was deposited on the electrodes. The array was then washed and AuNPs deposited to increase electroactive surface area and amplify the electrochemical signal of the arrays. Primary antibodies (Ab_1) were attached onto the GSH-AuNPs on the array via EDC-NHSS amidization overnight. The electrode array was washed and incubated with 2% BSA in PBS for 1 hr to block non-specific binding (NSB). A fresh AuNP-antibody array is inserted into the detection module for each assay.

2.3.7 On-line protein analyte capture and detection

The general strategy is illustrated in Figure 2.3. 40 µL of Ab_2-MP-HRP (1 mg mL^{-1} MPs) was added to 120 µL of 20 mM PBS, pH 7.4. This dispersion was then loaded into the 100 µL sample loop and injected at 100 µL min^{-1} into the capture chamber. 5 µL of protein analyte was diluted in calf serum and then loaded into the sample loop and injected into the chamber. A magnet bar (N55 neodymium magnet) was placed on top of the chamber before sample was injected to trap Ab_2-MP-HRP. After the capture chamber was filled with sample, flow was stopped and incubation was allowed for 30 min using the tiny stir bar for mixing.

The resulting protein-Ab_2-MP-HRP conjugates were then washed with PBS-Tween 20. Flow was then stopped and protein-Ab_2-MP-HRP conjugates in the reaction chamber were re-dispersed in the PBS-Tween 20 by removing the magnet. The valve was switched, and protein-Ab_2-MP-HRP was then pumped into the detection chamber. After the protein-Ab_2-MP-HRP conjugates filled the

detection chamber as evidenced by the red-brown color of MPs, flow was stopped and incubation was done for 15 min for capture of the beads by antibodies on the sensors. The array was then washed sequentially with PBSTween20 and 1 mM HQ in PBS. Amperometric detection was done at -0.2 V vs Ag/AgCl by injecting a mixture of 1 mM HQ and 100 µM H_2O_2 at 100 µL min^{-1} into the detection chamber via the sample loop.

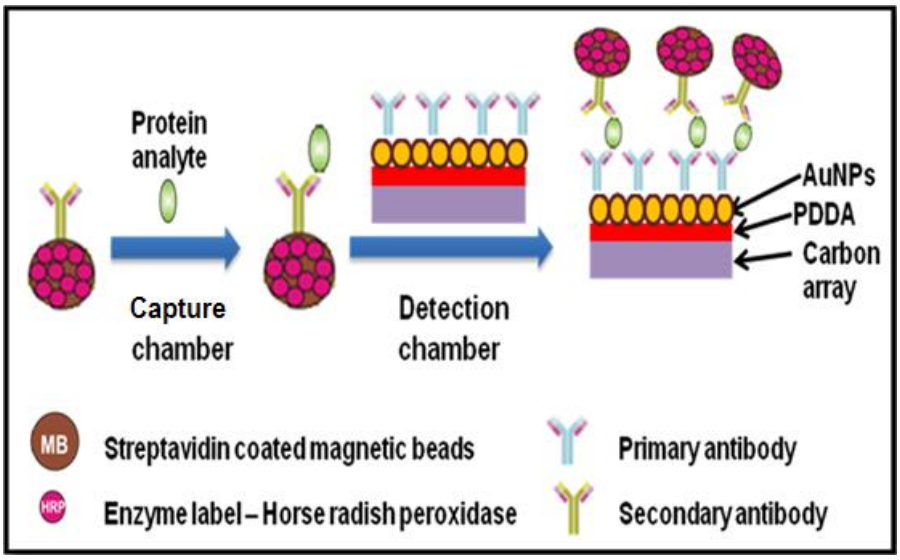

Figure 2.3: Conceptual strategy for ultrasensitive amperometric detection by microfluidic immunoarray. Protein analytes are captured on-line on Ab_2-MP-HRP bioconjugates in capture chamber. The protein-Ab_2-MP-HRP is then magnetically separated and washed in the chamber before being transported into the detection chamber.

During incubation in the detection chamber, the direction of flow from capture chamber can be sent to waste, so that the next sample can be loaded for capture with Ab_2-MP-HRP. Thus, both protein capture on sample 2 and detection on sample 1 can be done simultaneously to shorten assay time. Ideally, after the measurement of the first sample, the analysis time is ~30 min.

For multiplexed detection, a mixture of 20 µL of Ab_2-MP-HRP bioconjugate for each analyte reconstituted with 120 µL of PBS was loaded into the 100 µL sample loop and injected into the reaction chamber, followed by injection of a mixture of either two proteins (IL-6 and IL-8) or four proteins (IL-6, IL-1β, TNF-α and CRP) diluted in calf serum for standard calibrations. The procedure above was then used for simultaneous detection of the oral cancer biomarkers and oral mucositis biomarkers. All assay parameters were optimized for high sensitivity and high signal-to-noise ratio. Control experiments employed the full immunoassay procedure without antigen, and the response reflects the sum of residual non-specific binding and direct reduction of hydrogen peroxide.

2.4 Results

2.4.1 Array Characterization

The detection module of the system incorporates screen-printed carbon arrays coated with 5 nm GSH-AuNPs on ultrathin under-layers of poly(diallyldimethylamine) (PDDA) into a 63 µL microfluidic channel.[12] Tapping mode AFM images of uncoated carbon array sensors revealed a rough surface featuring hills and valleys with mean surface roughness of 17 ± 0.8 nm (Figure

2.4A). AFM images of array sensors with successively deposited layers of poly(diallyldimethyl amine) (PDDA) and 5 nm GSH-AuNPs, revealed nearly complete coverage of the underlying layer resulting in decreased mean surface roughness of 14.5 ± 1.2 nm (Figure 2.4B). AFM showed broader globular features after the immobilization of Ab_1 on the array (Figure 2.4C), with mean surface roughness slightly decreased to 12.4 ± 0.9 nm. The globular features are characteristic of immobilized primary antibody on the AuNP underlayer.[31] The electrochemical surface area after coating with AuNPs was estimated to be 2.53 (±0.26) × 10^{-3} cm^2 using cyclic voltammetry of 1 mM ferrocyanide and Randles-Sevcik equation.[12]

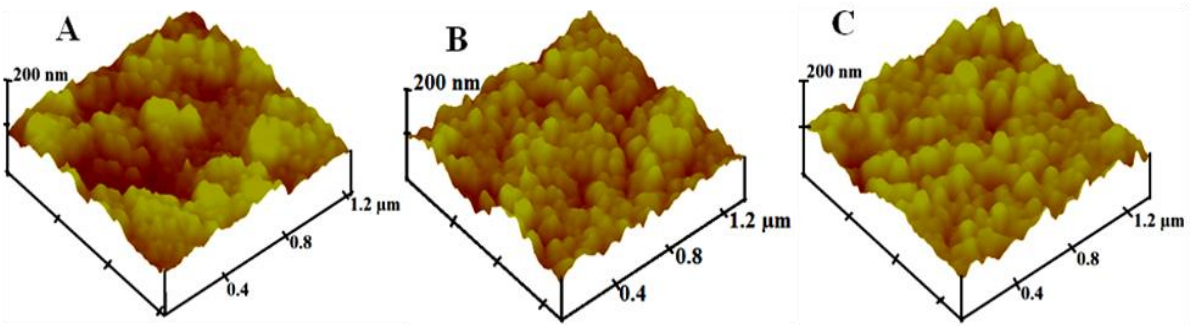

Figure 2.4: High resolution tapping mode AFM images of one of the array sensor electrodes of (A) bare screen printed carbon, (B) Carbon/PDDA/GSH-AuNPs and (C) Carbon/PDDA/GSH-AuNPs/Ab_1.

2.4.2 Immunoarray Calibration

We chose IL-6 and IL-8 as test analyte proteins because they are established biomarkers for oral, breast, prostate, and colorectal cancer.[32] IL-6 is

a 20 kDa cytokine implicated in inflammation, acute phase reaction, growth regulation and differentiation of cells.[33] Average concentration of IL-6 in serum of a healthy individual is < 6 pg mL^{-1} while in patients with oral cancer it ranges from 20 to over 1000 pg mL^{-1}.[34] IL-8 is an 8 kDa cytokine involved in inflammatory response, with serum levels in healthy individuals at ≤13 pg mL^{-1} compared to 20-1000 pg mL^{-1} or more in cancer patients.[35]

The microfluidic on-line capture system was first optimized for individual solutions of pure IL-6 and IL-8 in undiluted calf serum, a good surrogate for human serum in immunoarrays.[36] A key to achieving the best sensitivity and DLs is minimization of non-specific binding (NSB). For this purpose, the antibody coated array was incubated with 2% BSA for 1 hr prior to insertion in the detection chamber and all washing steps include 0.05% Tween-20. Optimization of surface concentrations of Ab_1 on the sensors and secondary antibody (Ab_2) on the MP are also critical. Best performance was obtained using 100 μg mL^{-1} Ab_1 for attachment to sensors, and 20 μg mL^{-1} Ab_2 for attachment to MPs.

MPs with attached HRP labels and antibodies for IL-6 or IL-8 were reconstituted in PBS, loaded into the sample loop, and injected into the capture chamber. Their positions are easily followed by their red-brown color. With the beads held in the capture chamber by a magnet, samples containing IL-6 or IL-8 were injected, and flow was stopped when the sample completely filled the capture chamber. After incubation to capture the analyte proteins on the beads and subsequent washing, the magnet is removed and flow is switched so that the

protein-bioconjugate beads are transported to the detection chamber. Again flow is stopped when the beads fill the detection chamber, and the beads are captured by the second set of antibodies on the sensors. Following protein capture and washing with PBS-Tween 20, a mixture of hydrogen peroxide to activate HRP and hydroquinone as mediator is then injected via the sample loop to develop the amperometric peaks (Figure 2.5A and C). A fresh 8-electrode array was inserted into the detection chamber for each sample, and this can be done while protein capture of the sample is occurring.

Using this protocol, peak currents increased linearly from 39 to 5,000 fg mL^{-1} for IL-6 and 9 to 2,500 fg mL^{-1} for IL-8. Peaks with no analyte protein (controls) are caused by a combination of direct reduction of hydrogen peroxide and NSB of the labeled magnetic particles on the array. Excellent array-to-array reproducibility is illustrated by the small error bars. The sensitivity of the immunoarray was 4.7 μA mL [fg protein]$^{-1}$ cm^{-2} for IL-6 and 2.0 μA mL [fg protein]$^{-1}$ cm^{-2} for IL-8 in undiluted calf serum.

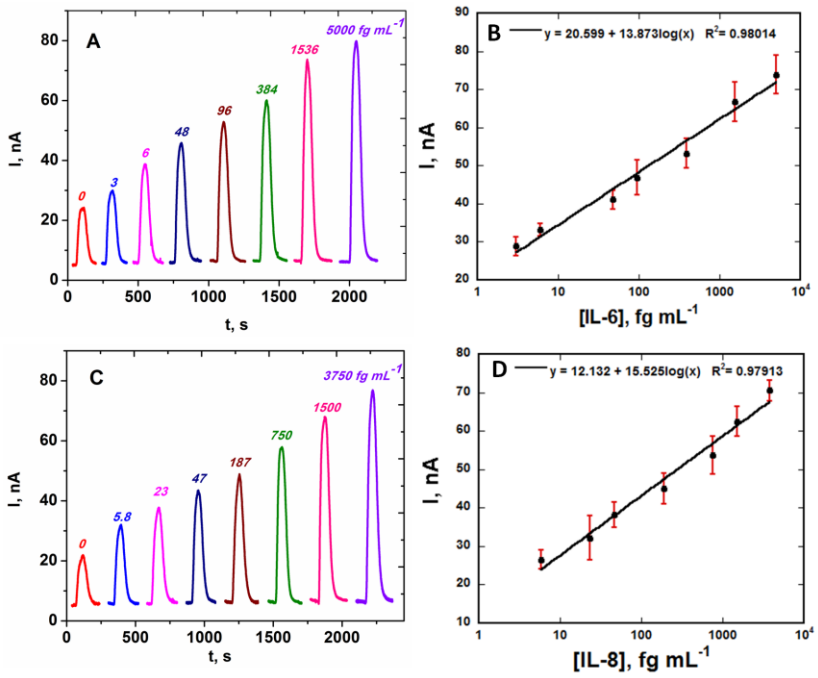

Figure 2.5: Amperometric responses for individual standard solutions of IL-6 and IL-8 in undiluted calf serum at -0.2 V vs. Ag/AgCl developed by injecting a mixture of 1 mM HQ and 0.1 mM H_2O_2 for (A) IL-6 and (C) IL-8, also showing calibration plots for (B) IL-6 and (D) IL-8 standards. Error bars represent standard deviations (n=8) for the eight electrodes of a single immunoarray.

NSB background can only result from residual NSB from the MPs having no captured analyte. The extent of NSB was compared to that of off-line capture in a small test tube using analyte-free controls (Figure 2.6A). There were no observable differences in peaks produced by on-line and offline protocols, showing that NSB is minimized to about the same extent by on-line and off-line capture methods. Reproducibility was also tested for 0 and 5 pg mL^{-1} IL-6 (Figure 2.6B) and IL-8 (Figure 2.6C) by running the immunoassays on different days with

different arrays. Relative standard deviation of the measurements for the two concentrations was <4 % confirming good array-to-array and day-to-day reproducibility.

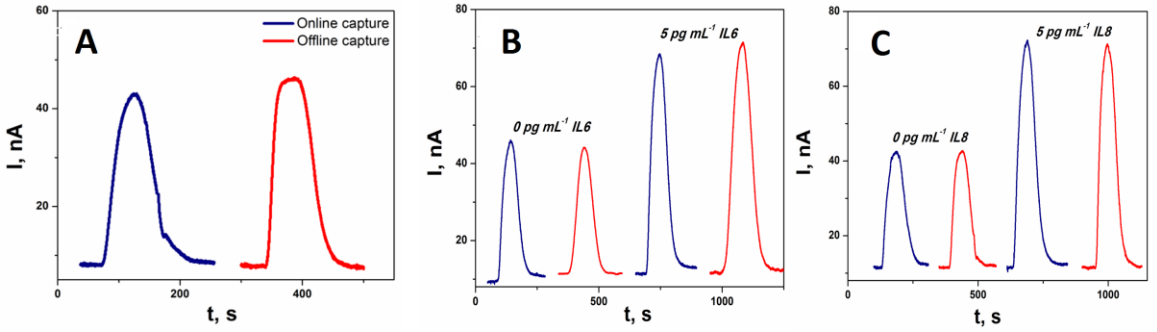

Figure 2.6: Amperometric signals for (A) on-line vs off-line capture protocol for control, (B) individual standard solutions of IL-6 and (C) IL-8 in undiluted calf serum at -0.2 V vs Ag/AgCl developed by injecting a mixture of 1 mM HQ and 0.1 mM H_2O_2 on different days with different arrays.

2.4.3 Determination of the cross-reactivity of the analytes

The immunosensor was also used to assess antibody cross reactivity using 5 pg mL^{-1} of IL-6 and IL-8. The immunoarrays were tested for cross reactivity of the protein with BSA and nonspecific antibodies before doing multiplexed detection. In these experiments, the arrays were coated with BSA and both IL-6 and IL-8 primary antibodies, however the Ab_2-MP-HRP-protein conjugate flown into the detection chamber were conjugated with only one type of protein. The amperometric measurements were recorded by injecting the mixture of 1 mM HQ and 0.1 mM H_2O_2. Amperometric responses for the cross

reactivity of the protein with non-specific antibodies is illustrated in Figure 2.7. Minimum cross reactivity between the analyte and non-specific antibodies was observed. Cross reactivity between IL-8 (protein analyte) with IL-6 capture antibodies was 3 ± 2% (Figure 2.7A) whereas the cross reactivity between IL-6 (protein analyte) with IL-8 capture antibodies was 4 ± 1% (Figure 2.7B) and considered to be within acceptable limits for simultaneous detection.

For multiplexed detection, specificity of the protein analyte was tested first before obtaining the calibration curves. IL-6 capture antibodies were spotted on the first four electrodes while IL-8 capture antibodies on the last four electrodes. A mixture of 10 pg mL^{-1} IL-6 and 6 pg mL^{-1} IL-8, were mixed and injected into the reaction to be captured with Ab_2-MP-HRP conjugates for both IL-6 and IL-8. After 30 min incubation in the reaction chamber, the protein-Ab_2-MP-HRP conjugate was washed and dispensed onto the electrodes housed in the detection chamber. Amperometric signals were recorded by injecting a mixture of 1 mM HQ and 0.1 mM H_2O_2. Figure 2.7C shows the amperometric differences between the response for the IL-6 on the first four electrodes and IL-8 on the last four electrodes indicating high selectivity.

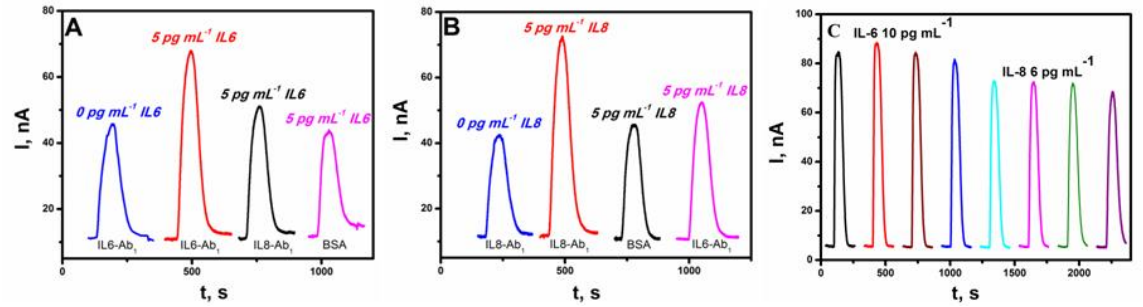

Figure 2.7: Cross reactivity of the analyte with non specific antibodies. The array was coated with BSA, IL-8 and IL-6 primary antibodies. (A) 5 pg mL^{-1} IL-6 and (B) 5 pg mL^{-1} IL-8 was injected and captured by the conjugate before being flown into the detection chamber. (C) Determination of specificity of the protein analyte on a single array. The first four electrodes show the amperometric response for IL-6 while the last four electrodes show the amperometric response for IL-8.

2.4.4 Detection of IL-6 and IL-8 in mixtures

For simultaneous detection of IL-6 and IL-8, capture antibodies for each protein were attached to four spots on the array (Figure 2.7C). Bioconjugate beads for IL-6 and IL-8 were combined, reconstituted in PBS, loaded into the sample loop, and injected into the reaction chamber, followed by injection of a mixture of IL-6 and IL-8. Incubation, washing, transport to the detection chamber, and detection were done as described above for the single protein standards.

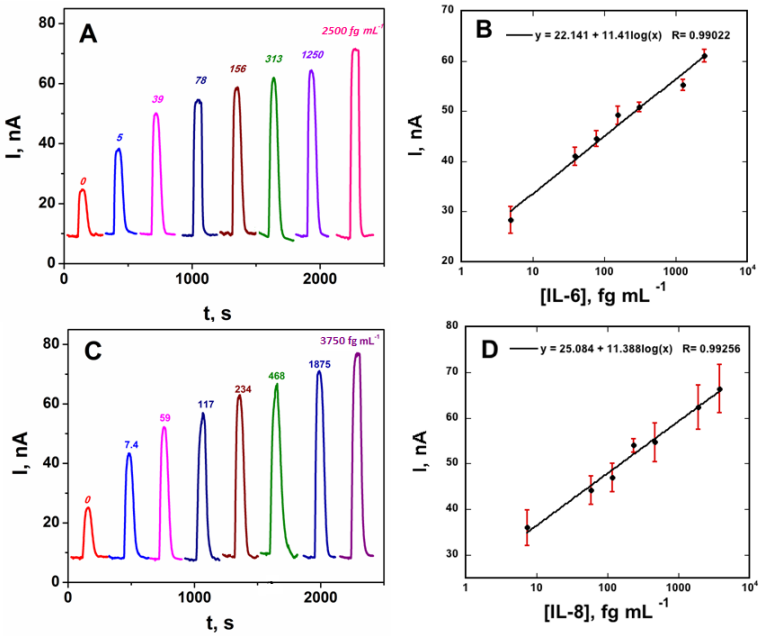

Figure 2.8: Amperometric responses for standard protein mixtures in undiluted calf serum at -0.2 V vs Ag/AgCl developed by injecting a mixture of 1 mM HQ and 0.1 mM H_2O_2 for (A) IL-6 and (C) IL-8, also showing calibration plots for (B) IL-6 and (D) IL-8. Error bars represent standard deviations (n=4) for the four IL-6 or IL-8 antibody-modified electrodes on a single immunoarray.

The peak currents increased linearly from 5 to 2,500 fg mL^{-1} for IL-6 and 7 to 3,750 fg mL^{-1} for IL-8 (Figure 2.8). Lower concentrations represent DLs, measured as three times the average standard deviation plus the zero protein control. The sensitivity of the immunoarray was 4.51 μA mL [fg protein]$^{-1}$ cm^{-2} for IL-6 and 4.45 μA mL [fg protein]$^{-1}$ cm^{-2} for IL-8 in undiluted calf serum.

2.4.5 Oral Mucositis Biomarkers

Assays were also designed to accurately measure normal serum biomarker levels as well as levels in patients undergoing oral cancer therapy. Reported mean serum levels of healthy individuals for IL-6, IL-1β, and TNF-α are 10-30 pg mL^{-1}, and 30 μg mL^{-1} for CRP. Serum levels before radiation therapy in patients with oral cancer were reported to increase to 20-190 pg mL^{-1} for IL-6, IL-1β and TNF-α, and ≥30 μg mL^{-1} for CRP.[37,38]

Primary antibodies for each protein were attached to two of the 8-electrodes on the array. HRP-labeled magnetic beads with antibodies for IL-6, TNF-α, CRP, and IL-1β were combined, re-dispersed in PBS, and injected as a mixture into the reaction chamber, followed by injection of a mixture of the four protein standards. All steps including incubation, washing, transport to detection chamber and detection were done as described above for oral cancer biomarkers. Binding studies related to the four protein analytes showed acceptably low cross-reactivity for all antibodies (Figure 2.9).

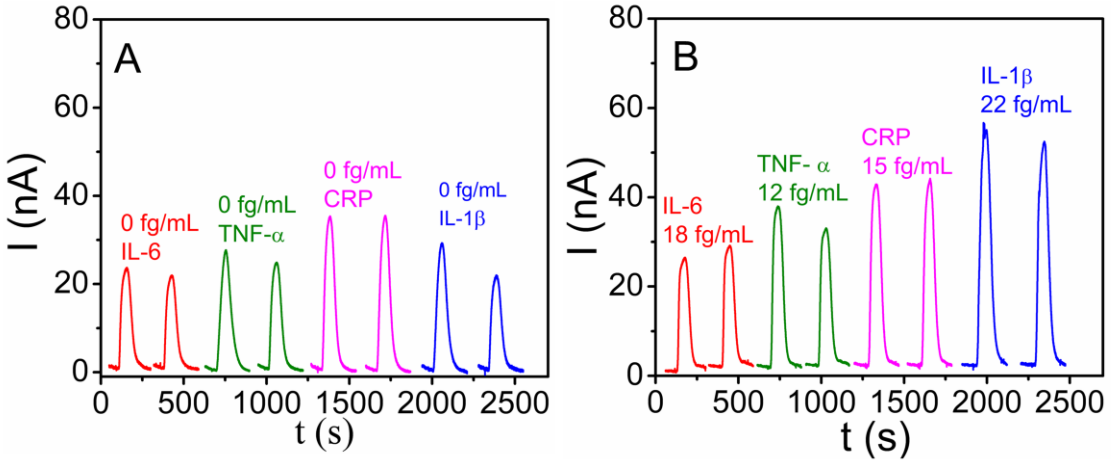

Figure 2.9: Duplicate responses measured simultaneously for (A) control mixture of 0 fg mL^{-1} for IL-6, TNF-α, CRP and IL-1β, and (B) standard mixture of 18 fg mL^{-1} IL-6, 12 fg mL^{-1} TNF-α, 15 fg mL^{-1} CRP, and 22 fg mL^{-1} IL-1β, illustrating reproducibility and selectivity.

Calibration data for the target proteins are shown in Figure 2.9.1. Detection limits (DLs) were 18 fg mL^{-1} for IL-6, 10 fg mL^{-1} for TNF-α, 15 fg mL^{-1} for CRP and 40 fg mL-1 for IL-1β for multiplex detection. Representative amperometric responses for multiplexed detection (Figure 2.9.1A,C,E,G) demonstrate high sensitivity in the pg/mL to low fg/mL range. Excellent reproducibility is illustrated by the small error bars obtained for calibration curves (Figure 2.9.1B,D,F,H), which were linear over 3 orders of magnitude concentration.

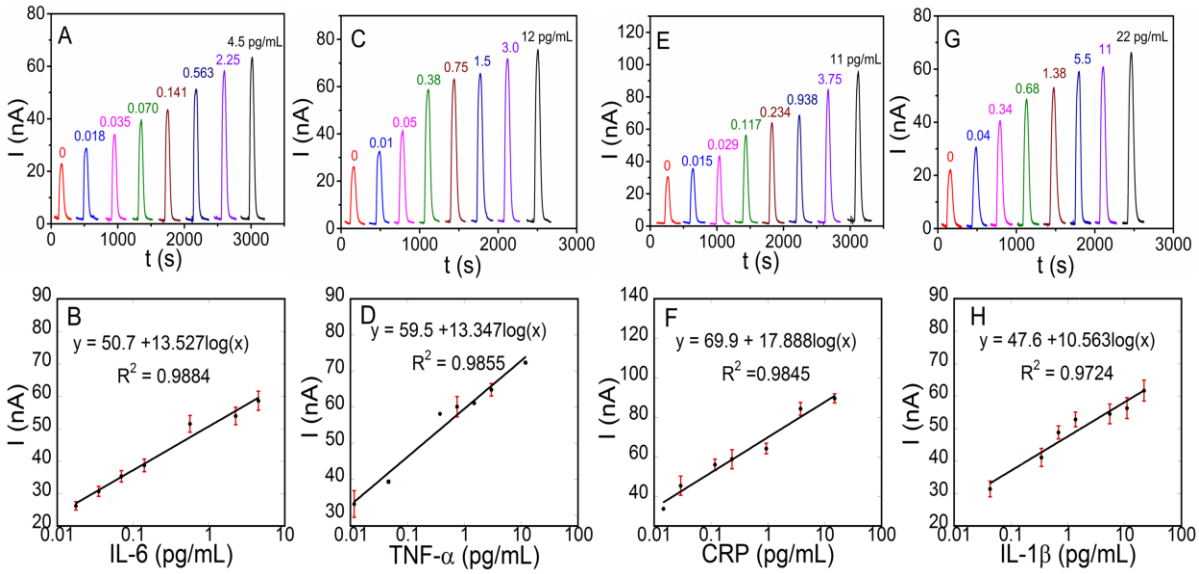

Figure 2.9.1: Amperometric responses for standard protein mixtures in 5-fold diluted calf serum for (A) IL-6, (C) TNF-α, (E) CRP, and (E) IL-1β, developed by injecting a mixture of 1 mM HQ and 0.1 mM H_2O_2 at -0.2 V vs. Ag/AgCl and the corresponding calibration plots for (B) IL-6, (D) TNF-α, (F) CRP, and (H) IL-β.

2.4.6 Assay Validation

2.4.6.1 Assay Validation with Conditioned Media from Oral Cancer Cells

Oral cancer or head and neck squamous cell carcinoma (HNSCC) is the sixth most common cancer in the developed world.[39] High mortality of HNSCC is related to frequent diagnoses at advanced stages.[40,41] IL-6 and IL-8 are associated with HNSCC, and hence accurate monitoring of their levels in patients holds promise for early detection and therapeutic monitoring.

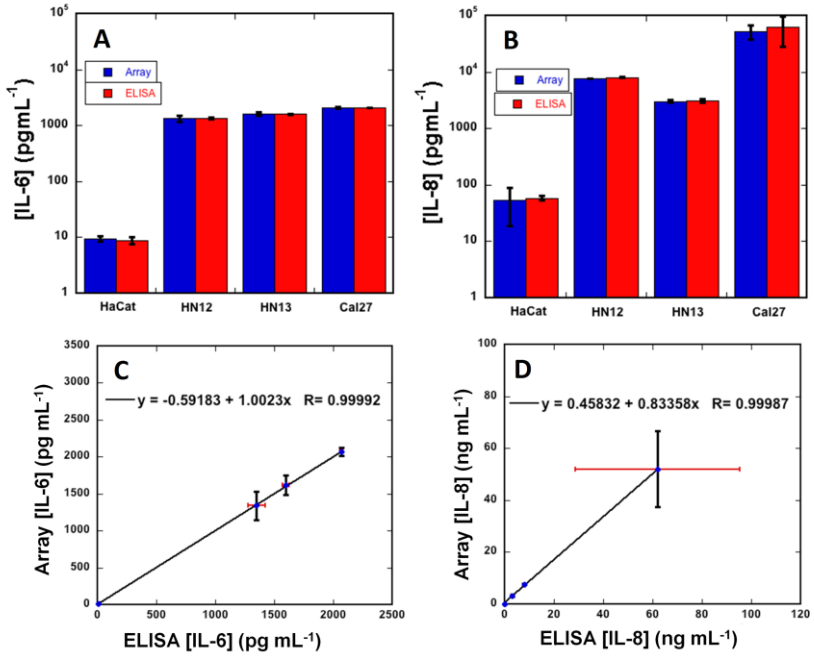

Figure 2.9.2: Correlation plots of immunoarray assay results for conditioned media of HaCat, HN12, HN13 and Cal27 cell lines vs. standard ELISA assays for (A) IL-6 and (B) IL-8. Error bars represent standard deviations for the immunoarray for n=4, and where not apparent are smaller than the point size.

To establish method accuracy, we used the microfluidic immunoarray to analyze levels of IL-6 and IL-8 in conditioned media from populations of HNSCC cell lines. Samples (5 µL) were diluted in PBS prior to injection into the capture chamber. Good accuracy of the immunoarray is illustrated by linear correlation plots with standard ELISA (Figure 2.9.2). The plots had slopes close to 1.0 (1.00 ± 0.01 for IL-6 and 0.83 ± 0.01 for IL-8) and intercepts close to zero (-0.592 ± 13.4 for IL-6 and 0.458 ± 0.29), confirming good correlation. Figure 2.9.2 shows comparative results for IL-6 and IL-8 in these samples by on-line capture

immunoassays and standard ELISA. Cancer cell lines HN12, HN13 and Cal27 secreted large amounts of IL-6 and IL-8 (>1,000 pg mL^{-1}), while immortalized HaCaT cells established from normal cancer-free epidermal cells showed low levels.

2.4.6.2 Assay validation with Human Serum Samples from H&N Cancer Patients

In order to validate accuracy, we used the microfluidic array to measure the levels of IL-6, TNF-α, and IL-1β simultaneously in ten serum samples from head and neck cancer patients undergoing radiation therapy. For patient samples CRP had to be measured separately due to its very high concentration in oral cancer patient serum.[37] For CRP, only 8 of the samples were analyzed as two of them had CRP levels well above our linear range after our standard dilution protocol, and amounts of sample were limited. In addition, CRP ELISA results were from a single sample run because of limited sample amounts. Serum samples collected on day 14 of radiation (1, 2, 3), day 35 of radiation (4, 5, 6, 7) and 21 days post-radiation (8, 9, 10) were used for these accuracy validation studies. Samples (5 μL) were diluted 30-fold in PBS prior to injection into the assay device to bring concentrations into the linear range of the calibrations. Several patient samples were spiked with different concentrations of standards to augment accuracy assessment and analytical recovery of the assay. By spiking the patient samples with 50, 100, 200, and 500 pg/mL of IL-6, TNF-α, and IL-1β

standards, a wider range of concentrations of the proteins was obtained for more representative correlation plots vs. ELISA. Good correlation of our results with those obtained from standard single-protein ELISA measurements are illustrated using bar graphs (Figure 2.9.3A).

Correlation was also assessed by linear plots of our immunoarray results vs. single protein ELISAs. Strong correlation between two assays is indicated by slopes approaching 1.0 and intercepts near 0. For this small sample set (≤ 10), linear plots resulted in slopes and R^2-values close to 1 and intercepts near 0 for all target proteins suggesting relatively good correlation for all the biomarker proteins (Figure 2.9.3B). The correlation plot slope for CRP (0.78) is a bit smaller than that of other proteins. This may be due to high levels of the protein in the μg/mL range requiring 1 million-fold serial dilutions that may generate volumetric errors, in addition to the fact that we have only one ELISA assay point for each sample for CRP. Nevertheless, as with all target proteins, CRP microfluidic immunoassay results gave self-consistent values for individual samples that were similar to ELISA values for most of the samples (Figure 2.9.3A).

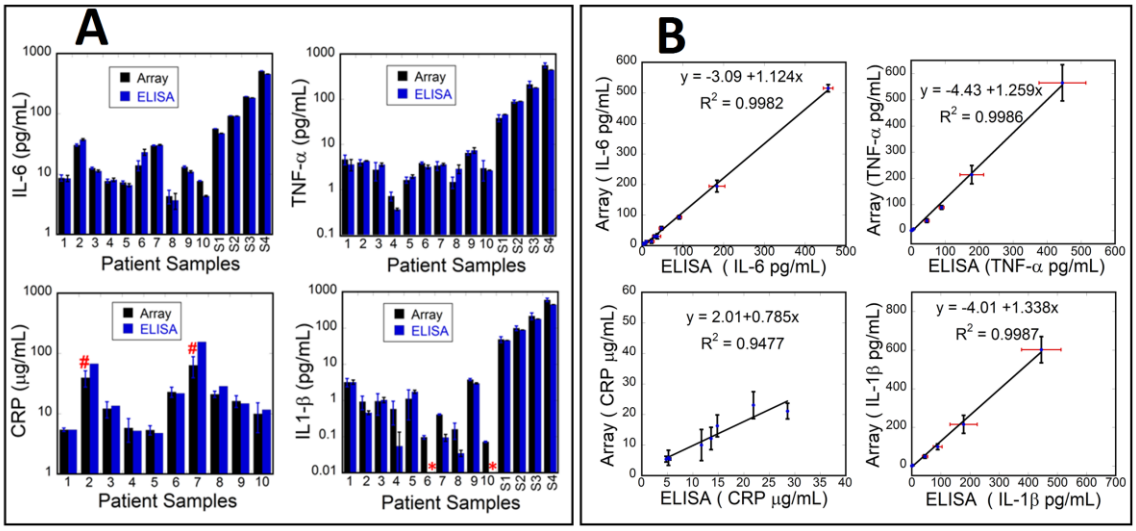

Figure 2.9.3: (A) Immunoarray and ELISA assay results from serum samples of Head and neck cancer patients for IL-6, TNF-α, CRP, and IL-1β. S1-S4 corresponds to patient samples spiked with 50, 100, 200, and 500 pg/mL respectively. (*) corresponds to values below the detection limits of ELISA and (#) corresponds to values above the dynamic range of the microfluidic immunoarray. (B) Linear correlation plots of immunoarray results against those from individual ELISAs for human serum samples from cancer patients for IL-6, TNF-α, CRP, and IL-1β. ELISA assays for CRP represent a single trial.

2.5 Discussion

Results described above demonstrate that the modular microfluidic system featuring on-line capture of protein biomarkers onto massively multi-labeled magnetic beads can accurately detect two protein cancer biomarkers in serum with high sensitivity and ultralow DLs. The MPs have high surface area to volume ratio here enabling attachment of 300,000 HRP labels and 40,000

antibodies to provide extremely efficient protein capture[42] as well as high sensitivity. Magnetic bead position is controlled magnetically in the on-line capture chamber for rapid binding of proteins, washing, and delivery to the detection chamber.

Sensitivities in undiluted calf serum from slopes of the calibration curves were 4.5 μA mL [fg protein]$^{-1}$ cm^{-2} for both IL-6 and IL-8. In contrast, assays using a similar microfluidic device with no capture chamber and off-line protein capture on beads with 400,000 HRP labels in simultaneous assays of 4 oral cancer proteins gave sensitivities of 5.9 μA mL [fg protein]$^{-1}$ cm^{-2} for IL-6 and 6.8 μA mL [fg protein]$^{-1}$ cm^{-2} for IL-8 in serum.[25] The slight decrease in sensitivity for the present on-line capture system can be attributed to fewer HRP labels used in Ab_2-MP-HRP. DLs of 5 fg mL^{-1} for IL-6 and 7 fg mL^{-1} for IL-8 for the on-line capture system were slightly better than the 10 fg mL^{-1} for both IL-6 and IL-8 in the earlier 4-protein off-line capture assay.[25]

Thus, the new on-line protein capture chamber incorporated into the earlier microfluidic detection system exhibited comparable sensitivity and about 2-fold better DLs from slopes of the calibration curves were 4.5 μA mL [fg protein]$^{-1}$ cm^{-2} for both IL-6 and IL-8. In contrast, assays using a similar microfluidic device with no capture chamber and off-line protein capture on beads with 400,000 HRP labels in simultaneous assays of 4 oral cancer proteins gave sensitivities of 5.9 μA mL [fg protein]$^{-1}$ cm^{-2} for IL-6 and 6.8 μA mL [fg protein]$^{-1}$ cm^{-2} for IL-8 in serum.[25] The slight decrease in sensitivity for the present on-line

capture system can be attributed to fewer HRP labels used in Ab_2-MP-HRP. DLs of 5 fg mL^{-1} for IL-6 and 7 fg mL^{-1} for IL-8 for the on-line capture system were slightly better than the 10 fg mL^{-1} for both IL-6 and IL-8 in the earlier 4-protein offline capture assay.[25] Thus, the new on-line protein capture chamber incorporated into the earlier microfluidic detection system exhibited comparable sensitivity and about 2-fold better DLs.

Very good accuracy of the assay system was confirmed by the correlation of immunoarray results on conditioned media for oral cancer cell lines with ELISA assays (Figure 2.9.1). Assays were done using 5 µL of conditioned media diluted in PBS to fit the dynamic range of the immunoassay. Selectivity was confirmed by accurate simultaneous detection of IL-6 and IL-8 in the conditioned cell media that also contains hundreds of other proteins, many at relatively high concentrations. In addition, the immunosensor gave good reproducibility as demonstrated by small array-to-array standard deviations (Figure 2.8) suggesting suitability for future clinical applications.

Inclusion of the on-line protein capture module provides a more automated strategy compared to the earlier device that required off-line capture since capture and washing are done in the microfluidic system, not manually as previously.[12,25] In the new system, most immunoassay steps are incorporated into the microfluidic device, requiring only loading of reagents, samples and wash solutions by the operator. The assay requires 30 min, which is less than 50 min for the off-line capture assay[25] and much less than standard ELISA (>5 hrs)[43]

and other commercial detection methods. Thus, assay time and level of automation begins to approach the needs of POC applications,[6,44] but further simplification of reagent addition will be required. The system has multiplexing capability for up to 8 proteins at attomolar levels with DLs 100-1,000 fold better than ELISA and commercial multiprotein bead assays, which have DLs of 1-10 pg mL^{-1} for many proteins.[2, 5,45]

2.6 Summary

In summary, we have fabricated and validated a modular microfluidic system featuring novel on-line capture of analyte proteins on magnetic beads to detect multiple cancer biomarker proteins. PDMS chambers are fabricated on machined molds, so that no lithography is needed. They are coupled to inexpensive commercial components so the system can be accessible to virtually any biomedical laboratory. Proof-of-concept was established by fast ultrasensitive, selective, reproducible detection of two proteins in biologically relevant mixtures. Partial automation and short analysis time suggest promise for clinical diagnosis of cancer and therapeutic monitoring, although further simplification is desirable. On-line capture on magnetic beads is also promising for integration into other low-cost microfluidic systems.

Preliminary correlation analysis of patient sample protein levels assayed in our work vs. standard metrics of oral mucositis severity suggested a strong correlation with IL-6, but results are inconclusive due to the limited number of samples. An ongoing related study by some of us (RVL, LAC, DEP) utilizing a

wider range of samples established tentative correlations with IL-6 and CRP as biomarkers for oral mucositis (unpublished data).

Future plans include assessing larger cohorts of patient samples at varying stages of therapy. This approach may ultimately lead to accurate, low-cost, rapid estimates of projected risk of oral mucositis in cancer patients, enabling improved therapeutic management. For example, human keratinocyte growth factor-1 (palifermin) is recommended for the prevention of oral mucositis in patients receiving autologous stem cell transplants.[46] However, this treatment is expensive, requires intravenous infusion, and is typically not indicated for the patient projected to develop only mild clinical mucositis. The development of such biomarkers to accurately predict who will develop severe mucositis can enable such expensive interventions for mucositis to be selectively used in a cost-effective manner. In turn, this would facilitate optimal delivery of cancer therapy and improve patient prognosis.

2.7 References

1. Etzioni, R.; Urban, N.; Ramsey, S.; McIntosh, M.; Schwartz, S.; Reid, B.; Radich, J.; Anderson, G.; Hartwell, L., The case for early detection. *Nat. Rev. Cancer* **2003,** *3*, 243-52.
2. Rusling, J. F.; Kumar, C. V.; Gutkind, J. S.; Patel, V., Measurement of biomarker proteins for point-of-care early detection and monitoring of cancer. *Analyst* **2010,** *135*, 2496-511.

3. Hanash, S. M.; Pitteri, S. J.; Faca, V. M., Mining the plasma proteome for cancer biomarkers. *Nature* **2008,** *452*, 571-9.
4. Kulasingam, V.; Diamandis, E. P., Strategies for discovering novel cancer biomarkers through utilization of emerging technologies. *Nat. Clin. Pract. Oncol.* **2008,** *5*, 588-99. 5, 588-599.
5. Lilja, H.; Ulmert, D.; Vickers, A. J., Prostate-specific antigen and prostate cancer: prediction, detection and monitoring. *Nat. Rev. Cancer.* **2008,** *8*, 268-78.
6. Gubala, V.; Harris, L. F.; Ricco, A. J.; Tan, M. X.; Williams, D. E., Point of care diagnostics: status and future. *Anal. Chem.* **2012,** *84*, 487-515.
7. Kingsmore, S. F., Multiplexed protein measurement: technologies and applications of protein and antibody arrays. *Nature Rev.* **2006,** *5*, 310-20.
8. Beveridge, J. S.; Stephens, J. R.; Williams, M. E., The use of magnetic nanoparticles in analytical chemistry. *Ann. Rev. Anal. Chem.* **2011,** *4*, 251 73.
9. Hawkridge, A. M.; Muddiman, D. C., Mass spectrometry-based biomarker discovery: toward a global proteome index of individuality. *Ann. Rev. Anal. Chem.* **2009,** *2*, 265-77.
10. Chin, C. D.; Laksanasopin, T.; Cheung, Y. K.; Steinmiller, D.; Linder, V.; Parsa, H.; Wang, J.; Moore, H.; Rouse, R.; Umviligihozo, G.; Karita, E.; Mwambarangwe, L.; Braunstein, S. L.; van de Wijgert, J.; Sahabo, R.;

Justman, J. E.; El-Sadr, W.; Sia, S. K., Microfluidics-based diagnostics of infectious diseases in the developing world. *Nature med.* **2011,** *17*, 1015-9.

11. Lee, H. J.; Wark, A. W.; Corn, R. M., Microarray methods for protein biomarker detection. *Analyst* **2008,** *133*, 975-83.
12. Chikkaveeraiah, B. V.; Mani, V.; Patel, V.; Gutkind, J. S.; Rusling, J. F., Microfluidic electrochemical immunoarray for ultrasensitive detection of two cancer biomarker proteins in serum. *Biosens. Bioelectron.***2011,** *26*, 4477-83.
13. Rusling, J. F., Nanomaterials-based electrochemical immunosensors for proteins. *Chem. Record.* **2012,** *12*, 164-76.
14. Rusling, J.; Munge, B.; Sardesai, N.; Malhotra, R.; Chikkaveeraiah, B., **2013**. Nanoscience based electrochemical sensors and arrays for detection of cancer biomarker proteins, In: Crespilho, F.N. (Ed), Nanobioelectrochemistry. Springer-Verlag, Berlin-Heidelberg, pp. 1-26.
15. Wang, J., Nanoparticle-Based Electrochemical Bioassays of Proteins. *Electroanalysis* **2007,** *19*, 769-776.
16. Wei, F.; Liao, W.; Xu, Z.; Yang, Y.; Wong, D. T.; Ho, C. M., A Bio-abiotic Interface Constructed by Nanoscale DNA-Dendrimer and Conducting Polymer for Ultra-sensitive Bio-molecular Diagnosis. *Small* **2009,** *5*, 1784-90.
17. Patolsky, F.; Zheng, G.; Lieber, C. M., Nanowire-based biosensors. *Anal. Chem.* **2006,** *78*, 4260-9.
18. Chin, C. D.; Linder, V.; Sia, S. K., Commercialization of microfluidic point ofcare diagnostic devices. *Lab chip* **2012,** *12*, 2118-34.

19. Gervais, L.; de Rooij, N.; Delamarche, E., Microfluidic chips for point-of-care immunodiagnostics. *Adv. Mater.* **2011,** *23* (24), H151-76.
20. Manz, A.; Harrison, D. J.; Verpoorte, E. M. J.; Fettinger, J. C.; Paulus, A.; Lüdi, H.; Widmer, H. M., Planar chips technology for miniaturization and integration of separation techniques into monitoring systems: Capillary electrophoresis on a chip*. J. Chromatogr. A* **1992,** *593*, 253-258.
21. Pan, Y.; Sonn, G. A.; Sin, M. L.; Mach, K. E.; Shih, M. C.; Gau, V.; Wong, P. K.; Liao, J. C., Electrochemical immunosensor detection of urinary lactoferrin in clinical samples for urinary tract infection diagnosis. *Biosens. Bioelectron.* **2010,** *26*, 649-54.
22. Wang, J.; Ahmad, H.; Ma, C.; Shi, Q.; Vermesh, O.; Vermesh, U.; Heath, J., A self-powered, one-step chip for rapid, quantitative and multiplexed detection of proteins from pinpricks of whole blood. *Lab chip* **2010,** *10*, 3157 62.
23. Whitesides, G. M., The origins and the future of microfluidics. *Nature* **2006,** *442*, 368-73.
24. Krause, C. E.; Otieno, B. A.; Latus, A.; Faria, R. C.; Patel, V.; Gutkind, J. S.; Rusling, J. F., Rapid microfluidic immunoassays of cancer biomarker proteins using disposable inkjet-printed gold nanoparticle arrays. *ChemistryOpen* **2013,** *2*, 141-5.
25. Malhotra, R.; Patel, V.; Chikkaveeraiah, B. V.; Munge, B. S.; Cheong, S. C.; Zain, R. B.; Abraham, M. T.; Dey, D. K.; Gutkind, J. S.; Rusling, J. F.,

Ultrasensitive detection of cancer biomarkers in the clinic by use of a nanostructured microfluidic array. *Anal. Chem.* **2012,** *84*, 6249-55.

26. Jeon, G. A.; Lee, J. S.; Patel, V.; Gutkind, J. S.; Thorgeirsson, S. S.; Kim, E. C.; Chu, I. S.; Amornphimoltham, P.; Park, M. H., Global gene expression profiles of human head and neck squamous carcinoma cell lines. *Int. J. Cancer.* **2004,** *112*, 249-58.
27. Sriuranpong, V.; Park, J. I.; Amornphimoltham, P.; Patel, V.; Nelkin, B. D.; Gutkind, J. S., Epidermal growth factor receptor-independent constitutive activation of STAT3 in head and neck squamous cell carcinoma is mediated by the autocrine/paracrine stimulation of the interleukin 6/gp130 cytokine system. *Cancer Res.* **2003,** *63*, 2948-56.
28. Pütter, J., 1983. Methods of Enzymatic Analysis 3. In: Becker, R., Bergmeyer, H.U. (Eds.),VerlugChemie, Deerfield Beach, FL. pp. 286-293.
29. Smith, P. K.; Krohn, R. I.; Hermanson, G. T.; Mallia, A. K.; Gartner, F. H.; Provenzano, M. D.; Fujimoto, E. K.; Goeke, N. M.; Olson, B. J.; Klenk, D. C., Measurement of protein using bicinchoninic acid. *Anal. Biochem.* **1985,** *150*, 76-85.
30. Wiechelman, K. J.; Braun, R. D.; Fitzpatrick, J. D., Investigation of the bicinchoninic acid protein assay: identification of the groups responsible for color formation. *Anal. Biochem.* **1988,** *175*, 231-7.
31. Mani, V.; Chikkaveeraiah, B. V.; Patel, V.; Gutkind, J. S.; Rusling, J. F., Ultrasensitive immunosensor for cancer biomarker proteins using gold

nanoparticle film electrodes and multienzyme-particle amplification. *ACS nano* **2009,** *3*, 585-94.

32. Xie, K., Interleukin-8 and human cancer biology. *Cytokine Growth Factor Rev*. **2001,** *12*, 375-91.
33. Deckert, F.; Legay, F., Development and validation of an IL-6 immunoreceptor assay based on surface plasmon resonance. *J. Pharm. Biomed. Anal.* **2000,** *23*, 403-12.
34. Riedel, F.; Zaiss, I.; Herzog, D.; Gotte, K.; Naim, R.; Hormann, K., Serum levels of interleukin-6 in patients with primary head and neck squamous cell carcinoma. *Anticancer Res.* **2005,** *25*, 2761-5.
35. Gokhale, A. S.; Haddad, R. I.; Cavacini, L. A.; Wirth, L.; Weeks, L.; Hallar, M.; Faucher, J.; Posner, M. R., Serum concentrations of interleukin-8, vascular endothelial growth factor, and epidermal growth factor receptor in patients with squamous cell cancer of the head and neck. *Oral Oncol.* **2005,** *41*, 70-6.
36. Yu, X.; Munge, B.; Patel, V.; Jensen, G.; Bhirde, A.; Gong, J. D.; Kim, S. N.; Gillespie, J.; Gutkind, J. S.; Papadimitrakopoulos, F.; Rusling, J. F., Carbon nanotube amplification strategies for highly sensitive immunodetection of cancer biomarkers. *J. Am. Chem. Soc.* **2006,** *128*, 11199-205.
37. Jablonska, E.; Piotrowski, L.; Grabowska, Z., Serum Levels of IL-1b, IL-6, TNF-a, sTNF-RI and CRP in Patients with Oral Cavity Cancer. *Pathol. Oncol.* **1997,** *3*, 126-129.

38. Brailo, V.; Vucicevic-Boras, V.; Lukac, J.; Biocina-Lukenda, D.; Zilic-Alajbeg, I.; Milenovic, A.; Balija, M., Salivary and serum interleukin 1 beta, interleukin 6 and tumor necrosis factor alpha in patients with leukoplakia and oral cancer. *Med. Oral Patol. Oral Cir. Bucal.* **2012,** *17*, e10-5.
39. Siegel, R.; Ward, E.; Brawley, O.; Jemal, A., Cancer statistics, 2011: the impact of eliminating socioeconomic and racial disparities on premature cancer deaths. *CA Cancer J. Clin.* **2011,** *61*, 212-36.
40. Horowitz, A. M.; Alfano, M. C., Performing a death-defying act. *J. Am. Dent. Assoc.* **2001,** *132*, 5s-6s.
41. Siegel, R.; Naishadham, D.; Jemal, A., Cancer statistics, 2012. *CA Cancer J. Clin.* **2012,** *62*, 10-29.
42. Mani, V.; Wasalathanthri, D. P.; Joshi, A. A.; Kumar, C. V.; Rusling, J. F., Highly efficient binding of paramagnetic beads bioconjugated with 100,000 or more antibodies to protein-coated surfaces. *Anal. Chem.* **2012,** *84*, 10485 91.
43. Findlay, J. W.; Smith, W. C.; Lee, J. W.; Nordblom, G. D.; Das, I.; DeSilva, B. S.; Khan, M. N.; Bowsher, R. R., Validation of immunoassays for bioanalysis: a pharmaceutical industry perspective. *J. Pharm. Biomed. Anal.* **2000,** *21*, 1249-73.
44. Soper, S. A.; Brown, K.; Ellington, A.; Frazier, B.; Garcia-Manero, G.; Gau, V.; Gutman, S. I.; Hayes, D. F.; Korte, B.; Landers, J. L.; Larson, D.; Ligler, F.; Majumdar, A.; Mascini, M.; Nolte, D.; Rosenzweig, Z.; Wang, J.; Wilson,

D., Point-of-care biosensor systems for cancer diagnostics/prognostics. *Biosens. Bioelectron*. **2006,** *21*, 1932-42.

45. Ward, A. M.; Catto, J. W.; Hamdy, F. C., Prostate specific antigen: biology, biochemistry and available commercial assays. *Ann. Clin. Biochem.* **2001,** *38*, 633-51.
46. Lalla, R. V.; Bowen, J.; Barasch, A.; Elting, L.; Epstein, J.; Keefe, D. M.; McGuire, D. B.; Migliorati, C.; Nicolatou-Galitis, O.; Peterson, D. E.; Raber-Durlacher, J. E.; Sonis, S. T.; Elad, S., MASCC/ISOO clinical practice guidelines for the management of mucositis secondary to cancer therapy. *Cancer* **2014,** *120*, 1453-61.

CHAPTER THREE

Ultrasensitive Multiplexed Detection of Parathyroid Hormone related Peptides (PTHrP) Using Gold Nanoparticle Immunoarrays

3.1 Abstract

Parathyroid hormone-related peptide (PTHrP) is a paraneoplastic protein recognized as the major causative agent of humoral hypercalcemia of malignancy (HHM). Independent of hypercalcemia, PTHrP has also been implicated in tumor progression and metastasis of a variety of human cancers. Conventional PTHrP detection methods such as immunoradiometric assay (IRMA) lack the sensitivity required to measure its levels prior to the development of hypercalcemia and pose potential health hazards due to the use of radioactive isotope labels. Here, we describe the first ultrasensitive multiplexed assay to measure intact PTHrP1-173 isoform as well as its fragments consisting of N-terminal and C-terminal peptides. We employed a microfluidic system featuring a small microfluidic chamber for on-line capture of the peptides from serum onto magnetic beads labeled with multiple copies of peptide-specific antibodies and signal-transducing enzyme labels. The magnetic bead-peptide conjugate was then washed and sent to a detection chamber housing antibody-modified 8-electrode array fabricated by ink-jet printing of gold nanoparticles. Limits of detection (LOD) of 3 fg mL^{-1} (~1000 fold lower than IRMA) were achieved for simultaneous detection of PTHrP isoforms and fragments within 30 min. Very

good correlation was observed with IRMA (n=57); r^2=0.99 using PTHrP1-173 and 1-86 fragment. Analysis of the sample data by ROC resulted in area under the curve of 0.96, 80-83% sensitivity and 96-100% specificity. Our study suggests that PTHrP1-173 isoform is the predominant circulating form of PTHrP. This new ultrasensitive, rapid, multiplexed, assay for PTHrP isoforms and fragments can aid in diagnosis, prognosis and therapeutic monitoring of cancer patients from early to advanced stages and help examine underlying mechanisms of PTHrP overproduction.

3.2 Introduction

The existence of a parathyroid hormone (PTH)-like factor was first postulated by Albright over 60 years ago[1] as a humoral factor responsible for the development of hypercalcemia in cancer patients and later described as humoral hypercalcemia of malignancy (HHM).[2] The true nature of this PTH-like factor remained elusive as it escaped detection by immunoassays using antibodies raised against PTH[3,4] but could be detected using bioassays based on activation of the PTH receptor.[5,6] This lead to the cloning and characterization of this PTH-like factor now known as parathyroid hormone-related peptide (PTHrP)[7,8] and to the development of specific immunoassays.[9,10]

Human PTHrP comprises of three isoforms of 139, 141 and 173 amino acids proteins through alternative mRNA splicing at the 3'end.[11] All the isoforms have identical amino acid sequence through residue 139 and undergo posttranslational cleavage generating N-terminal, mid-region and C-terminal

peptides with distinct physiological functions. Because of the N-terminal homology, PTHrP exerts PTH-like actions in bone and kidney by binding and activating the same guanylyl nucleotide-binding (G) protein-linked receptor (PTH1R) causing hypercalcemia.[12,13]

In addition to its PTH-like effect leading to hypercalcemia, PTHrP display properties distinct from those of PTH.[14,15] PTHrP is widely expressed in both normal and cancerous human tissues.[16,17] It acts as endocrine, autocrine, paracrine, or intracrine factor in a vast range of important physiological roles including normal skeletal development, placental calcium transport, smooth muscle relaxation, and mammary gland development.[15] Circulating levels of PTHrP have also been shown to correlate with disease progression in a variety of human cancers including breast, prostate, melanoma e.t.c[18-21] and development of bone metastasis in several studies.[22-24] However, PTHrP in the vast majority of cases can only be detected in the blood circulation when hypercalcemia develops.[9,10] Once hypercalcemia is present, there is approximately 50 percent chance the patient will die within 30 days.[25] Therefore, current PTHrP assays are limited to confirming the humoral origin of hypercalcemia but cannot provide tools for early detection of PTHrP producing tumors prior to the development of hypercalcemia. Early detection requires PTHrP assays with much higher sensitivity and/or specificity. Conventional assays for measuring the level of PTHrP in cancer patients include radioimmunoassay (RIA) and immunoradiometric assay (IRMA).[9,10,26] Despite the

specificity, ease of isotope conjugation and stability against interference from assay components such as serum/plasma, there are still several drawbacks limiting IRMA use in a normal clinical setup. The high energy isotopes employed such as ^{125}I pose substantial health hazard, require expertise to handle, and strict regulations to be met. These isotopes also have a short halflife which translates to a short shelf-life of the labeled reagents.[27,28] Assays that do not require radioisotope labeling such as enzyme linked immunosorbent assay (ELISA),[29] immunofluorometric assay[30] and mass spectrometry[27,31] have been developed for PTHrP detection. However, most of these assays lack the sensitivity required to measure levels of PTHrP in cancer patients early in the disease process prior to the development of hypercalcemia. Furthermore, none of these assays are designed to measure specific PTHrP isoforms and in particular the human specific PTHrP1-173 isoform.

In this chapter, we adapted a recently developed novel semi-automated modular microfluidic device[32] to detect peptides for the first time. The microfluidic system first delivers the sample to a capture chamber, where enzyme-labeled magnetic beads equipped with antibodies capture each target peptide. Then, the beads are washed and delivered to 8-sensor gold immunoarray (~$0.2 per array)[33] decorated with a second set of antibodies that recognize and bind the magnetic bead-bound target peptides. The peptides are measured simultaneously by activation of enzyme labels and electrochemical detection. Intact PTHrP isoforms as well as N- and C-terminal fragments were detected

simultaneously in serum. LOD of 3 fg mL^{-1} was achieved, which is 1000 fold lower than any commercially available PTHrP assay. Good correlation between the microfluidic immunoarray and IRMA results in cancer patients' serum/plasma demonstrates the diagnostic potential of the new assay. To the best our knowledge, this is the first ultrasensitive assay to simultaneously detect the intact PTHrP isoforms and its fragments.

3.3 Experimental Section

3.3.1 Chemicals and Materials

Horseradish peroxidase (HRP), sterile filtered bovine calf serum, Tween-20, bovine serum albumin (BSA), gold (III) chloride trihydrate ($HAuCl_4 \cdot 3H_2O$, 99.9%), sodium borohydride (99%), tetrocylammonium bromide, 3-mercaptopropionic acid (MPA), 1-dodecane thiol, poly(amic acid), 1-(3-(Dimethylamino)propyl)-3-ethylcarbodiimide hydrochloride (EDC), Nhydroxysulfosuccinimide (NHSS) and hydroquinone (HQ, ≥ 99%) were from Sigma-Aldrich. Hydrogen peroxide (H_2O_2, 30%) was from Fisher. Kapton FPC film (127 mM thick) was purchased from American Durafilm. The poly(dimethoxy)silane (PDMS) kit was purchased from Dow Corning. Immunoreagents (monoclonal antibodies, polyclonal antibodies, BSA, horseradish peroxidase (HRP)) were dissolved in pH 7.4 phosphate saline buffer (PBS, 5.9 mM Na_2HPO_4, 3.9 mM NaH_2PO_4, 2.7 mM KCL, 120 mM NaCl). 400 mM EDC and 100 mM NHSS were dissolved in water immediately before use. All

solutions were prepared with 18 MΩ·cm water purified through use of a Hydro water purification system (Durham, NC, USA).

3.3.2 PTHrP peptides and Antibodies

Intact PTHrP 1-173 was produced from cDNA encoding the PTHrP 1-173 isoform. Human PTHrP fragments 1-33, 151-169, 140-173 were purchased from Sheldon Biotechnology Center (McGill University). Human recombinant PTHrP 1-86 expressed in E.Coli was purchased from Sigma-Aldrich. Monoclonal antibodies M45 (IgM) and PA158 (IgG) were raised against PTHrP1-33; monoclonal antibody PA104 (IgG) was raised against PTHrP 140-173; monoclonal antibody PA6 (IgG) was raised against PTHrP 151-169, PA104, PA158. All monoclonal antibodies were purified by affinity chromatography (Medilabs, Quebec) and found highly specific with no cross reactivity with PTH and other unrelated peptides.[34] The bioactivity of these monoclonal antibodies was tested previously both in vitro and in vivo. Polyclonal antibodies against human PTHrP 1-173 (IgY lots 3103 and 3104) were raised in chicken and purified commercially (Genway Biotech, San Diego, CA).

3.3.3 Immunoradiometric assay (IRMA) for PTHrP

We used a commercial PTHrP assay for correlation purposes (PTHrP RUO, Active® IRMA catalog # DSL8100 Beckman Coulter Canada Inc, Montreal, Canada). This IRMA has been previously described to measure PTHrP in various cancer stages and to establish normal control values. It uses an N-terminal

monoclonal antibody raised against PTHrP1-40 and a mid-region monoclonal antibody raised against PTHrP 57-80. It has a sensitivity of 3 pg/mL and linearity up to 2100 pg/mL. Internal controls were made using pooled patients samples and conditioned media from PTHrP producing cells lines. The inter-assay variability was 4.4% and the intra-assay variability was 4.7%, according to the manufacturer's specifications. Normal values obtained from 40 healthy volunteers range from 0-15 pg/mL.

3.3.4 Human Serum Samples

Human serum samples from 22 healthy subjects and 37 cancer patients were obtained from McGill University Health Center. Samples were stored at or below -80°C until analyzed.

3.3.5 Array Fabrication

Immunoarrays were fabricated from 4 nm dodecanethiol decorated gold nanoparticles (AuNPs) on Kapton sheet as previously described using Dimatix inkjet materials printer (Figure 3.1).[33] Gold nanoparticle ink was prepared at 100 mg mL^{-1} in toluene and filtered using a 0.2 mm cutoff PTFE filter. The ink was then injected into a Dimatrix cartridge for use in the Dimatrix Inkjet materials printer. Upon printing, the electrode arrays were annealed 15 minutes at 200°C to drive off the thiol layer. The arrays lightened in color indicating the loss of the dodecane thiol layer and Au cores coalescing. Immediately after being annealed, the arrays were returned to the Dimatrix Inkjet materials printer to print the

poly(amic acid) insulation layer. The poly(amic acid) ink was prepared by diluting the 10% (m/m) poly(amic acid) solution in pure N-methyl-2-pyrrolidone (NMP) to 1% (m/m) and the adding the solution to a liquid crystal Dimatrix printer cartridge immediately prior to use.

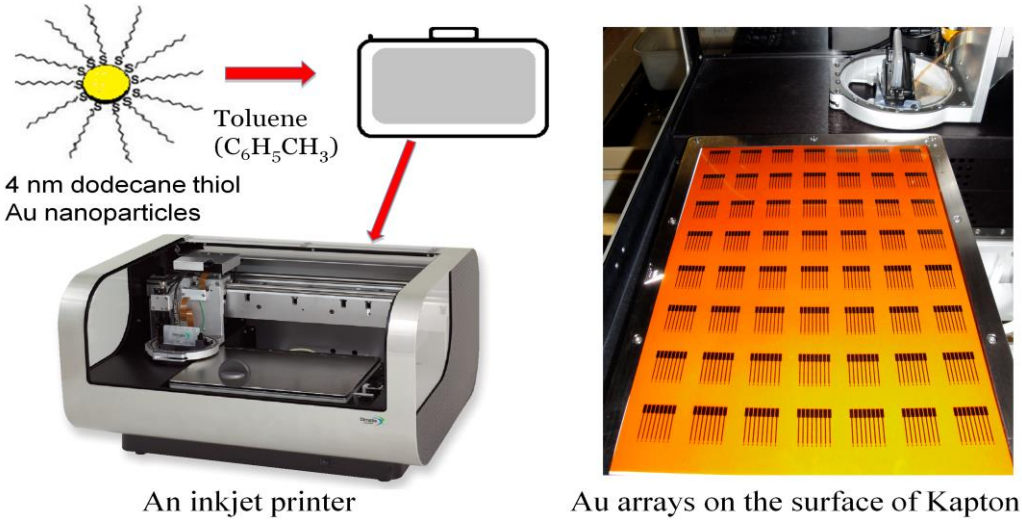

Figure 3.1: A photograph of Dimatix Inkjet Materials Printer from Fujifilm and printed gold nanoparticles (AuNPs) arrays on surface of Kapton Sheet.

The electrode arrays were then cleaned in 0.18 M sulfuric acid, by cycling potential between 1.5 and -0.2 V vs. saturated calomel electrode (SCE) to remove gold oxide from the surface. The electrode arrays were coated with self assembled monolayer (SAM) of mercaptopropionic acid (MPA) to introduce carboxyl groups on the surface of the array. The surface carboxyl groups were activated by freshly prepared EDC and NHSS to attach monoclonal antibodies (Ab_1) to array elements through amidization overnight. The arrays-modified with

Ab_1 were then washed with PBS-T20 to remove excess unbound Ab_1 and incubated with 2% BSA for 1 hr to minimize non-specific binding (NSB). The Ab_1-modified arrays were then fitted into the detection chamber for amperometric measurement. A new array was employed for each measurement.

3.3.6 Derivatization of Magnetic Beads

Magnetic bead bioconjugates [tosyl-activated magnetic beads (MBs)-Horseradish peroxidase (HRP)-Antibody (Ab_2)] were prepared using as previously described[35] with slight modification to reduce the bead conjugate preparation time from 42 to 24 hr. Briefly, tosylactivated magnetic beads (MB) (0.2 mg) were washed 3x with sodium borate buffer (pH 9.5), then reconstituted in 3 M ammonium sulfate + 0.1 M sodium borate buffer (volume 1:1). Horseradish peroxidase (HRP) (3 mg) and polyclonal antibody (Ab_2) (0.8 mg) were then simultaneously added to the dispersion and incubated at 37 ˚C for 18 hrs. The magnetic bead bioconjugates (HRP-MB-Ab_2) were then washed with PBS-T20 and reconstituted in 0.5% BSA at 37 ˚C for 6 hrs to block NSB. The resulting beads were washed 3x with 0.1% BSA, reconstituted in 600 µL of 0.1% BSA and stored at 4 ˚C. The number of Ab_2 per MB was estimated to be (4–11) $\times 10^4$ for different polyclonal antibodies for PTHrP using a protein assay kit (Bicinchoninic acid assay, BCA).[36] Activity assays showed that the number of HRP per MB was (1.3-2.6) $\times$ 10^5 (Table 3.1).[37]

Table 3.1: Characterization of Magnetic Bead Conjugate

Antibodies (Ab_2)	ABTS (#HRP per bead)	BCA (#Ab_2 per bead)
MA45	256,000 ± 20,000	40,000 ± 6,000
IgY 3103	165,000 ± 19,000	96,000 ± 7,000
IgY 3104	127,000 ± 5,000	114,000 ± 11,000

3.3.7 Detection of PTHrP isoforms and fragments

The semi-automated microfluidic system was constructed as previously reported[32] (Figure 3.2) and electrochemical measurements were all done at room temperature with a CHI 1040A eight-channel potentiostat at conditions optimized for high sensitivity and low S/N. The capture and detection chamber were first connected to the microfluidic system and subjected to a flow of PBS-T20 to block for NSB. 30 µL of HRP-MB-Ab_2 conjugate was reconstituted in 130 µL of 20 mM PBS buffer (pH 7.4), loaded into the 100 µL sample loop and injected into the capture chamber at 100 µL/min flow rate. 5 µL of PTHrP standard reconstituted in 5x diluted calf serum was loaded into the sample loop and injected into the capture chamber. HRP-MB-Ab_2 conjugate were held in the capture chamber, through use of a neodymium magnet positioned above the top PMMA plate, as the peptide standard or serum/plasma sample was injected. For simultaneous detection of N-terminal (1-33 or 1-86), and C-terminal peptides (151-169, 140-173) or intact 1-173 isoform, 10 µL of HRP-MB-Ab_2 conjugate for each peptide was reconstituted in 130 µL of PBS buffer, loaded into the sample loop and

injected into the capture chamber followed by injection of a mixture of the three standard peptides diluted in calf serum. Flow was then stopped, magnet removed and incubation was allowed for 30 mins with stirring for the peptide to be captured by HRP-MB-Ab_2 conjugate.

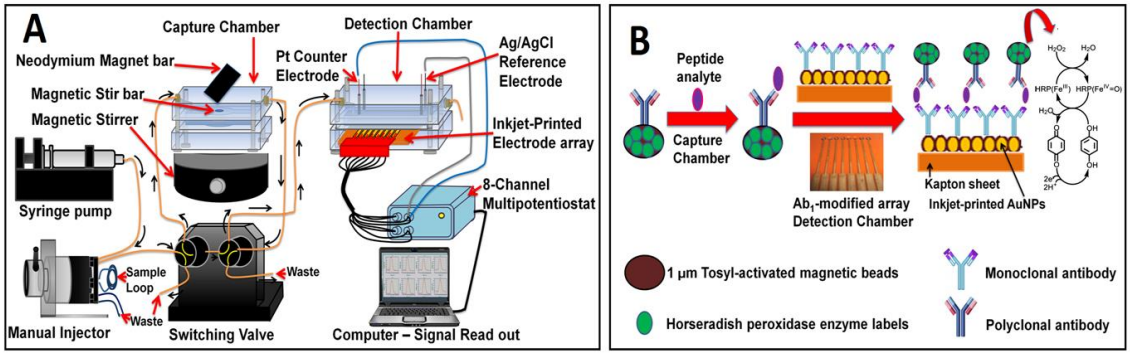

Figure 3.2: Immunoarray set-up for on-line peptide capture: (A) microfluidic device and (B) detection pathway.

The resulting peptide-Ab_2-MB-HRP conjugates were washed by flushing the capture chamber with PBS-T20 while holding the magnet bar on top of the PMMA plate and then re-dispersed in PBS-T20. The direction of flow was changed and the peptide-Ab_2-MB-HRP conjugates were transported into the detection chamber housing the Ab_1-modified 8-electrode array. After peptide-Ab_2-MB-HRP conjugates filled the detection chamber, flow was stopped and incubation was allowed for 15 mins for Ab_1 on the array to capture the bead conjugate. Unbound bead conjugate was then washed off by resuming buffer flow.

To perform amperometric measurements, the arrays were further subjected to a flow of buffer containing 1 mM hydroquinone in PBS for 4 mins. The 8 electrodes of the array were then connected to the working electrode leads of a CHI 1040 multi-potentiostat, and the Pt and Ag/AgCl wires were connected to the counter and reference leads, respectively. Amperometric detection was performed at -0.3 V vs Ag/AgCl by injecting a mixture of 1 mM hydroquinone and 0.1 mM hydrogen peroxide into the detection chamber via the sample loop at 100 µL/min. Hydrogen peroxide activates HRP on the peptide-Ab_2-MB-HRP conjugates to ferryloxy-HRP, which, in turn oxidizes hydroquinone to benzoquinone. Signal is generated as benzoquinone is reduced through a 2-electron transfer at the electrode surface.

3.4 Results

3.4.1 Single Peptide Detection

PTHrP generally undergoes post-translational proteolytic cleavage at lysine or arginine residue to generate smaller biologically active N-terminal, midregion and C-terminal peptide fragments.[10,11] We therefore first designed single peptide assays for N-terminal (1-33 & 1-86) and C-terminal fragments (151-169 & 140-173) as well as intact PTHrP 1-173 isoform. PA158, PA6 & PA104 were employed as capture antibody on the sensor elements while M45, IgY3103 & IgY3104 were attached onto magnetic bead conjugate as detection antibody (Table 3.2). Standards for the peptide fragments were prepared in 5x

diluted calf serum as a surrogate for human serum.[38] Control experiments employed full immunoassay reagents without the peptide analyte.

Table 3.2: Antibody and Peptide Pairing for Sandwich Assay

Peptide Fragments	Antibody on the Sensor	Antibody on the Beads	Single Detection (DL fg/mL)	Sensitivity (μA/cm²)/(C)	Fragment size (no. of aa)
1-33	PA158	MA45	5	2.22	33
151-169	PA6	IgY3103	4	2.12	19
140-173	PA104	IgY3104	3	1.98	33
1-86	PA158	IgY3103	4	4.89	86
1-173	PA104	IgY3104	3	3.55	173

To establish optimal conditions for the assays as well as to improve on both the signal to noise ratio and sensitivity, antibody concentrations were first optimized on the beads and sensors prior to obtaining calibration curves. N-terminal fragments (1-33 & 1-86) were paired with antibodies PA158 and MA45, while the C-terminal fragments (151-169 & 140-173) were paired with antibodies (PA6 & PA104) and (IgY3103 & IgY3104) (Table 3.2). We began with optimizing the antibody concentrations on the magnetic beads keeping a consistent Ab_1 antibody concentration of 100 μg mL^{-1}, and employing standard concentration of 0, 2.5, and 5 pg mL^{-1} for standard peptide fragments (of 151-169, 140-173, and 1-33). The optimal secondary antibody concentration was determined from the greatest signal difference between the control and sample concentration for

IgY3103 50 µg mL^{-1}, for IgY3104 50 µg mL^{-1}, and for M45 20 µg mL^{-1} (Figure 3.3 D,E,F).

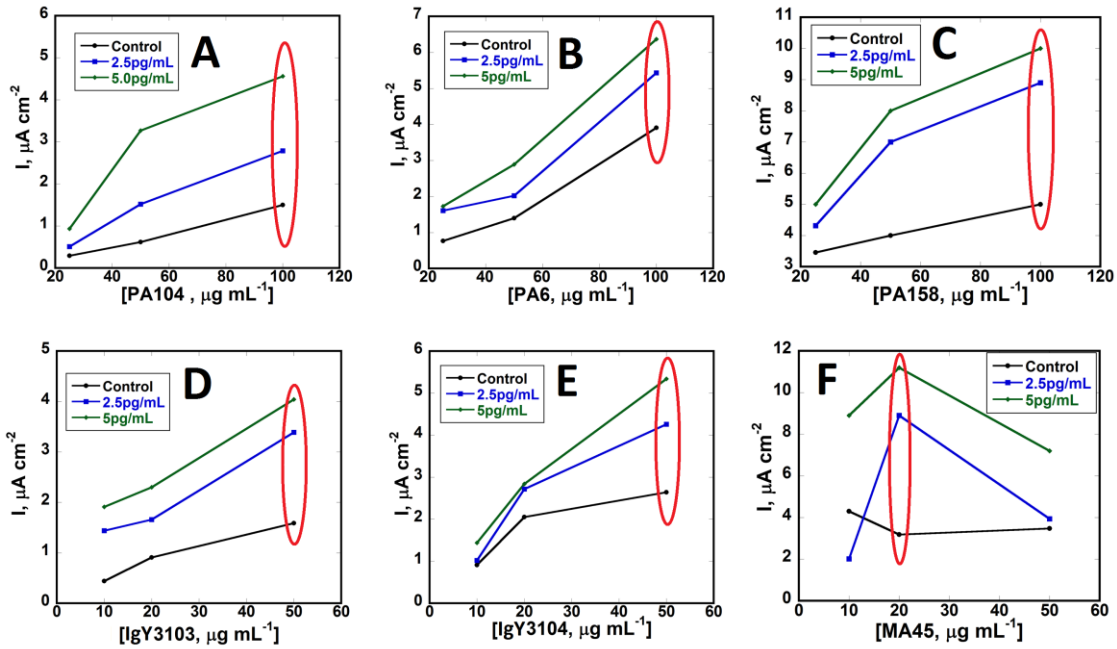

Figure 3.3: Optimization of Ab_1 and Ab_2 concentration using a control and standard concentrations of 2.5, 5 pg mL^{-1} for (A) PA104, (B) PA6, (C) PA158, (D) IgY3103, (E) IgY3104, and (F) MA45. Optimal concentrations for both Ab_1 and Ab_2 are circled.

Once the secondary antibody concentration was confirmed for the conjugate magnetic beads the optimal concentration of primary antibody on the surface of arrays was established using a consistent optimized secondary antibody concentration (IgY3103 50 µg mL^{-1}, IgY3104 50 µg mL^{-1}, and M45 20 µg mL^{-1}) again employing standard concentrations of 0, 2.5, and 5 pg mL^{-1} for standard peptide fragments (of 151-169, 140-173, and 1-33). The greatest signal

difference between control and sample concentration indicated the optimal primary antibody concentration to be 100 µg mL^{-1} for all monoclonal antibodies (Figure 3.3 A,B,C).

Using the optimized concentrations of Ab_1 and Ab_2, calibration plots for the individual peptide fragments were obtained (Figure 3.4). Control signals resulted from a combination of NSB of the magnetic bead conjugate on the sensor elements and direct reduction of hydrogen peroxide. Current density increased linearly with log C for all the peptide fragments from 3 fg mL^{-1} to 16 pg mL^{-1}. LOD measured as three times the standard deviation above the control ranged from 3-5 fg mL^{-1} for all the peptides (Table 3.2). These LODs are 1000-fold better than IRMA and commercial ELISA kits (3-5.5 pg mL^{-1}). Good assay reproducibility is indicated by the small error bars for the standard points in the calibration plot. Sensitivities, obtained from the slope of the calibration plot, were dependant on the peptide fragment size. For the smaller peptide fragments (1-33, 140-173 & 151-169), sensitivities were in the range of 1.98 – 2.12 µA cm^{-2} $[\log C]^{-1}$ while the larger peptide fragments exhibited a much higher sensitivity (3.55 – 4.98 µA cm^{-2} $[\log C]^{-1}$) (Table 3.2).

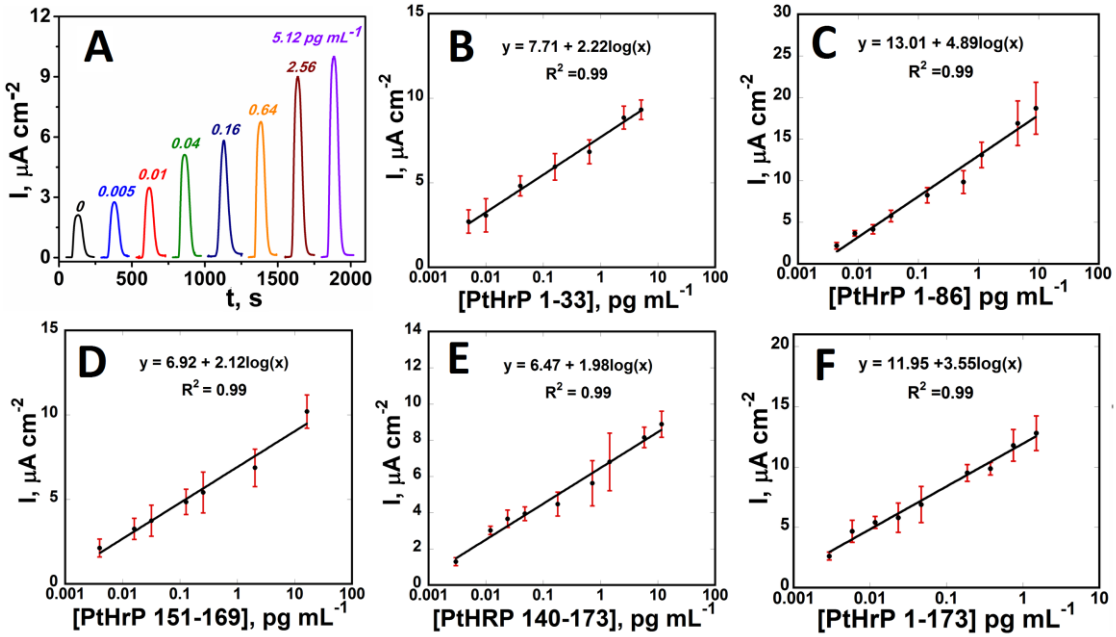

Figure 3.4: Responses for (A) 1-33 obtained at -0.3 V vs Ag/AgCl. Calibration plots for PTHrP peptide fragments in 5x diluted calf serum: (B) 1-33, (C) 1-86, (D) 151-169, (E) 140-173 and (F) intact PTHrP 1-173 (n=8).

3.4.2 Multiplexed Peptide Detection

Based on the sensitivities observed during single peptide detection, the larger peptide fragments (1-86 & 1-173) were selected for multiplexed detection (Table 3.2). Employing the 8-electrode array, a sandwich assay was build up on the first three electrodes for detection of 1-173 using PA104 and IgY3103, the next three electrodes for detection of 1-86 using PA158 and MA45 and the last two electrodes for detection of 1-173 using PA6 and IgY3104 (Figure 3.5A). Magnetic bead conjugate (10 µL each) with MA45, IgY3103 and IgY3104 were combined, dispersed in PBS and injected into the capture chamber via the sample loop. A mixture of standards for 1-86 and 1-173 (volume ratio 1:2) was

then introduced into the capture chamber with the aid of the magnet bar positioned above the capture chamber. All steps, from washing the resulting peptide-bead conjugate to amperometric detection, were performed as illustrated above for single peptide detection. Prior to obtaining calibration plots, binding studies were done to determine the specificity of the antibodies towards the peptide fragments (Figure 3.5B). Minimal cross-reactivity was observed between the antibodies for 1-173 and 1-86 peptide analytes.

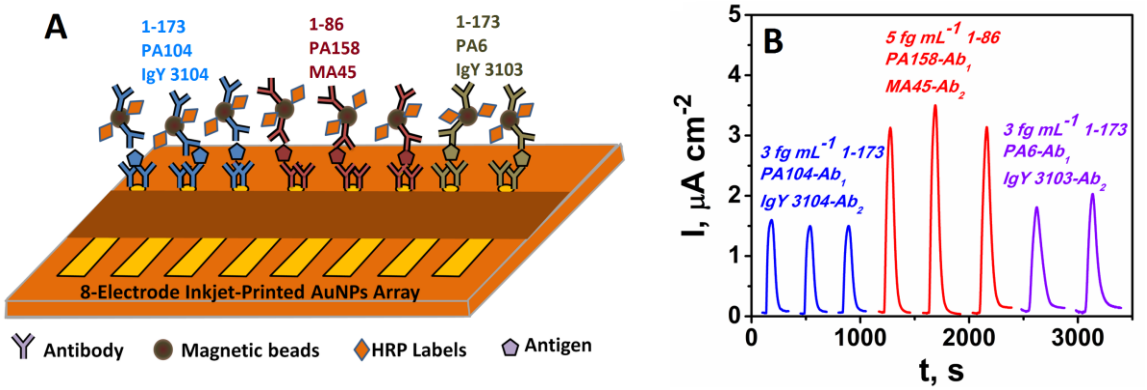

Figure 3.5: A) Multiplexing strategy for the peptide fragments on a single 8-electrode inkjet-printed AuNPs array. B) Representative amperometric response for detection of a mixture of 1-173 and 1-86 on a single 8-electrode array.

Calibration plots for detection of a mixture of the peptides are shown in Figure 3.6. Current density increased linearly with log C of the peptides from 3 fg mL^{-1} to 12 pg mL^{-1}. LODs were 4 fg mL^{-1} for 1-86, 6 fg mL^{-1} for 1-173 (PA104) and 3 fg mL^{-1} for 1-173 (PA6). Excellent reproducibility is illustrated with small error bars for the standards mixtures. In addition, combination of PA104 &

IgY3104 and PA6 & IgY3103 exhibited similar sensitivity towards detection of intact PTHrP1-173 isoform (4.49 vs 4.48 μA cm^{-2} $[\log C]^{-1}$) (Figure 3.6B & F). This is consistent with the observations made during specificity (Figure 3.5B) and the binding studies previously done by our collaborators.[34]

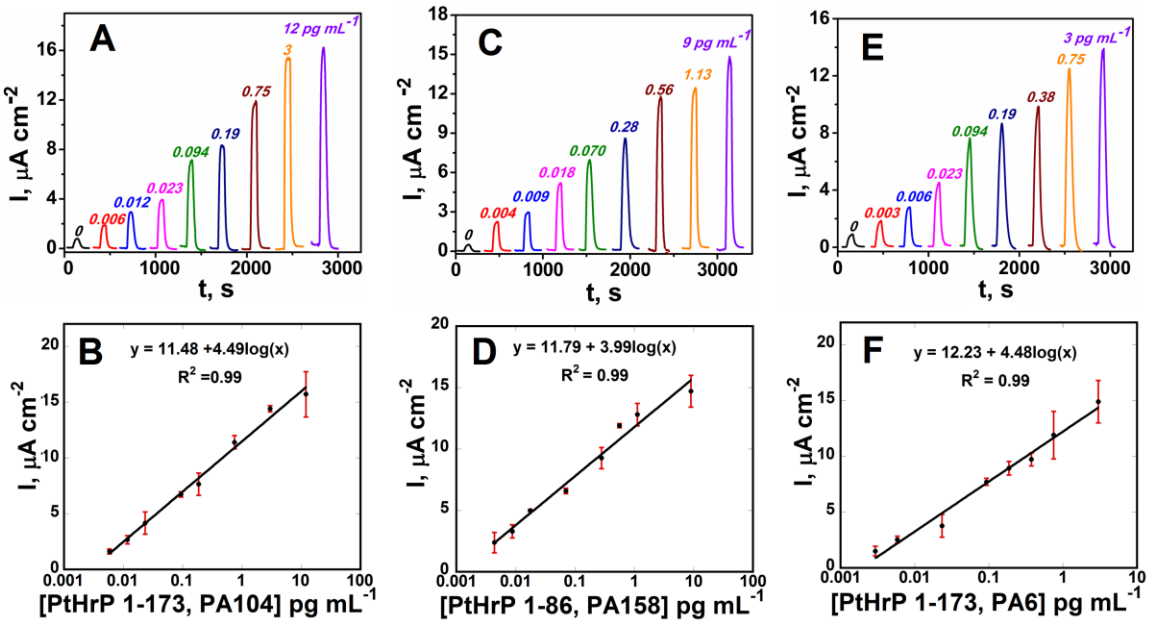

Figure 3.6: Amperometric responses for standard peptide mixtures in 5x diluted calf serum at -0.3 V vs Ag/AgCl for (A) intact PTHrP 1-173 using PA104, (C) 1-86 peptide fragment (E) intact PTHrP 1-173 using PA6 and also showing calibration plots for intact PTHrP 1-173 (B & F) and 1-86 fragment (D) (n=3).

3.4.3 Validation using Cancer serum samples

Serum and plasma samples from cancer patients and cancer-free individuals were assayed and compared with IRMA results to validate accuracy. The antibody used for 1-86 peptide binds all three PTHrP isoforms and their N-

terminal fragments. The antibody used for 1-173 binds PTHrP 1-173 and shorter fragments such as 140-173 and 151-169.[34] A significant difference in the PTHrP levels between the healthy individuals and cancer patients was observed; 2-sample t-test at the 95% confidence level confirmed great difference between the two cohorts (P<0.001) (Table 3.3).

Table 3.3: Serum Samples Data

	Number of Samples (n)	Mean PTHrP (pg/mL)	Stdev
Healthy Individuals	22	6.69	2.07
Cancer Patients	35	23.99	22.77

Cancer patient samples had larger amounts of PTHrP upto 90 pg mL^{-1} compared to healthy individuals (<10 pg mL^{-1}, Figure 3.7A,B). Assays by the immunoarray and IRMA gave similar levels of PTHrP; t test at the 95% confidence level confirmed no significant difference between the two methods (Figure 3.7C). Our assay detected PTHrP levels in all samples including 4 that were undetectable by IRMA. Immunoarray results gave good linear correlation plots with IRMA for all 57 samples (22 controls and 35 cancer subjects) with slopes close to 1 (0.90 ± 0.02 for 1-86 & 0.82 ± 0.01 for 1-173), intercepts near 0 (1.33 ± 0.51 for 1-86 & 0.39 ± 0.28 for 1-173) and correlation coefficients of 0.99 (Figure 3.7D; Table 3.4). Values obtained with assay measuring intact PTHrP 1-173 and its fragments (red) were only slightly lower than values obtained with the assay recognizing all three isoforms and its fragments labeled as 1-86 (blue)

suggesting that PTHrP 1-173 is the form of PTHrP in these samples (Figure 3.7C).

Table 3.4: Correlation plot table

PTHrP	Slope	Intercept	R^2
1-86	0.90 ± 0.02	1.33 ± 0.51	0.99
1-173	0.82 ± 0.01	0.39 ± 0.28	0.99

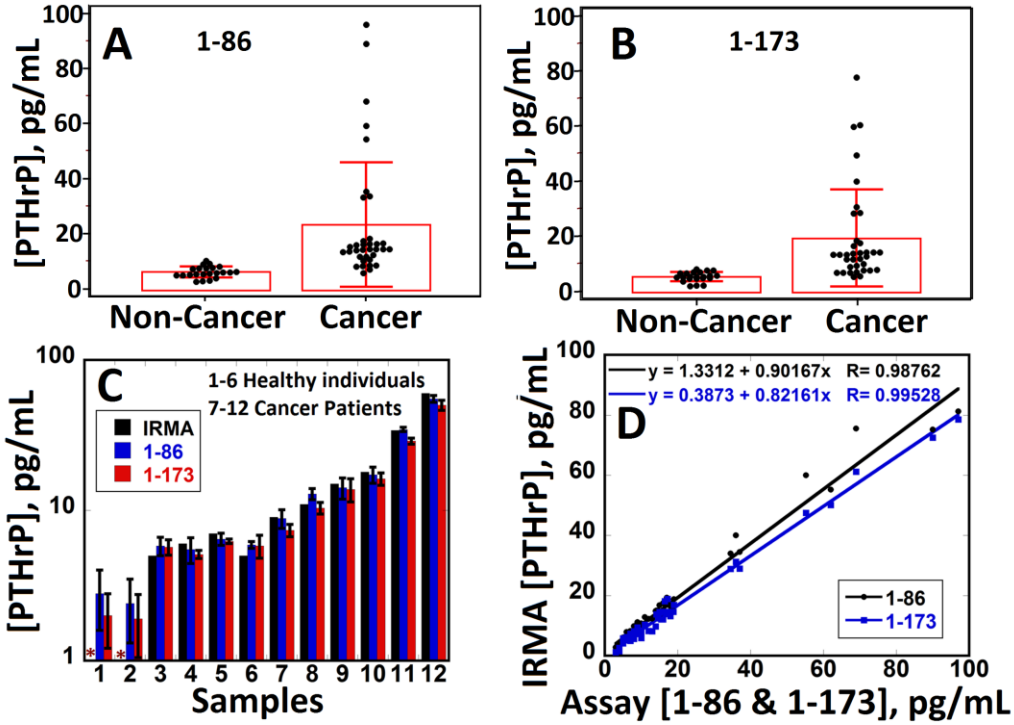

Figure 3.7: Distributions of PTHrP levels in serum and plasma from cancer patients (37) and cancer-free individuals (22) for (A) 1-86; (B) PTHrP 1-173; (C) bar graph comparing IRMA and immunoarray (1-86 & 1-173) results for PTHrP (n=12) and (D) correlation plot of IRMA and immunoarray data (1-86 & 1-173) (n=57). Asterisk (*) denotes value below IRMA LOD.

3.4.4 ROC Analysis

Analysis of the patient PTHrP data was also done using Receiver Operating Characteristic (ROC) plots. ROC is commonly used in clinical tests to determine the accuracy of the test and obtain cut-off values in diagnostic tests. In ROC curves, sensitivity (true positive rate) is plotted against 100-specificity (false positive rate) for different cut-off points. Each point on the ROC curve represents a sensitivity/specificity pair corresponding to a particular decision threshold. A test with perfect discrimination has a ROC curve that passes through the upper left corner (100% sensitivity, 100% specificity).[39] Therefore, the closer the ROC curve is to the upper left corner, the higher the overall accuracy of the test. The area under a ROC curve (AUC) quantifies the overall ability of the test to discriminate between those individuals with the disease and those without the disease. A truly perfect test with zero false positives and zero false negatives has an AUC of 1.00.

For PTHrP (n=57) the ROC plot had AUC of 0.96 for the 1-86 fragment assay and 0.94 the PTHrP1-173 assay (Figure 3.8). 1-86 fragments gave 80% sensitivity and 100% specificity while intact PTHrP1-173 gave 82.9% sensitivity and 95.5% specificity. The cancer vs. non-cancer cut-off PTHrP was 10.9 pg mL^{-1} using the 1-86 assay and 8 pg mL^{-1} using the 1-173 assay, which is in agreement with IRMA results. However, curves for individual peptides (Figure 3.8A) gave relatively similar sensitivity and specificity when using normalized, mean values of the two peptides (Figure 3.8B).

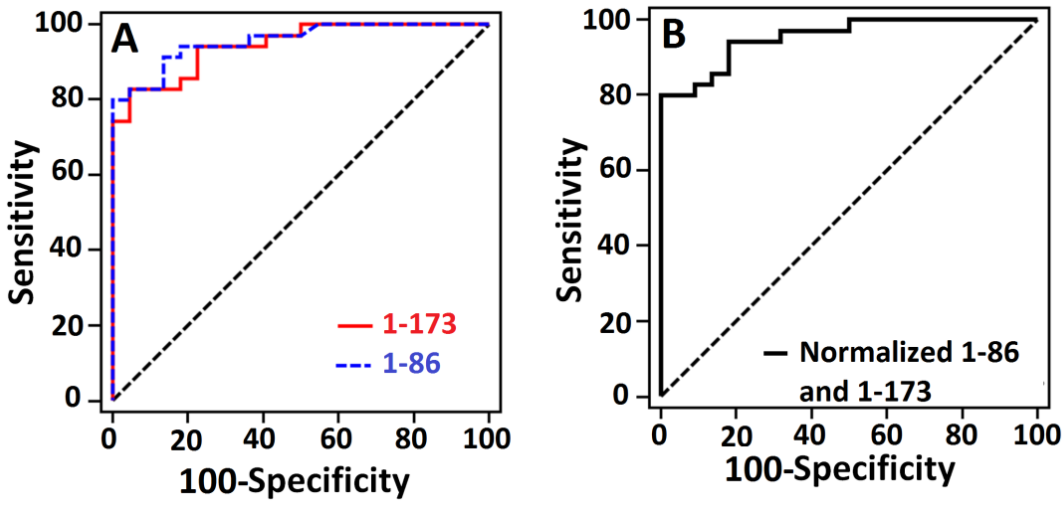

Figure 3.8: Receiver operating characteristic (ROC) curves for (A) serum assays for 1-173 (red) with AUC 0.94, 95.5% specificity and 82.9% sensitivity & 1-86 (blue) with AUC 0.96, 100% specificity and 80% sensitivity; and (B) normalized value for both 1-86 and 1-173 with AUC 0.96, 100% specificity and 80% sensitivity.

3.5 Discussion

Results described above demonstrate development of the first assay for simultaneous detection of PTHrP and its peptide fragments in serum/plasma down to 3 fg mL^{-1}. The 1 µm superparamagnetic beads with 250,000 HRP labels and 120,000 antibodies (Ab_2) per bead enabled high capture efficiency and ultrahigh sensitivity to be achieved in 30 mins assays. 1-86 peptide assays measured the level of all the three PTHrP isoforms (PTHrP1-139, 1-141 and 1-173) and their fragments containing N-terminal end of the peptides while assay using 1-173 measured the long isoform PTHrP1-173 and shorter fragments of it

such as 140-173, 80-173 e.t.c in serum. A novel and interesting observation is that circulating concentrations of the PTHrP 1-173 isoform and its fragments was only slightly lower than the concentrations of all three isoforms and their fragments suggesting that PTHrP 1-173 is the predominant circulating form of PTHrP, a finding that requires further investigation in larger cohorts.

Sensitivities of the single-detection assays ranged from 2–5 μA cm^{-2} [log C]$^{-1}$. The highest sensitivities were obtained for peptide fragments 1-86 & 1-173, which were used for multiplexed detection of patient samples. Assay results revealed a significant difference between the levels of PTHrP in healthy individuals (<10 pg mL^{-1}) compared to cancer patients and our assays could also detect PTHrP levels in all the samples (Figure 3.7). In agreement, ROC analyses (Figure 3.8) gave 80-83% sensitivity and 96-100% specificity for clinical detection of cancer. While the sample size is small and many more need to be analyzed, results suggest a high potential of PTHrP 1-86, 1-173 immunoassay for early stage cancer diagnostics.

Fragments of PTHrP are under investigation to determine their diagnostic potential in variety of human cancers. Washam et al, identified N-terminal fragment of PTHrP 12-48 as a plasma biomarker for breast cancer bone metastasis with sensitivity of 91% and specificity of 93%.[40] Using mass spectrometry, PTHrP 12-48 was significantly elevated in plasma of breast cancer patients with bone metastasis compared to controls without metastasis (P<0.0001). Combination of a clinical serum marker N-telopeptide of type I

collagen (NTx) with plasma PTHrP 12-48 greatly increased the diagnostic specificity and accuracy (AUC=0.99). However, mass spectrometry is costly, time consuming, and technically complex, and unlikely to be feasible for point-of-care peptide assays. Our assay, on the other hand, can detect PTHrP levels using both large and small fragment sizes at levels as low as 3 fg mL^{-1}.

The microfluidic immunoarray offers a simple, rapid, low cost way to simultaneously detect PTHrP peptide fragments. Inkjet printing technology offers both a simple and elegant way to fabricate disposable low-cost sensor electronics for the immunoarray. A single 8-electrode array cost ≈$0.2, and up to 56 arrays can be printed in a single run.[33] Thus, ease of fabrication and utilization of commercial components makes this approach accessible to virtually any biomedical laboratory at low cost. Capture and detection chamber are made by templating PDMS channels on machined aluminium molds to avoid lithography, and mounted on hard plastic PMMA housings with inlet and outlet lines. The microfluidic device requires only small sample volume (5 µL) and offers a degree of automation and reliability to enhance reproducibility and throughput. These advantages make the microfluidic immunoarrays a promising tool for development of sensitive, integrated, portable, clinical diagnostic devices in a short time with minimal sample and reagent requirements.

In summary, we present above a novel approach for simultaneous detection of isoforms of PTHrP in a single assay suitable for comparisons of circulating forms. The assay permits accurate analysis of both normal and

pathological clinical samples with numerous potential applications in pathologies and physiological conditions in which PTHrP has been implicated. Results of cancer patient samples support the diagnostic usefulness of such assays. This technology is amenable at examining PTHrP overproduction in a variety of cancer patients from early to late stages of disease.

3.6 References

1. Albright, F.; Case records of the Massachusetts General Hospital, No. 27461. *N. Engl. J. Med.* **1941,** *225,* 789-91.
2. Stewart, A. F.; Horst, R.; Deftos, L. J.; Cadman, E. C.; Lang, R.; Broadus, A. E., Biochemical evaluation of patients with cancer-associated hypercalcemia: evidence for humoral and nonhumoral groups. *N. Engl. J. Med.* **1980,** *303*, 1377-83.
3. Riggs, B. L.; Arnaud, C. D.; Reynolds, J. C.; Smith, L. H., Immunologic differentiation of primary hyperparathyroidism from hyperparathyroidism due to nonparathyroid cancer. *J. Clin. Invest.* **1971,** *50*, 2079-83.
4. Powell, D.; Singer, F. R.; Murray, T. M.; Minkin, C.; Potts, J. T., Jr., Nonparathyroid humoral hypercalcemia in patients with neoplastic diseases. *N. Engl. J. Med.* **1973,** *289*, 176-81.
5. Rodan, S. B.; Insogna, K. L.; Vignery, A. M.; Stewart, A. F.; Broadus, A. E.; D'Souza, S. M.; Bertolini, D. R.; Mundy, G. R.; Rodan, G. A., Factors associated with humoral hypercalcemia of malignancy stimulate adenylate cyclase in osteoblastic cells. *J. Clin. Invest.* **1983,** *72*, 1511-5.

6. Stewart, A. F.; Insogna, K. L.; Goltzman, D.; Broadus, A. E., Identification of adenylate cyclase-stimulating activity and cytochemical glucose-6-phosphate dehydrogenase-stimulating activity in extracts of tumors from patients with humoral hypercalcemia of malignancy. *Proc. Natl. Acad. Sci. USA* **1983,** *80*, 1454-8.
7. Suva, L. J.; Winslow, G. A.; Wettenhall, R. E.; Hammonds, R. G.; Moseley, J. M.; Diefenbach-Jagger, H.; Rodda, C. P.; Kemp, B. E.; Rodriguez, H.; Chen, E. Y.; et al., A parathyroid hormone-related protein implicated in malignant hypercalcemia: cloning and expression. *Science* **1987,** *237*, 893-6.
8. Strewler, G. J.; Stern, P. H.; Jacobs, J. W.; Eveloff, J.; Klein, R. F.; Leung, S. C.; Rosenblatt, M.; Nissenson, R. A., Parathyroid hormonelike protein from human renal carcinoma cells. Structural and functional homology with parathyroid hormone. *J. Clin. Invest.* **1987,** *80*, 1803-7.
9. Ratcliffe, W. A.; Norbury, S.; Heath, D. A.; Ratcliffe, J. G., Development and validation of an immunoradiometric assay of parathyrin-related protein in unextracted plasma. *Clin. Chem.* **1991,** *37*, 678-85.
10. Suehiro, M.; Murakami, M.; Fukuchi, M., Circulating forms of immunoreactive parathyroid hormone-related protein for identifying patients with humoral hypercalcemia of malignancy: a comparative study with C-terminal(109-141)- and N-terminal(1-86)-region-specific PTHrP radioassay. *Ann. Nucl. Med.* **1994,** *8*, 231-7.

11. Yasuda, T.; Banville, D.; Hendy, G. N.; Goltzman, D., Characterization of the human parathyroid hormone-like peptide gene. Functional and evolutionary aspects. *J. Biol, Chem.* **1989,** *264*, 7720-5.
12. Luparello, C., Parathyroid Hormone-Related Protein (PTHrP): A Key Regulator of Life/Death Decisions by Tumor Cells with Potential Clinical Applications. *Cancers* **2011,** *3*, 396-407.
13. Simmonds, C. S.; Kovacs, C. S., Role of parathyroid hormone (PTH) and PTH-related protein (PTHrP) in regulating mineral homeostasis during fetal development. *Crit. Rev. Eukaryot. Gene Expr.* **2010,** *20*, 235-73.
14. Sebag, M.; Henderson, J.; Goltzman, D.; Kremer, R., Regulation of parathyroid hormone-related peptide production in normal human mammary epithelial cells in vitro. *Am. J. Physiol.* **1994,** *267*, C723-30.
15. McCauley, L. K.; Martin, T. J., Twenty-five years of PTHrP progress: from cancer hormone to multifunctional cytokine. *J. Bone Miner. Res.* **2012,** *27*, 1231-9.
16. Kremer, R.; Woodworth, C. D.; Goltzman, D., Expression and action of parathyroid hormone-related peptide in human cervical epithelial cells. *Am. J. Physiol.* **1996,** *271*, C164-71.
17. El Abdaimi, K.; Papavasiliou, V.; Goltzman, D.; Kremer, R., Expression and regulation of parathyroid hormone-related peptide in normal and malignant melanocytes. *Am. J. Physiol. Cell Physiol.* **2000,** *279*, C1230-8.

18. Pecherstorfer, M.; Schilling, T.; Blind, E.; Zimmer-Roth, I.; Baumgartner, G.; Ziegler, R.; Raue, F., Parathyroid hormone-related protein and life expectancy in hypercalcemic cancer patients. *J. Clin. Endocrinol. Metab.* **1994,** *78*, 1268-70.
19. Li, J.; Karaplis, A. C.; Huang, D. C.; Siegel, P. M.; Camirand, A.; Yang, X. F.; Muller, W. J.; Kremer, R., PTHrP drives breast tumor initiation, progression, and metastasis in mice and is a potential therapy target. *J. Clin. Invest.* **2011,***121*, 4655-69.
20. Huang, D. C.; Yang, X. F.; Ochietti, B.; Fadhil, I.; Camirand, A.; Kremer, R., Parathyroid hormone-related protein: potential therapeutic target for melanoma invasion and metastasis. *Endocrinology* **2014,** *155*, 3739-49.
21. Dougherty, K. M.; Blomme, E. A.; Koh, A. J.; Henderson, J. E.; Pienta, K. J.; Rosol, T. J.; McCauley, L. K., Parathyroid hormone-related protein as a growth regulator of prostate carcinoma. *Cancer Res.* **1999,** *59*, 6015-22.
22. Rabbani, S. A.; Gladu, J.; Harakidas, P.; Jamison, B.; Goltzman, D., Overproduction of parathyroid hormone-related peptide results in increased osteolytic skeletal metastasis by prostate cancer cells in vivo. *Int. J. Cancer* **1999,** *80*, 257-64.
23. Guise, T. A.; Yin, J. J.; Taylor, S. D.; Kumagai, Y.; Dallas, M.; Boyce, B. F.; Yoneda, T.; Mundy, G. R., Evidence for a causal role of parathyroid hormonerelated protein in the pathogenesis of human breast cancer-mediated osteolysis. *J. Clin. Invest.* **1996,** *98*, 1544-9.

24. Miki, T.; Yano, S.; Hanibuchi, M.; Kanematsu, T.; Muguruma, H.; Sone, S., Parathyroid hormone-related protein (PTHrP) is responsible for production of bone metastasis, but not visceral metastasis, by human small cell lung cancer SBC-5 cells in natural killer cell-depleted SCID mice. *Int. J. Cancer* **2004,** *108*,511-5.

25. Stewart, A. F., Clinical practice. Hypercalcemia associated with cancer. *N. Engl. J. Med.* **2005,** *352*, 373-9.

26. Takahashi, S.; Hakuta, M.; Aiba, K.; Ito, Y.; Horikoshi, N.; Miura, M.; Hatake, K.; Ogata, E., Elevation of circulating plasma cytokines in cancer patients with high plasma parathyroid hormone-related protein levels. *Endocr. Relat. Cancer* **2003,** *10*, 403-7.

27. Lu, C. M.; Burton, W. D.; Fitzgerald, R. L.; Deftos, L. J.; Buchholz, B. A.; Vogel, J. S.; Herold, D. A., Mass spectrometric immunoassay for parathyroid hormone-related protein. *Anal. Chem.* **2002,** *74*, 5507-12.

28. Shan, G.; Huang, W.; Gee, S. J.; Buchholz, B. A.; Vogel, J. S.; Hammock, B. D., Isotope-labeled immunoassays without radiation waste. *Proc. Natl. Acad. Sci. USA* **2000,** *97*, 2445-9.

29. Nordholm, A.; Rix, M.; Olgaard, K.; Lewin, E., Parathyroid hormone-related peptide plasma concentrations in patients on hemodialysis. *Scand. J. Clin. Lab Invest.* **2014,** *74*, 206-12.

30. Canario, A. V.; Rotllant, J.; Fuentes, J.; Guerreiro, P. M.; Rita Teodosio, H.; Power, D. M.; Clark, M. S., Novel bioactive parathyroid hormone and related peptides in teleost fish. *FEBS Lett.* **2006,** *580*, 291-9.
31. Kushnir, M. M.; Rockwood, A. L.; Strathmann, F. G.; Frank, E. L.; Straseski, J. A.; Meikle, A. W., LC-MS/MS Measurement of Parathyroid Hormone-Related Peptide. *Clin. Chem.* **2016,** *62*, 218-26.
32. Otieno, B. A.; Krause, C. E.; Latus, A.; Chikkaveeraiah, B. V.; Faria, R. C.; Rusling, J. F., On-line protein capture on magnetic beads for ultrasensitive microfluidic immunoassays of cancer biomarkers. *Biosens. Bioelectron.* **2014,** *53*, 268-74.
33. Jensen, G. C.; Krause, C. E.; Sotzing, G. A.; Rusling, J. F., Inkjet-printed gold nanoparticle electrochemical arrays on plastic. Application to immunodetection of a cancer biomarker protein. *Phys. Chem. Chem. Phys.* **2011,** *13*, 4888-94.
34. Kremer, R. B.; Huang, D. C.; PTHRP, its isoforms and antagonists thereto in the diagnosis and treatment of disease. US patent# 7,897,139B2 Issued March 1, 2011.
35. Krause, C. E.; Otieno, B. A.; Latus, A.; Faria, R. C.; Patel, V.; Gutkind, J. S.; Rusling, J. F., Rapid microfluidic immunoassays of cancer biomarker proteins using disposable inkjet-printed gold nanoparticle arrays. *ChemistryOpen* **2013,** *2*, 141-5.

36. Smith, P. K.; Krohn, R. I.; Hermanson, G. T.; Mallia, A. K., Gartner, F. H.; Provenzano, M. D.; Fujimoto, E. K.; Goeke, N. M.; Olson, B. J.; Klenk, D. C., Measurement of protein using bicinchoninic acid. *Anal. Biochem.* **1985**, 150, 76–85.
37. Chikkaveeraiah, B. V.; Mani, V.; Patel, V.; Gutkind, J. S.; Rusling, J.F.; Microfluidic electrochemical immunoarray for ultrasensitive detection of two cancer biomarker proteins in serum. *Biosens. Bioelectron.* **2011**, 26, 4477 83.
38. Yu, X.; Munge, B.; Patel, V.; Jensen, G.; Bhirde, A.; Gong, J. D.; Kim, S. N.; Gillespie, J.; Gutkind, J. S.; Papadimitrakopoulos, F.; Rusling, J. F.; Carbon nanotube amplification strategies for highly sensitive immunodetection of cancer biomarkers. *J. Am. Chem. Soc.* **2006,** *128*, 11199-205.
39. Zweig, M. H.; Campbell, G.; Receiver operating characteristics (ROC) plots: a fundamental evaluation tool in clinical medicine. *Clin. Chem.* **1993**, *39*, 561-77.
40. Washam, C. L.; Byrum, S. D.; Leitzel, K.; Ali, S. M.; Tackett, A. J.; Gaddy, D.; Sundermann, S. E.; Lipton, A.; Suva, L. J., Identification of PTHrP(12-48) as a plasma biomarker associated with breast cancer bone metastasis. *Cancer Epidemiol. Biomarkers Prev.* **2013,** *22*, 972-83.

CHAPTER FOUR

Ultrasensitive Electrochemical Microfluidic Immunoarray for Assessment of Aggressive vs Indolent forms of Prostate Cancer

4.1 Abstract

Prostate cancer is the most common cause of cancer-related death in men in the US and throughout the world. Current practices for detection and staging of prostate cancer often fall short in terms of sensitivity, specificity and inability to distinguish between aggressive and indolent forms of prostate cancer. These limitations lead to unnecessary treatments that adversely affect the patients' quality of life with minimal or no gain. Measurement of small panels of molecular signature biomarkers in serum holds tremendous potential for cancer diagnostics and personalized therapy. Here we describe a simple, low-cost, modular microfluidic system for on-line capture and detection of prostate cancer protein biomarkers. The protein panel includes PSA, vascular endothelial growth factor-D (VEGF-D), pigment epithelial derived factor (PEDF), insulin growth factor-1 (IGF-1), insulin growth factor binding protein-3 (IGFBP-3), monocyte differentiation antigen CD-14 (CD14), V-Ets avian erythroblastosis virus E26 oncogene homolog ETS-related gene (ERG), and Golgi membrane protein 1 (GOLM-1), many of which are thought to be specific for aggressive prostate cancer. The system features a 1 or 2-channel small chamber for on-line protein capture from serum by magnetic beads labeled with many copies of analyte

specific antibodies and signal-transducing enzyme labels, positioned upstream of a 1 or 2-channel detection chamber housing a nanostructured 8 electrode sensor array. Nanostructured commercial screen printed carbon arrays ($3) are fitted into the microfluidic detection chamber to achieve high sensitivity. Ultralow detection limit in the low fM range was achieved in a 45 mins assay while higher detection limits in pM range was achieved in 25 mins assay for multiplexed detection of the biomarker proteins. Measurements of this panel of selected biomarkers will be tested with prostate cancer patient samples from US and Ireland to assess its diagnostic capability in discriminating aggressive from indolent forms of prostate cancer.

4.2 Introduction

Prostate cancer is the second most common cause of cancer-related death and the most male non-cutaneous malignancy in US and Ireland.[1] Recent statistic from American Cancer Society[2] and Irish Cancer Society[3] demonstrate that just as many men die from prostate cancer as women die from breast cancer. In US alone 2.8 million men live with prostate cancer, 200,000 new cancer cases are diagnosed every year and approximately 30,000 die each year.[2,4] In Ireland, more than 3,300 prostate cancer cases are diagnosed resulting in more than 500 patient death each year.[3] The lifetime risk of men developing prostate cancer in these countries is 1 in 7 men. In a population with increased longevity, it is likely that prostate cancer will become even more clinically prevalent in future. This projected increase is a major public health

concern, especially when there are dilemmas associated with both detection and treatment of prostate cancer.[4]

Current practices for initial assessment of prostate cancer include prostate specific antigen (PSA) blood test and digital rectal exam (DRE).[5,6] If either PSA level is above 4 ng mL^{-1} or the DRE test is suspicious or abnormal, then the patient undergoes transrectal ultrasound (TRUS) biopsy. These practices have led to early detection of prostate cancer and improved the patient survival rate and treatment outcomes. However, they have also led to inaccurate assessments often resulting in unnecessary or unwarranted treatments that adversely affect patient quality of life with little or minimal gain.[7-9] PSA, for example, has low specificity to prostate cancer as the levels are also elevated in conditions such as benign prostatic hypertrophy (BPH), prostatitis, and catheterization. In addition, PSA has limited predictive power and inability to clearly distinguish aggressive forms of prostate cancer from indolent forms.[10-12] During DRE, the tip index finger only reaches a small area of the prostate gland, and tumors in the anterior and medial lobes of the prostate may be undetectable. Biopsy on the other hand is invasive, and again only a partial representation of the entire prostate can be sampled and there is a chance of missing small but significant areas. All these limitations have led to over-diagnosis and ultimately over-treatment of the indolent forms of prostate cancer that would otherwise not become clinically manifest over a patient's lifetime or not result in cancer-related death.[8,9,13] Therefore, more strategies are needed to accurately detect and stage

prostate cancer and most importantly to better stratify patients for appropriate treatment options.

Measurement of a small panel of signature molecular biomarkers in serum holds tremendous promise for future cancer diagnostics and personalized therapy.[14-16] Biomarker discovery research for prostate cancer has been the focus of many laboratories across the world. The main aim is to identify new biomarkers that can better detect prostate cancer and at the same time reduce the number of unnecessary biopsy.[17] Several protein biomarkers including VEGF-D[18,19], PEDF[18,20,21], IGF-1[18], IGFBP-3[18], CD-14[18], ERG[22-24], and GOLM-1[22] have recently been shown to be associated with prostate cancer. Oon et al, for example, validated a panel of VEGF-D, PEDF, IGF-1, IGFBP-3 and CD-14 in patients from the Irish Cancer Research Consortium. The biomarker panel was validated with an AUC of 76.6%, and a sensitivity and specificity of 80% and 75% respectively.[18] Using a 2D-DIGE, PEDF and zinc-α2-glycoprotein (ZAG) have been identified as serum markers for the progression of prostate cancer.[20] However, conflicting findings have also been reported regarding correlation of the levels of these biomarkers with severity of prostate cancer.[25-27] Therefore, a multiple biomarker based diagnostic assay needs to be conducted to ascertain the correlation of these biomarkers to prostate cancer grade and their ability to distinguish aggressive from indolent form of prostate cancer.

Our laboratory recently developed a semi-automated 8-electrode electrochemical microfluidic immunoarray for on-line capture and detection of

upto 4 cancer protein biomarkers (Figure 4.1).[28,29] Protein analytes were captured on-line in a small microfluidic device from serum by heavily labeled magnetic beads, magnetically separated, washed and re-dispersed in buffer prior to introduction into a second microfluidic device, detection chamber. The detection chamber houses primary antibody (Ab_1)-modified array that sorts and bind the protein-bead conjugate to complete the sandwich format. Protein analytes were detected amperometrically by activation of the enzyme label. Massively labeled magnetic beads, modular microfluidic platform, and nanostructured sensor enable rapid, ultrasensitive, simultaneous detection of biomarker proteins in small volume serum samples (~5 μL).

In this chapter, we fabricated a novel 16-electrode electrochemical microfluidic immunoarray for simultaneous detection of 8 prostate cancer protein biomarkers (Figure 4.2). The protein panel includes PSA, PEDF, VEGF-D, ERG, GOLM-1, CD-14, IGF-1 and IGFBP-3, many of which are thought to be associated with aggressive prostate cancer.[18-22] The microfluidic system features a 2- channel capture chamber in which protein analytes are captured from serum by heavily labeled magnetic beads upstream a 2-channel detection housing two 8- electrode Ab_1-modified array. Capture chamber and detection chamber are interfaced with an automated syringe pump, a manual injector and switching valves. The protein analytes are captured and detected sequentially in the channels. Detection limits in the fM range were obtained on the 8-electrode system while higher detection limits in pM range were obtained on the 16-

electrode system by tailoring the assay time. Patient samples will be analyzed and compared with standard ELISA to ascertain the accuracy of immunoarray and also to determine the diagnostic utility of these protein markers in distinguishing aggressive from indolent forms of prostate cancer.

4.3 Experimental Section

4.3.1 Antibodies & Proteins

Human Vascular Endothelial Growth Factor-D (VEGF-D) duoset (catalog# DY622), Human Kallikrein 3/ Prostate Specific Antigen (PSA) duoset (catalog# DY1344), Human Insulin Growth Factor Binding Protein 3 (IGFBP-3) duoset (catalog# DY675), Human Insulin Growth Factor 1 (IGF-1) duoset (catalog# DY291), Human monocyte Cluster of Differentiation 14 (CD-14) duoset (catalog# DY383) and Human serpin F1/ Pigment Epithelial Derived Factor (PEDF) duoset (catalog# DY1177-05) were from R&D Systems. All the duosets contain monoclonal primary antibody, biotinylated-secondary antibody and recombinant protein (antigen). Human Golgi membrane protein 1 (GOLM-1) [Biotinylated Secondary Antibody clone 2D6 (catalog# TA700480), Purified Human Protein (catalog# TP314745) and Capture Antibody clone 2F3 (catalog# TA600480)] and Human ETS-related gene (ERG) [Biotinylated Secondary Antibody clone 5F12 (catalog# TA700176), Purified Human Protein (catalog# TP308093) and Capture Antibody clone 8A9 (catalog# TA600177)] were from OriGene Technologies, Inc.

4.3.2 Human Serum Samples

Human serum samples were collected from prostate cancer patients and healthy individuals from George Washington University. The study protocol was IRB approved and written Informed Consent of participants was obtained prior to sample collection. All samples were stored at or below -80 ^{0}C until use. Serum samples will be assayed directly and in selected cases spiked with biomarker proteins for validation tests.

4.3.3 Chemicals & Materials

Screen printed carbon 8-sensor array chips were designed to our specifications (700 μm) by Kanichi Research, Ltd (Manchester, UK). Sodium borohydride (99%), poly (diallyldimethylammonium chloride) (PDDA, MW 100,000-200,000, 20%), N-hydroxyxulfosuccinimide (NHSS), 1-(3-(dimethylamino)propyl)-3-ethylcarbodiimide hydrochloride (EDC), L-Glutathione reduced (GSH, 99%), gold (III) chloride trihydrate (HAuCl4.3H2O, 99.9%), Tween- 20, calf serum, lyophilized 99% bovine serum albumin (BSA) and hydroquinone (HQ, ≥90%) were from Sigma Aldrich. Dynabeads® MyOne™ Streptavidin T1 and biotinylated-Horseradish peroxidase (HRP), enzyme label were purchased from Life Technology. Hydrogen peroxide was from Fisher Scientific and polydimethylsiloxane (PDMS) kit was from Dow corning. Tubing and switching valves were from IDEX Health & Science. Immunoreagents (monoclonal primary antibodies, BSA, biotinylated secondary antibodies and biotinylated HRP) were dissolved in pH 7.4 phosphate saline (PBS) buffer (0.01

M phosphate, 0.14 M NaCl, 2.7 mM KCl) unless otherwise noted. EDC and NHSS were dissolved in water immediately before use. All solutions were prepared with water purified by Hydro water purification system to 18mΩ.cm.

4.3.4 Preparation of Magnetic-bead Conjugates (Ab_2-MP-HRP)

Biotinylated antibodies (Ab_2) and biotinylated HRP were chemically bonded onto 1 μm diameter streptavidin-coated super-paramagnetic particles (MPs) as previously described in chapter two. The number of HRP labels per MP ranged from 300,000-500,000 (±37,000) from enzyme activity assays. The bicinchoninic acid assay **(**BCA**)** was used to estimate 40,000 -100,000 (± 15,000) Ab_2 per MP.[28,29]

4.3.5 Array Fabrication

Screen printed carbon sensors in the array were coated with sequential layers of polycation PDDA and 5 nm GSH-AuNPs using layer-by-layer electrostatic adsorption as previously reported in chapter two.[28,29] Surface carboxyl groups on the GSH-AuNP layer were activated by freshly prepared EDC and NHSS to attach primary antibodies (Ab_1) to array elements through amidization. The arrays were then washed and incubated with 2% BSA in PBS for 1 hr to block non-specific binding (NSB). For amperometric measurements, the Ab_1-modified array was positioned in a detection chamber, which consisted of a microfluidic channel with reference and counter wire electrodes. A new AuNP-antibody array was used for each assay.

4.3.6 Single Detection of Protein Biomarkers

The microfluidic system (Figure 4.1) was used in concert with Ab_2-MP-HRP detection labels and Ab_1-decorated sensor arrays. Briefly, 40 µL of Ab_2-MP-HRP (1 mg mL^{-1} MPs) was dispersed in 120 µL of 20 mM PBS pH 7.4, loaded into a 100 µL sample loop and injected at 100 µL min^{-1} into the capture chamber. Subsequently, 5 µL of protein analyte diluted in calf serum was loaded into the sample loop and injected into the chamber. Once the capture chamber was filled with sample, flow was stopped for 30 min with stirring in the chamber to facilitate analyte capture. The protein-Ab_2-MP-HRP conjugates were then washed, dispersed in PBS-Tween-20, and a valve was switched to transport them into the detection chamber. When protein-Ab_2-MP-HRP conjugates filled the detection chamber, flow was stopped for 15 min for capture of the conjugate on the Ab_1-modified sensor surfaces. Buffer flow was then resumed to remove any unbound conjugate from the microfluidic channel.

The eight sensors in the array were connected to the leads of a multipotentiostat while the Pt counter and Ag/AgCl reference wires were connected to the appropriate CHI 1040A leads. To generate amperometric peaks, a mixture of 1 mM HQ mediator and 0.1 mM H_2O_2 was injected into the microfluidic device through the 100 µL sample loop. Amperometric signals were measured via the multipotentiostat with the array potential at -0.2 V vs. Ag/AgCl. HRP on the antigen-Ab_2-MP-HRP conjugates is activated by hydrogen peroxide, resulting in the oxidized ferryloxy form of HRP. The electron mediator (HQ) then

reduces the ferryloxy-HRP, regenerating HRP. The signal is developed by the reduction of oxidized mediator (benzoquinone) at the sensor surface.

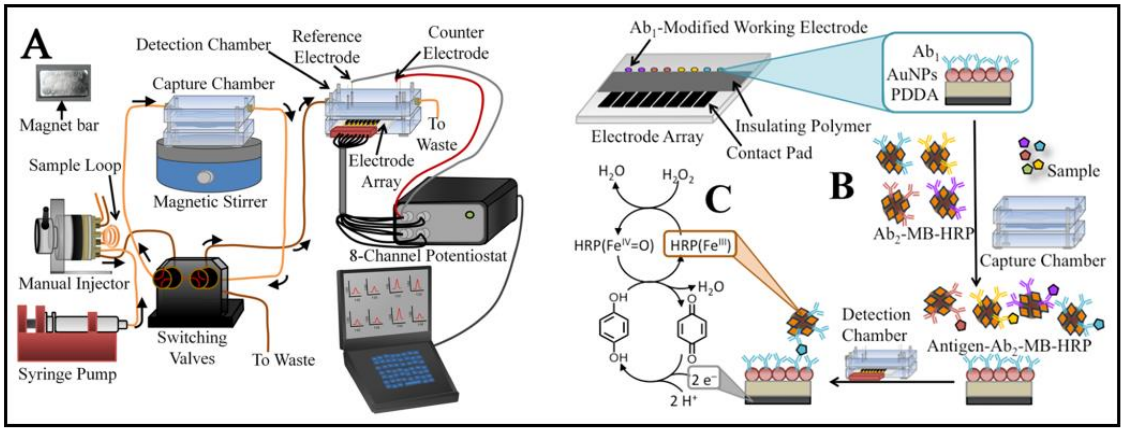

Figure 4.1: (A) Illustration of the microfluidic set up for on-line capture and detection of cancer protein biomarkers. (B) Protein analytes are captured onto the Ab_2-MP-HRP in the capture chamber to form protein-bead bioconjugates. (C) Amperometric signal generation by injecting a mixture of 1 mM HQ, electron mediator, and 0.1 mM H_2O_2 into the detection chamber.

4.3.7 Multiplexed Detection of Protein Biomarkers

For multiplexed detection of the 8-panel protein cancer biomarkers, a novel 16-electrode system was designed (Figure 4.2A). The system features a two-channel detection chamber housing two 8-electrode array (Figure 4.2C) and two-channel capture chamber with ports on the top poly (methylmethacrylate) (PMMA) plate to hold the magnet bar (Figure 4.2B). Each reaction chamber channel is 100 µL in size while the detection chamber channel is 70 µL in size.

The system is connected to an automated syringe pump, switching valves and manual injector to introduce reagents and sample.

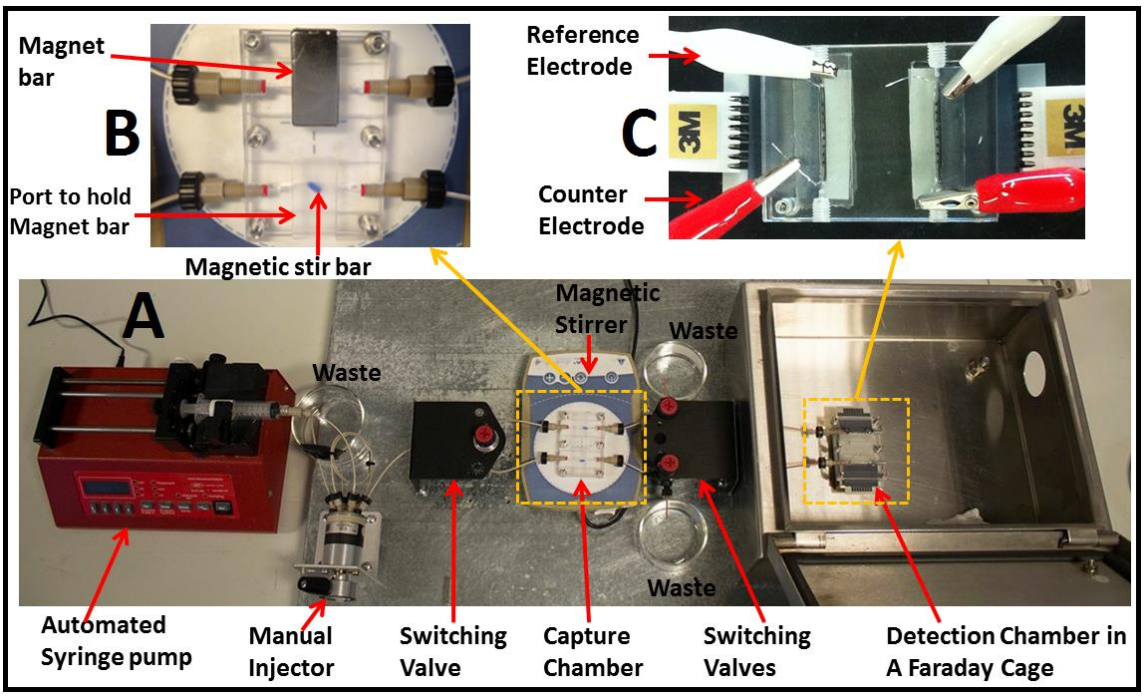

Figure 4.2: (A) Photograph of the automated 16-electrode microfluidic system featuring (B) a two-channel capture chamber with ports to hold the magnet bar and (C) a two-channel detection chamber housing two 8-electrode arrays.

The protein panel was segregated into two groups consisting of the proteins with low concentration in serum (PSA, ERG, IGF-1, VEGFD) and those with high concentration in serum (GOLM-1, PEDF, IGFBP-3, CD-14) (Figure 4.3). 10 µL each of the magnetic bead conjugate for the first group were mixed and reconstituted in 120 µL of PBS. The mixture of the magnetic bead conjugate was introduced into the channel 1 of the capture chamber followed by introduction of

a mixture of protein analytes. Incubation was then allowed for 10 min as the bead conjugate and sample were introduced onto channel two. The protein-bead conjugate was then washed and transferred onto the detection for additional 10 min incubation. Detection was performed as previously described on the 8-electrode system.

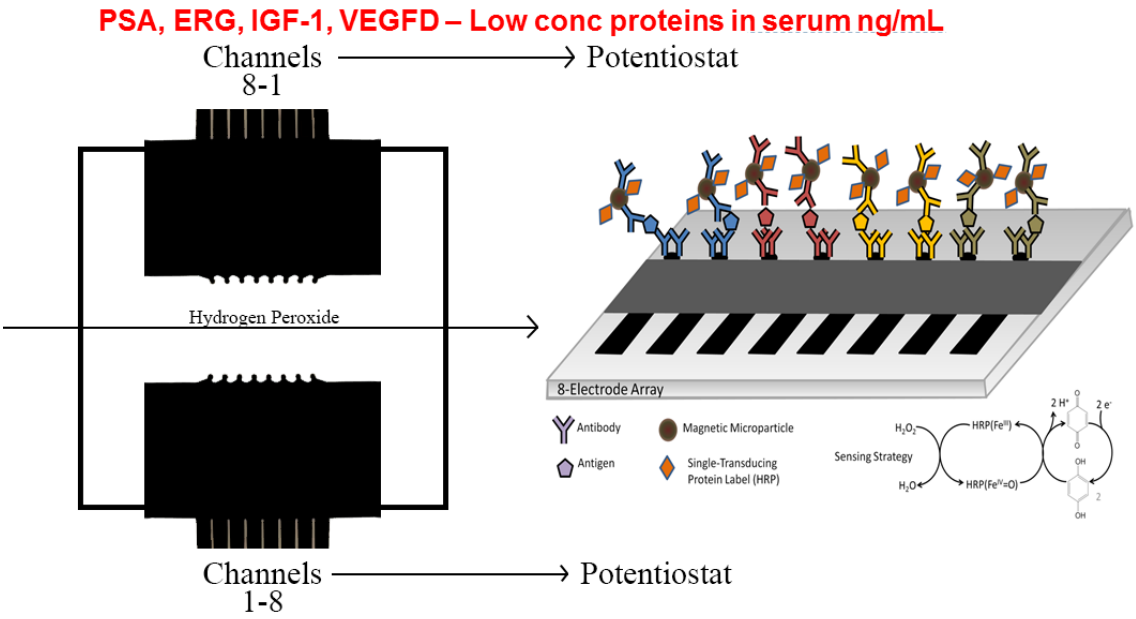

Figure 4.3: Multiplexing strategy for the 8-panel protein on the 16-electrode system. High and low concentration proteins in serum are assayed on separate channels of the system.

4.4 Results

4.4.1 Optimization of the Biomarker Panel

The microfluidic array was first optimized separately for all the 8-protein panel in 5-fold diluted calf serum, a good surrogate for human serum.[30] Optimal surface concentrations of antibody on each Ab_2-MP-HRP conjugate were established prior to obtaining calibration curves by comparing amperometric responses between analyte standards and controls. Control experiments featured the full immunoassay procedure without the protein analyte. Control signals result from a combination of direct reduction of hydrogen peroxide and NSB of the labeled bioconjugate beads on the sensors. To minimize NSB, 0.1% BSA was used in the preparation of the magnetic particle bioconjugates, while 2% BSA was incubated on sensors for 1 hr prior to incorporation into the microfluidic device. Further control of NSB was established by washing with PBS Tween-20 in both capture and detection chamber.

Optimal concentration of Ab_1 on the surface of the sensor arrays was determined by varying concentrations of Ab_1 from 25 to 100 μg mL^{-1} on the arrays while keeping the concentration of Ab_2 constant on the magnetic bead conjugate. A control (5x diluted calf serum) and a sample (diluted protein standard) were then run on the arrays with different concentrations of Ab_1. The concentration of Ab_1 that resulted in the highest difference between control and sample was selected as the optimal concentration of Ab_1 (Figure 4.4).

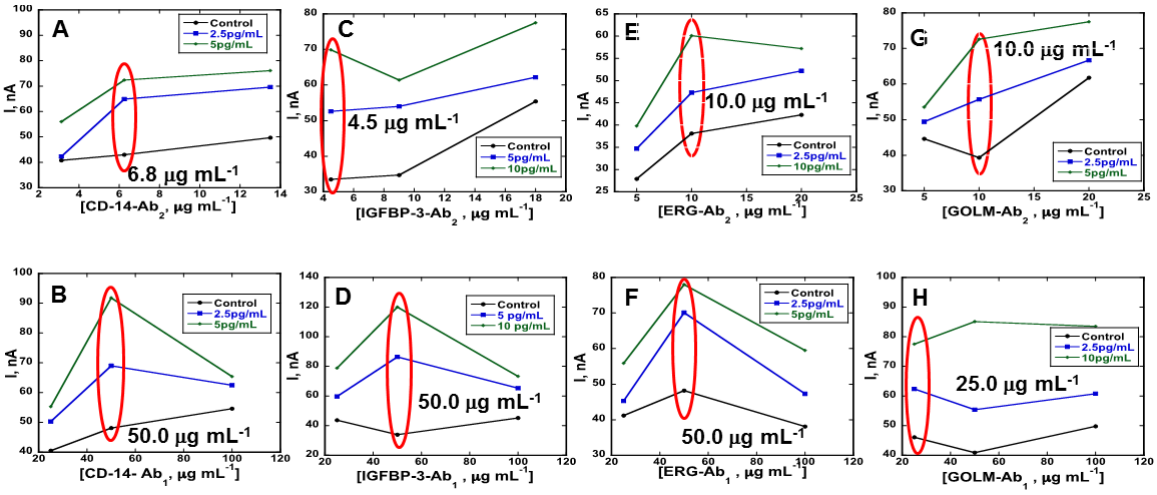

Figure 4.4 A-H: Optimization of Ab_1 and Ab_2 concentration using a control and standard concentrations of 2.5, 5 or 10 pg mL^{-1} for (A) CD-14 Ab_2, (B) CD-14 Ab_1, (C) IGFBP-3 Ab_2, (D) IGFBP-3 Ab_1, (E) ERG Ab_2, (F) ERG Ab_1, (G) GOLM Ab_2, and (H) GOLM Ab_1. Optimal concentrations for both Ab_1 and Ab_2 are circled.

Similarly, the concentration of Ab_2 was also optimized on the magnetic bead conjugate. This was done by keeping the concentration of Ab_1 constant on the surface of the array and varying the concentration of Ab_2 on magnetic beads from 4.5 to 10 µg mL^{-1}. A control and sample were run and the concentration of Ab_2 that gave the highest signal difference between the control and sample was selected as the optimal concentration of Ab_2 (Figure 4.4). The key factors that play a role here are surface coverage and orientation of the antibodies on the beads and sensor surface.

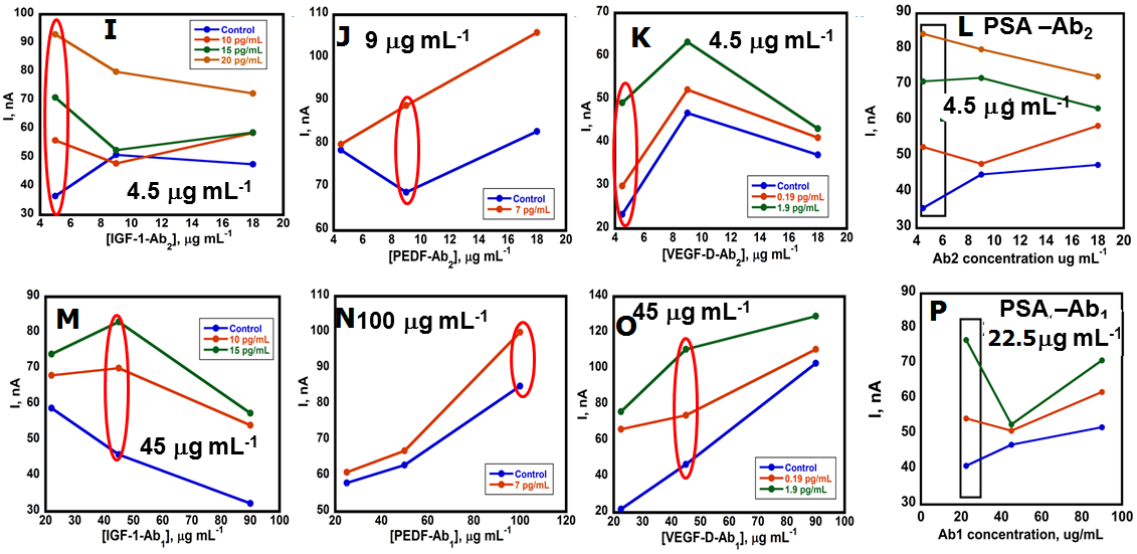

Figure 4.4 I-P: Optimization of Ab_1 and Ab_2 concentration using a control and standard concentrations for (I) IGF-1 Ab_2, (M) IGF-1 Ab_1, (J) PEDF Ab_2, (N) PEDF Ab_1, (K) VEGF-D Ab_2, (O) VEGF-D Ab_1, (L) PSA Ab_2, and (P) PSA Ab_1. Optimal concentrations for both Ab_1 and Ab_2 are circled.

4.4.2 8-Electrode System: Single Biomarker Detection

Using the above optimal conditions for Ab_1 and Ab_2, individual calibration curves were developed for the 8-protein panel. Peak currents increased linearly from 3 fg mL^{-1} to 15 pg mL^{-1} when these proteins were analyzed alone in 30 min assay (Figure 4.5 A-H & I-N). Peaks without target analyte are caused by a combination of direct peroxide reduction and non-specific adsorption of the labeled magnetic particles on the electrode surface. Detection limits measured as 3 times the standard deviation above the control were 3 fg mL^{-1} for IGFBP-3, 88 fg mL^{-1} for ERG, 4 fg mL^{-1} for GOLM-1, 5 fg mL-1 for CD-14, 5 fg mL^{-1} for IGF-1, 70 fg mL^{-1} for PEDF and 8 fg mL^{-1} for VEGF-D for single detection. Good

reproducibility is illustrated by the small error bars obtained for calibration curves (Figure 4.5 A-D & I-K), which were linear over 2 orders of magnitude concentration.

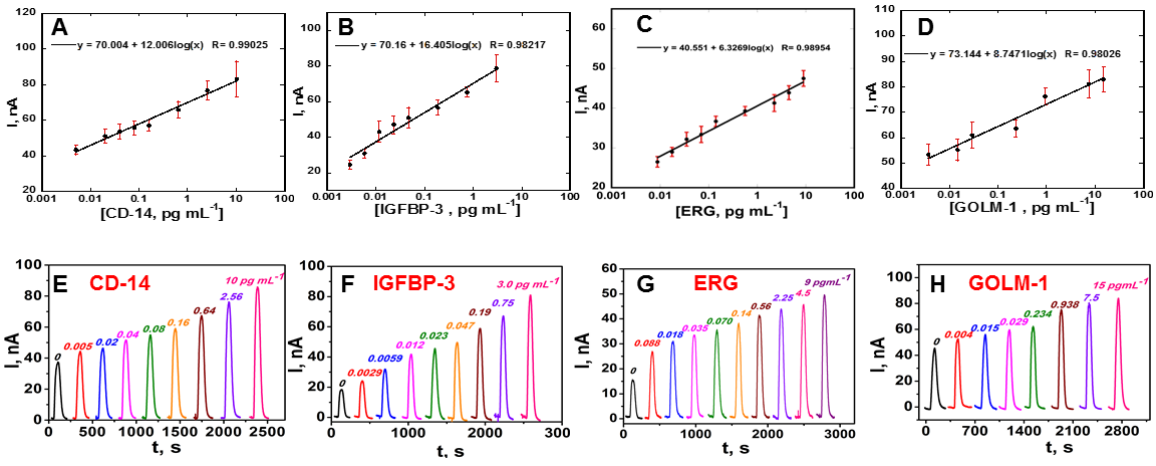

Figure 4.5 A-H: Calibration plots for individual protein in 5x diluted calf serum at -0.2 V vs Ag/AgCl for (A) CD-14, (B) IGFBP-3, (C) ERG, (D) GOLM; and also showing amperometric responses for (E) CD-14, (F) IGFBP-3, (G) ERG, (H) GOLM.

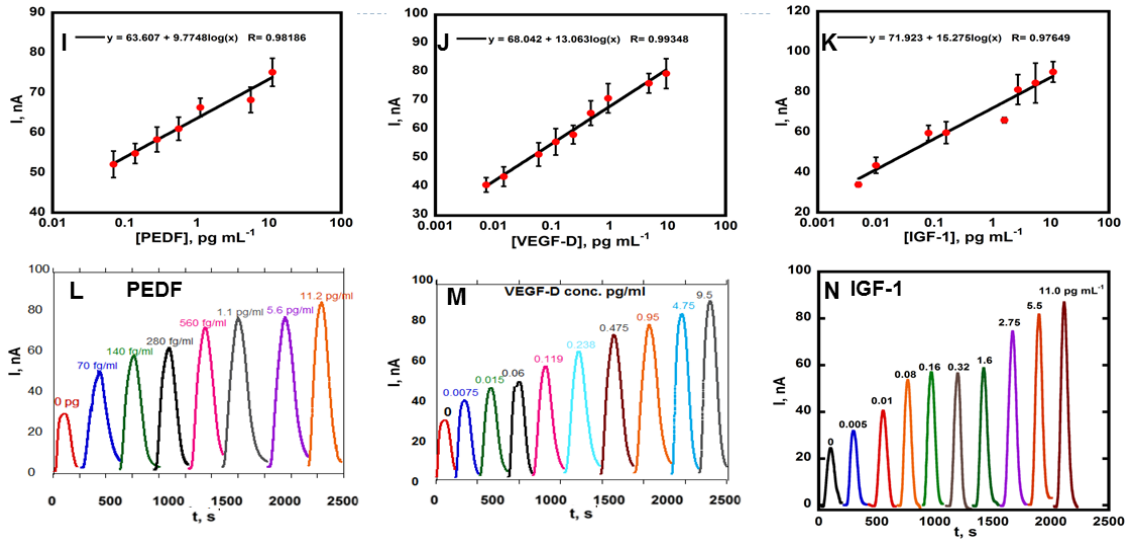

Figure 4.5 I-N: Calibration plots for individual protein in 5x diluted calf serum at -0.2 V vs Ag/AgCl for (I) PEDF, (J) VEGF-D, (K) IGF-1, and also showing amperometric responses for (L) PEDF, (M) VEGF-D, (N) IGF-1.

4.4.3 16-Electrode System

4.4.3.1 Single Biomarker Detection

The optimal conditions for Ab_1 and Ab_2 obtained on the 8-electrode system above (Figure 4.4), were utilized for single biomarker detection on the 16-electrode system. The Ab_1-modified array was first placed into the detection chamber, connected to the microfluidic set-up and washed for 2 min with PBS-T20 to block for NSB. The direction of flow was then switched to direct flow from the capture chamber to waste. Magnetic bead conjugate was then injected into the loop and flow resumed to introduce the conjugate into channel 1. The magnet bar was placed on the port of the capture chamber to trap the beads in the channel as the protein analyte was introduced. Incubation was then allowed for

10 min for the protein to be captured by the bead conjugate. Direction of flow, was then switched to introduce the second magnetic bead conjugate and protein analyte in channel 2. 10 min incubation was allowed on channel 2 for the analyte to be captured by bead conjugate.

After 10 min incubation on capture chamber, direction of flow was changed and the protein-bead conjugate was then introduced into the detection chamber, followed by a 10 min incubation to allow the protein-bead conjugate to be captured by the Ab_1 on the array. The array was then washed for 3 min with PBS-T20 to remove any unbound conjugate followed by washing for additional 3 min with 1 mM HQ solution. Amperometric signal was then generated by injecting a mixture of 1 mM HQ and 0.1 mM H_2O_2. The same protocol was employed on channel 2 for the second protein analyte. Total assay time from incubation with protein analyte to detection is ~45 ± 5 min for the two protein analytes (~25 min for each protein analyte).

Employing the above protocol, calibration plots were developed for the all the 8 proteins. Peak current increased linearly with increasing concentration of the protein analyte from 8 pg mL^{-1} to 68 ng mL^{-1} (Figure 4.6 A-H & I-P). Detection limits measured as 3 times the standard deviation above the control were 80 pg mL^{-1} for IGFBP-3, 10 pg mL^{-1} for ERG, 8 pg mL^{-1} for GOLM-1, 140 pg mL^{-1} for PSA, 250 pg mL^{-1} for CD-14, 10 pg mL^{-1} for IGF-1, 90 pg mL^{-1} for PEDF and 20 pg mL^{-1} for VEGF-D for single detection (Table 1). These detection limits and dynamic range were higher than the ones observed on the 8-electrode system.

This is due to the reduction of the assay time from 45 min for individual protein on the 8 electrode system to ~25 min for each protein analyte on the 16-electrode system. This dynamic range is suitable for the protein panel since most of the proteins have concentrations in the ng mL^{-1} to ug mL^{-1} range in serum samples. The sensitivity of the immunoarray from the slope of the calibration curve ranged from 5.73 to 12.8 μA mL [ng protein]$^{-1}$ cm^{-2} for all the protein standards in undiluted calf serum.

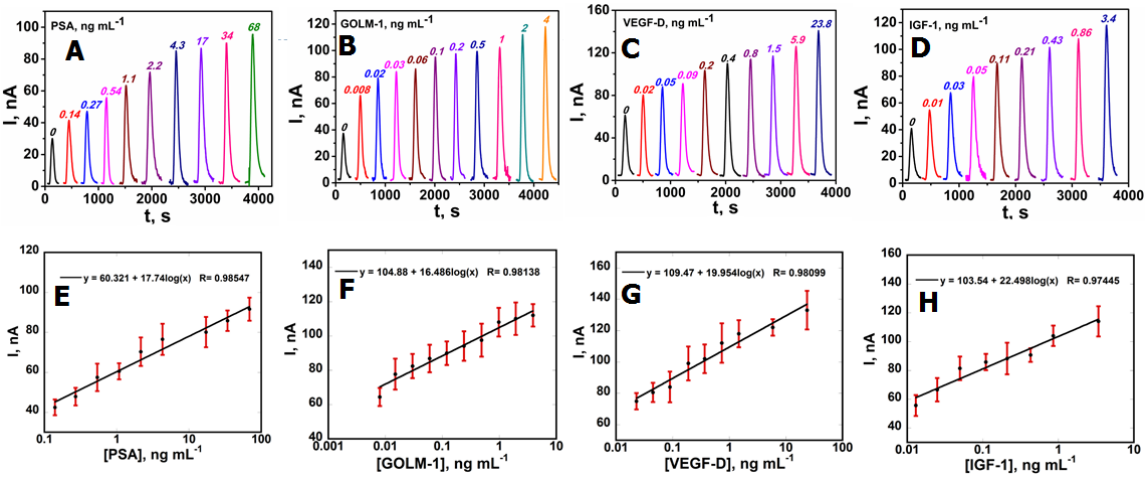

Figure 4.6 A-H: Amperometric responses for individual protein in 5x diluted calf serum at -0.2 V vs Ag/AgCl for (A) PSA, (B) GOLM, (C) VEGF-D, (D) IGF-1; and also showing calibration plots for (E) PSA, (F) GOLM, (G) VEGF-D, (H) IGF-1.

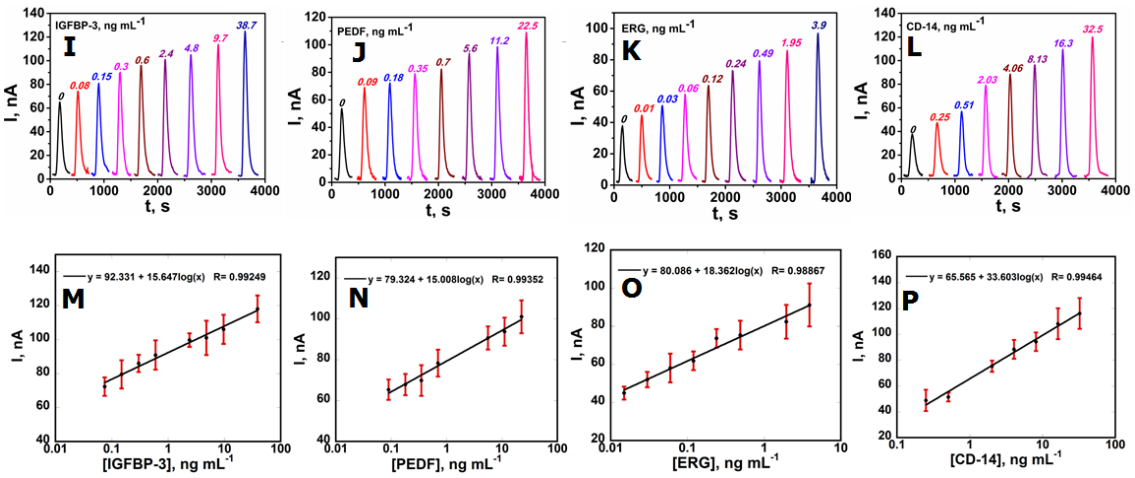

Figure 4.6 I-P: Amperometric responses for individual protein in 5x diluted calf serum at -0.2 V vs Ag/AgCl for (I) IGFBP-3, (J) PEDF, (K) ERG, (L) CD-14; and also showing calibration plots for (M) IGFBP-3, (N) PEDF, (O) ERG, (P) CD-14.

4.4.3.2 Multiplex Biomarker Detection

For multiplexed detection of the protein panel on the 16 electrode system, the protein panel was grouped into two depending on their reported concentration range in serum samples (Figure 4.3). Low concentration protein panel (PSA, ERG, IGF-1 and VEGF-D) were assayed on channel 1 while the high concentration protein panel (GOLM-1, PEDF, IGFBP-3 and CD-14) were assayed on channel 2. Furthermore, IGF-1 was separated from IGFBP-3 to minimize cross-reactivity. Primary antibodies for each protein were attached to two of the 8-electrodes on the array. HRP-labeled magnetic beads with antibodies for PSA, ERG, IGF-1 and VEGF-D were combined, re-dispersed in PBS, and injected as a mixture into the capture chamber channel 1, followed by injection of a mixture of the four protein standards. Similarly, HRP-labeled

magnetic beads with antibodies GOLM-1, PEDF, IGFBP-3 and CD-14 were combined, re-dispersed in PBS, and injected as a mixture to capture chamber channel 2, followed by injection of a mixture of these four protein standards. All steps including incubation, washing, transport to detection chamber and detection were done as described above for single biomarkers on the 16-electrode system.

Calibration data for the target proteins are shown in Figure 4.7. Good reproducibility is illustrated by the small error bars obtained for calibration curves (Figure 4.7), which were linear over 2 orders of magnitude concentration. The sensitivity of the immunoarray from the slope of the calibration curve ranged from 4.17 to 9.98 μA mL [ng protein]$^{-1}$ cm^{-2} for all the protein standards in undiluted calf serum (Table 1). The decrease in sensitivity is due to cross-reactivity between the protein analytes.

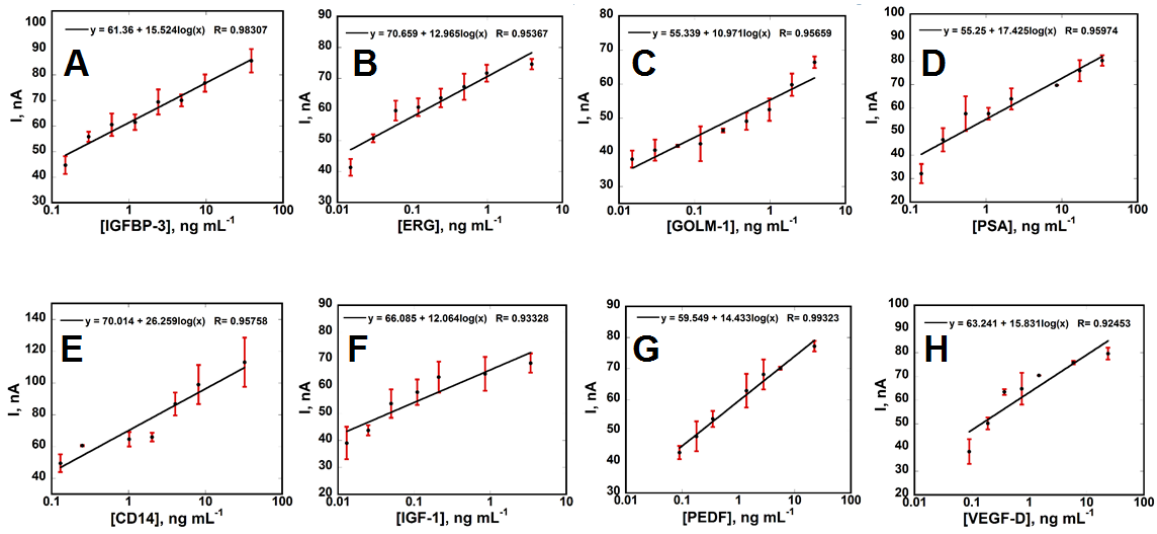

Figure 4.7: Calibration plots for a mixture of protein analytes in 5x diluted calf serum at -0.2 V vs Ag/AgCl for (A) IGFBP-3, (B) ERG, (C) GOLM, (D) PSA, (E) CD-14, (F) IGF-1, (G) PEDF and (H) VEGF-D.

Table 4.1: Detection limits and sensitivities of the 8-protein panel on the 16-electrode system.

Proteins	Detection Limit (pg/mL)	Single Detection Sensitivity (Slope/Area)	Multiplex Detection Sensitivity (Slope/Area)
PSA	140	6.74	6.62
GOLM-1	8	6.27	4.17
VEGF-D	20	7.59	6.02
PEDF	90	5.73	5.49
IGFBP-3	80	5.95	5.91
IGF-1	10	8.55	4.59
ERG	10	6.97	4.92
CD-14	250	12.8	9.98

4.5 Discussion

Results described above demonstrate that the novel 16-electrode system can accurately detect a panel of 8 proteins simultaneously in diluted calf serum. Inclusion of automated syringe pump and 2-channel capture with ports to hold the magnet bar, enhances a degree of automation to the new set up. Only loading of reagents and samples is required by the operator, unlike the 8-electrode system which still required the operator to hold the magnet bar manually on the capture chamber. As in the 8-electrode system, the magnetic beads can be easily manipulated by external magnets enabling wash steps to be done with much ease in the microfluidic device. The beads also provide a high surface to enable efficient capture of secondary and enzyme label for signal amplification.[28] A clear advantage is the speed, sample size, and multiplicity of the immunoassays over ELISA, which requires 100 µL serum for each single protein assay.[28,29]

Sensitivities of immunoarray assays obtained from the slope of the calibration curves ranged from 5.73 to 12.8 µA mL [ng protein]$^{-1}$ cm^{-2} for single detection and 4.17 to 9.98 µA mL [ng protein]$^{-1}$ cm^{-2} for multiplexed detection of the proteins on the 16-electrode system. The decrease in sensitivity was due to minimal cross-reactivity observed across the protein panel. However, a wide dynamic range (8 pg mL^{-1} to 68 ng mL^{-1}) was obtained that would enable detection of the proteins in serum samples. The overall accuracy of the assay in complex mixtures will be determined by correlation between immunoarray results

with those obtained by standard ELISAs for human patient serum levels. The hypothesis that these biomarker proteins could distinguish between aggressive and indolent forms of prostate cancer would also be investigated by assaying serum samples from prostate cancer patients in Ireland and US.

4.6 References

1. Thorne, H.; Willems, A. J.; Niedermayr, E.; Hoh, I. M.; Li, J.; Clouston, D.; Mitchell, G.; Fox, S.; Hopper, J. L.; Bolton, D. Decreased prostate cancer specific survival of men with BRCA2 mutations from multiple breast cancer families. *Cancer Prev. Res.* **2011**, *4*, 1002–1010.
2. American Cancer Society, **2016,** *Cancer Facts & Figures 2016.*
3. Irish Cancer Society, **2016,** *Cancer Facts & Figures 2016*
4. Siegel, R. L.; Miller, K. D.; Jemal, A., Cancer statistics, 2016. *CA. Cancer J. Clin.* **2016,** *66*, 7-30.
5. Kawachi, M. H.; Bahnson, R. R.; Barry, M.; Carroll, P. R.; Carter, H. B.; Catalona, W. J.; Epstein, J. I.; Etzioni, R. B.; Hemstreet, G. P., 3rd; Howe, R. J.; Kopin, J. D.; Lange, P. H.; Lilja, H.; Mohler, J.; Moul, J.; Nadler, R. B.; Patterson, S.; Pollack, A.; Presti, J. C.; Stroup, A. M.; Urban, D. A.; Wake, R.; Wei, J. T., Prostate cancer early detection. Clinical practice guidelines in oncology. *J. Natl. Compr. Canc. Netw.* **2007,** *5*, 714-36.
6. Smith, R. A.; Cokkinides, V.; Brooks, D.; Saslow, D.; Brawley, O. W., Cancer Screening in the United States, 2010: A Review of Current American Cancer

Society Guidelines and Issues in Cancer Screening. *CA: A Cancer J. Clin.* **2010,** *60*, 99-119.

7. Cary, K. C.; Cooperberg, M. R., Biomarkers in prostate cancer surveillance and screening: past, present, and future. *Ther. Adv. Urol.* **2013,** *5*, 318-29.
8. Loeb, S.; Bjurlin, M.; Nicholson, J.; Tammela, T. L.; Penson, D.; Carter, H. B.; Carroll, P.; Etzioni, R., Overdiagnosis and Overtreatment of Prostate Cancer. *Eur. Urol.* **2014,** *65*, 1046-55.
9. Klotz, L., Prostate cancer overdiagnosis and overtreatment. *Curr. Opin. Endocrinol. Diabetes Obes.* **2013,** *20*, 204-9.
10. Assinder, S. J.; Nicholson, H. Prostate Disease: Prostate hyperplasia and prostate cancer and prostatitis. In Pathophysiology and Treatment of Male Sexual and Reproductive Dysfunction; Kandeel, E.F., Ed.; Marcel Dekker Inc.: New York, NY, USA, **2007**; pp. 423–439.
11. Velonas, V.; Woo, H.; Remedios, C.; Assinder, S., Current Status of Biomarkers for Prostate Cancer. *Int. J. Mol. Sci.* **2013,** *14*, 11034.
12. Qu, M.; Ren, S. C.; Sun, Y. H., Current early diagnostic biomarkers of prostate cancer. *Asian J. Androl.* **2014,** *16*, 549-54.
13. Bangma, C.H.; Roemeling, S.; Schroder, F.H. Overdiagnosis and overtreatment of early detected prostate cancer. *World J. Urol*. **2007**, *25*, 3 9.
14. Kulasingam, V.; Diamandis, E. P., Strategies for discovering novel cancer biomarkers through utilization of emerging technologies. *Nat Clin Pract Oncol.* **2008,** *5*, 588-99.

15. Hanash, S. M.; Pitteri, S. J.; Faca, V. M., Mining the plasma proteome for cancer biomarkers. *Nature* **2008,** *452*, 571-9.
16. Rusling, J. F.; Kumar, C. V.; Gutkind, J. S.; Patel, V., Measurement of biomarker proteins for point-of-care early detection and monitoring of cancer. *Analyst* **2010,** *135*, 2496-511.
17. Sciarra, A.; Panebianco, V.; Cattarino, S.; Busetto, G. M.; De Berardinis, E.; Ciccariello, M.; Gentile, V.; Salciccia, S., Multiparametric magnetic resonance imaging of the prostate can improve the predictive value of the urinary prostate cancer antigen 3 test in patients with elevated prostate specific antigen levels and a previous negative biopsy. *BJU Int.* **2012,** *110*, 1661-5.
18. Oon, S. F.; Fanning, D. M.; Fan, Y.; Boyce, S.; Murphy, T. B.; Fitzpatrick, J. M.; Watson, R. W., The identification and internal validation of a preoperative serum biomarker panel to determine extracapsular extension in patients with prostate cancer. *Prostate* **2012,** *72*, 1523-31.
19. Kaushal, V.; Mukunyadzi, P.; Dennis, R. A.; Siegel, E. R.; Johnson, D. E.; Kohli, M., Stage-specific characterization of the vascular endothelial growth factor axis in prostate cancer: expression of lymphangiogenic markers is associated with advanced-stage disease. *Clin. cancer Res.* **2005,** *11*, 584 93.
20. Byrne, J. C.; Downes, M. R.; O'Donoghue, N.; O'Keane, C.; O'Neill, A.; Fan, Y.; Fitzpatrick, J. M.; Dunn, M.; Watson, R. W., 2D-DIGE as a strategy to

identify serum markers for the progression of prostate cancer. *J. Proteome Res.* **2009,** *8*, 942-57.

21. Qingyi, Z.; Lin, Y.; Junhong, W.; Jian, S.; Weizhou, H.; Long, M.; Zeyu, S.; Xiaojian, G., Unfavorable prognostic value of human PEDF decreased in highgrade prostatic intraepithelial neoplasia: a differential proteomics approach. *Cancer Invest.* **2009,** *27*, 794-801.
22. Yamoah, K.; Johnson, M. H.; Choeurng, V.; Faisal, F. A.; Yousefi, K.; Haddad, Z.; Ross, A. E.; Alshalafa, M.; Den, R.; Lal, P.; Feldman, M.; Dicker, A. P.; Klein, E. A.; Davicioni, E.; Rebbeck, T. R.; Schaeffer, E. M., Novel Biomarker Signature That May Predict Aggressive Disease in African American Men With Prostate Cancer. *J. clin. Oncol.* **2015,** *33*, 2789-96.
23. Culig, Z., Distinguishing indolent from aggressive prostate cancer. *Recent Results Cancer Res.* **2014,** *202*, 141-7.
24. Rosen, P.; Sesterhenn, I. A.; Brassell, S. A.; McLeod, D. G.; Srivastava, S.; Dobi, A., Clinical potential of the ERG oncoprotein in prostate cancer. *Nat. Rev. Urol.* **2012,** *9*, 131-7.
25. Ismail A, H.; Pollak, M.; Behlouli, H.; Tanguay, S.; BÉGin, L. R.; Aprikian, A. G., Insulin-Like Growth Factor-1 and Insulin-Like Growth Factor Binding Protein-3 for Prostate Cancer Detection in Patients Undergoing Prostate Biopsy. *J. Urol.* **2002** *168*, 2426-2430.
26. Ismail, H. A.; Pollak, M.; Behlouli, H.; Tanguay, S.; Bégin, L. R.; Aprikian, A. G., Serum insulin-like growth factor (IGF)-1 and IGF-binding protein-3 do not

correlate with Gleason score or quantity of prostate cancer in biopsy samples. *BJU Intl.* **2003,** *92*, 699-702.

27. Kimura, T.; Furusato, B.; Miki, J.; Yamamoto, T.; Hayashi, N.; Takahashi, H.; Kamata, Y.; van Leenders, G. J. H. L.; Visakorpi, T.; Egawa, S., Expression of ERG oncoprotein is associated with a less aggressive tumor phenotype in Japanese prostate cancer patients. *Pathol. Intl.* **2012,** *62*, 742-748.
28. Otieno, B. A.; Krause, C. E.; Latus, A.; Chikkaveeraiah, B. V.; Faria, R. C.; Rusling, J. F., On-line protein capture on magnetic beads for ultrasensitive microfluidic immunoassays of cancer biomarkers. *Biosens. Bioelectron.* **2014,** *53*, 268-274.
29. Krause, C. E.; Otieno, B. A.; Bishop, G. W.; Phadke, G.; Choquette, L.; Lalla, R. V.; Peterson, D. E.; Rusling, J. F., Ultrasensitive microfluidic array for serum pro-inflammatory cytokines and C-reactive protein to assess oral mucositis risk in cancer patients. *Anal. Bioanal. Chem.* **2015,** *407*, 7239-43.
30. Yu, X.; Munge, B.; Patel, V.; Jensen, G.; Bhirde, A.; Gong, J. D.; Kim, S. N.; Gillespie, J.; Gutkind, J. S.; Papadimitrakopoulos, F.; Rusling, J. F., Carbon nanotube amplification strategies for highly sensitive immunodetection of cancer biomarkers. *J. Am. Chem. Soc.* **2006,** *128*, 11199-205.

CHAPTER FIVE

Bioconjugation of Antibodies and Enzyme Labels onto Magnetic Beads

5.1 Abstract

Immunoassays employ antibodies and labels to capture and detect target macromolecular analytes, often from complex sample matrices such as serum, plasma, or saliva. The high affinity and specificity of antibody-antigen interactions makes immunoassays critically important analytical techniques for clinical diagnostics as well as other research applications in the areas of pharmaceutical and environmental analysis. Integration of magnetic beads (MBs) into immunoassays and other bioanalytical methodologies is a valuable approach to allow efficient target capture, enrichment and convenient separation. In addition, large signal amplification can be achieved by pre-concentration of the target and by attaching many thousands of enzyme labels to the MBs. These features have enabled MB-based biosensors to achieve ultra-low detection limits needed for advanced clinical diagnostics that are challenging or impossible using traditional immunoassays. MBs are employed either as mobile substrates for target analyte capture, as detection labels (or label carriers), or simultaneously as substrates and labels. For optimal assay performance it is crucial to apply an easy, efficient and robust bead-probe conjugation protocol, and to thoroughly characterize the bioconjugated products. Herein, we describe methods used in our laboratory to

functionalize MBs with antibodies and enzyme labels for ultrasensitive detection of protein analytes. We also present detailed strategies for characterizing the magnetic bead bioconjugates.

5.2 Introduction

Novel technologies are greatly needed to enhance laboratory productivity and provide rapid, accurate and sensitive methods for detection of various macromolecules such as protein biomarkers, DNA and small molecules for early disease diagnosis.[1] Recent advances in nanotechnology, in particular in the areas of nanomaterials, have advanced immunoassays towards the development of new generation of point-of-care (POC) devices that could significantly enhance test speed and sensitivity.[2] Integration of nanomaterials, such as magnetic beads (MBs), quantum dots and carbon nanotubes, into immunoassays as detection labels, or as substrates onto which target is captured have important advantages.[3, 4] Nanomaterials of various sizes, shapes and compositions have been developed and extensively utilized, providing exciting possibilities for rapid and highly sensitive detection systems.[5]

Among these nanomaterials, MBs have attracted much attention in immunoassays owing to their unique properties. The most useful MBs for bioconjugation feature a magnetic core surrounded by a non-magnetic polymer coating for attachment of biomolecules (Figure 5.1). Iron oxides such as magnetite (Fe3O4) or maghemite (γFe2O3) are preferentially used as core

material due to their stability. The outer polymer coating serves to add surface functional coating to the beads and protects the metal oxide from external media.[6, 7] To prevent agglomeration, superparamagnetic nanoparticles are usually dispersed or embedded into a matrix such as polystyrene, silica, dextran and albumin. The most commonly employed MBs in immunoassays are superparamagnetic or non-remnant. These beads have nominally zero magnetization in the absence of a magnetic field but become magnetic in an applied magnetic field. When fabricated with a dense superparamagnetic nanoparticle center embedded in polymer housing, the resulting MBs behave as non-magnetic particles in the absence of magnetic fields, although a bit of aggregation may result from small non-ideal magnetic properties. A great advantage of superparamagnetic beads as opposed to non-magnetic particles is their ease of manipulation with simple, inexpensive permanent magnets or electromagnets. Very efficient isolation of target analytes from biomedical samples can be achieved by both manual and automated systems.[2, 4, 6, 8]

Magnetic beads of various sizes, densities, magnetic susceptibilities, material composition and a wide variety of surface chemistries are commercially available from companies such as Invitrogen, Solulink, Micromod, Bangs Labs, and Merck with diameter ranging from 10 nm to 50 μm. The user can choose the desired surface chemistry to link the molecules of interest. MBs conjugated with antibodies provide large surface area per unit volume to enable efficient capture of target analytes. As a result, the sensitivity of the assays is increased due to

the high efficiency of interaction between the sample and reagents that can provide large pre-concentration factors. Moreover, MBs can be easily dispersed into the sample matrix with gentle shaking hence faster binding kinetics can be achieved.[3, 6] In addition to the ease of manipulation, shorter assay time and high sensitivity, MBs are compatible with diverse detection and signal processing approaches, including electrochemiluminiscence,[9,10] surface Plasmon resonance[11, 12] and electrochemical detection.[2, 4, 8]

Our laboratory has exploited MBs conjugated with massive copies of antibodies and enzyme labels in electrochemical immunosensors for a series of prostate and oral cancer biomarkers.[13-17] MBs conjugated with 10s of thousands of detection antibodies (Ab_2) and up to a half million horseradish peroxidase (HRPs) labels have been used to enhance the sensitivity of the immunoassays.[13-15, 17, 18] Ab_2 and HRP attachment onto MBs, and purification of the bead bioconjugates (MB-Ab_2-HRP) is facilitated by magnetic separations. When integrated with microfluidic systems, position of the resulting bioconjugate beads can be magnetically controlled to facilitate faster assay times. Heavily labeled detection particles have led to detection limits in low fg/mL range, enhancing sensitivity 100-1000 times as opposed to conventional immunoassays using singly-labeled Ab_2's.[8, 16, 19] High local concentrations of antibodies on the beads greatly favor the binding of protein analytes[20] while the multiple enzyme labels amplify signals.[3, 21] However, in order to obtain the high sensitivity and

reproducibility of immunoassays, an easy, efficient and robust bead-probe conjugation protocol needs to be employed.

5.3 Bioconjugation of Magnetic beads

For optimal bioanalytical performance, it is crucial to employ a suitable and reproducible method for bioconjugation of MBs with specific recognition and signal triggering elements. Choice of conjugation strategy is dictated by a combination of factors including MBs size, nature of the MB surface coating, available functional groups, or the type of biological molecule and its chemical composition.[5, 21] Commercial MBs are available with a wide variety of functional groups such as amine, carboxyl, epoxy, tosyl, hydroxyl, N-hydroxysuccinimide as well as biological molecules such as biotin, streptavidin, protein A, protein G and antibodies (Figure 5.1).[6, 7]

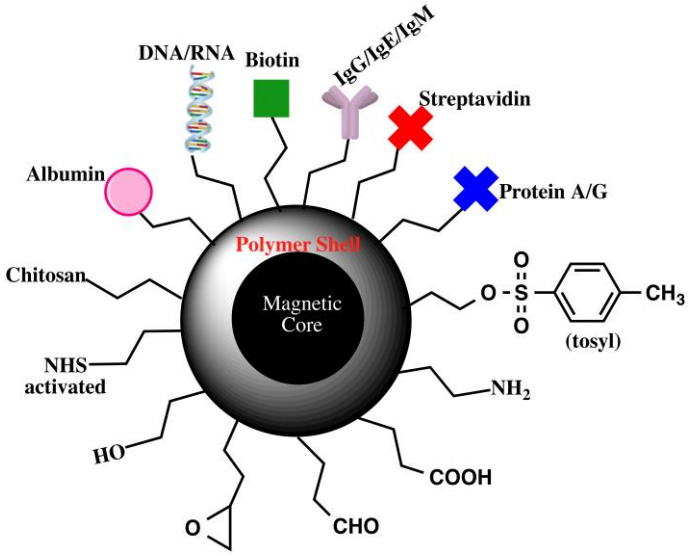

Figure 5.1: Variety of commercially available functionalized MBs with coatings of either organic functional group to attach biomolecules or biomolecules that can bind specific moieties.

Biomolecules can be conjugated to the surface coatings of MBs either directly, or using cross-linkers or other reagents (see Figure 5.1). Bioconjugation approaches usually include non-covalent interaction such as physical adsorption, specific affinity interaction, entrapment of molecules around the magnetic beads, and covalent interaction of biomolecules with the functional groups on MBs surface.[5, 21] Functional groups can be activated for coupling using EDC-NHSS chemistry for carboxylates or glutaraldehyde for amines to attach appropriate functional groups of biomolecules. Particles pre-coated with streptavidin can capture biotin-labeled biomolecules. Surface tosyl-, NHS-activated and epoxide groups on MBs can be used to attach biomolecules directly without crosslinking

agents. Protein A coated particles can selectively bind to Fc regions of antibodies for oriented immobilization.[6]

Herein, we provide detailed protocols used in our laboratory to functionalize MBs with both antibodies as recognition elements and HRP as signal triggering element, also known as dual-labeling of MBs, for ultrasensitive detection of protein cancer biomarkers. We provide protocols used for conjugation of streptavidin-coated MBs as well as tosyl-activated MBs and highlight the strategies employed for optimization and characterization of the bioconjugates.

5.4 Preparation of dual-labeled magnetic beads

5.4.1. Tosyl-activated Magnetic Beads

Tosyl-activated magnetic beads provide reactive sulphonyl esters that covalently link antibodies or other ligands that contain primary amino or sulphydryl groups to the magnetic particle surface (Figure 5.2). Immobilization of antibodies on these MBs occurs via the Fc region thus ensuring optimal orientation of the antibody, resulting in higher capture yield of the target analyte. The physical adsorption of the antibodies to the magnetic particle surface is rapid, however the formation of covalent bonds requires more time. Therefore, preparation of these conjugates should take place at 37^{o}C for 24 hours. Additional incubation with blocking buffers containing 0.01-0.5% BSA solution aid in minimizing non-specific binding (NSB) from occurring and increase the functionality of the coupled antibodies and enzyme labels. Buffers used for

preparation of antibody conjugates should be removed of any reactive groups including amines, thiols, and hydroxyls as well as any sugars and stabilizers that may interfere with binding. To facilitate the coupling efficiency buffers with high ionic strength should be used as they stimulate hydrophobic interactions. In addition tosyl groups are more reactive at higher pH, therefore sodium borate buffer (pH 9.5) should be used.

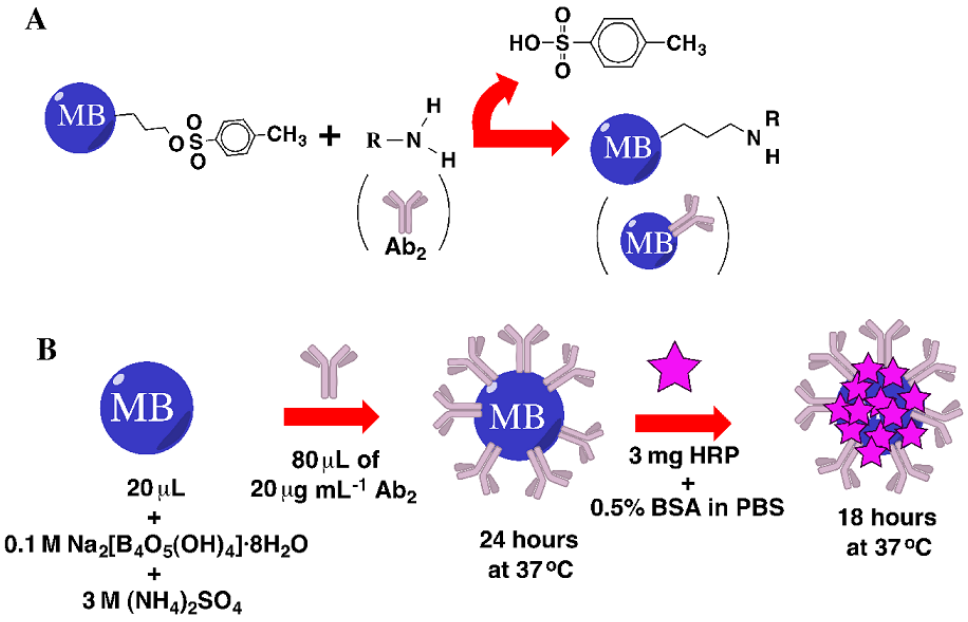

Figure 5.2: (A) The covalent attachment of antibodies to the tosyl functionalized magnetic particles. The tosyl groups act as leaving groups for surface amine groups present on antibodies to attach. (B) The complete conjugation protocol for both the attachment of antibodies as well as HRP enzyme labels.

1. Vortex the medium slurry of the tosyl-activated MBs (Dynabeads® MyOne™ Tosylactivated product no. 65501) to homogeneity before dispensing.

2. Transfer 20 µL (100 mg/mL) of tosyl-activated MBs to a 1.5 mL microcentrifuge tube and suspend in 600 µL of 0.1 M sodium borate buffer (pH 9.5).
3. Place the microcentrifuge tube on a magnet (Invitrogen Dynal magnet) for 2 mins and discard the supernatant. Resuspend the tosyl-acivated magnetic beads in 600 µL of 0.1 M sodium borate buffer (pH 9.5).
4. Repeat step 3 once more to ensure the excess sulphonyl esters are removed from tosyl-activated MBs. Once supernatant is removed, resuspend MBs in 290 µL of 0.1 M sodium borate buffer (pH 9.5), 207 µL of 3 M ammonium sulfate (pH 9.5) and 80 µL (0.02-1 mg/mL) of desired concentration of antibody (Ab_2), all into the microcentrifuge tube.
5. Incubate the microcentrifuge tube with its contents (MB-Ab_2) at 37^{o}C for 24 hours with slow tilt rotatation (Invitrogen Dynabeads MX mixer).
6. Following incubation place the microcentrifuge tube on a magnet (Invitrogen Dynal magnet) for 2 mins and discard the supernatant removing any excess unbound antibody (Ab_2). Resuspend the bioconjugates with 600 µL of 20 mM phosphate buffer containing detergent Tween-20 (pH 7.4).
7. Place the microcentrifuge again on the magnet (Invitrogen Dynal magnet) for 2 mins and discard the supernatant. Resuspend the MB-Ab_2 with 625 µL of 3 mg HRP in 0.5% BSA in phosphate buffer (pH 7.4).

8. Incubate the bioconjugate for 18 hours at 37 ^{o}C with slow rotation to attach HRP to MB-Ab_2 to form HRP-MB-Ab_2.
9. Place the BSA blocked HRP-MB-Ab_2 bioconjugates on a magnet (Invitrogen Dynal magnet) for 2 mins and discard the supernatant removing any excess unbound HRP. Resuspend the HRP-MB-Ab_2 bioconjugate in 625 µL 0.1% BSA in phosphate buffer (pH 7.4).
10. Repeat wash (step 9) 3 times. Once sufficiently washed re-suspend the HRP-MB-Ab_2 bioconjugates in 625 µL 0.1% BSA in phosphate buffer (pH 7.4). Place the conjugates at 4^{o}C until further use. These HRP-MB-Ab_2 can be used for 2-3 weeks without noticeable degradation in performance.[13]

5.4.2. Streptavidin-coated Magnetic Beads

Streptavidin magnetic beads contain a monolayer of streptavidin covalently coupled to the surface of the beads. This streptavidin monolayer has a high affinity for biotinylated biomolecules (Figure 5.3). The binding of streptavidin to biotin is one of the strongest known non-covalent biological interactions with femtomolar affinity constants.[22] Once the streptavidin tetramer is bound to the surface of the magnetic beads there are two or three biotin binding sites available for each streptavidin molecule on the surface of the bead after immobilization. Streptavidin's high affinity for biotin enables biotinylated biomolecules to be captured within 25 mins at 37 ^{o}C, this greatly reduces conjugate preparation

times. We recommend a ratio of 1:2:4 for MBs:Ab_2:HRP when preparing the streptavidin MB conjugates.

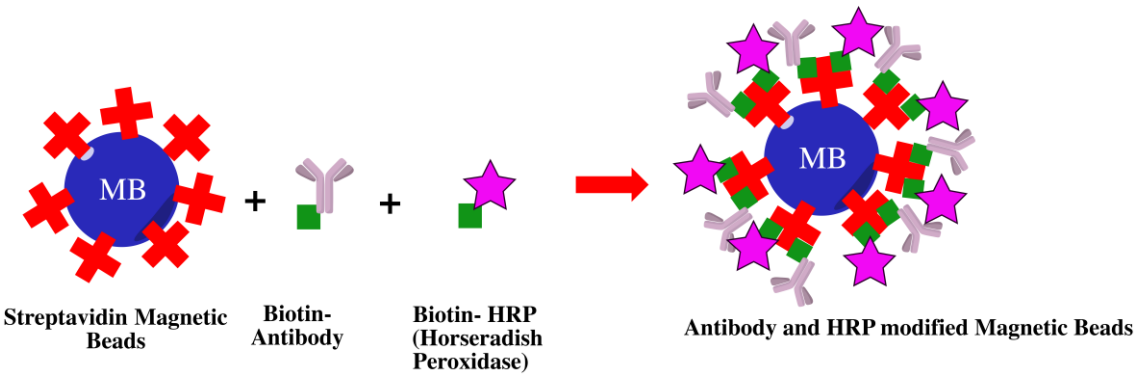

Figure 5.3: The non-covalent attachment of biotin-antibodies and biotin-Horseradish Peroxidase labels to the surface of streptavidin-coated MBs.

1. Vortex the medium slurry of the streptavidin MBs (Dynabeads® MyOne™ streptavidin T1 product no. 65601) to homogeneity before dispensing.
2. Transfer 20 µL (10 mg/mL) of streptavidin MBs to a 1.5 mL microcentrifuge tube and suspend in 200 µL of 0.1% BSA in phosphate buffer (pH 7.4).
3. Place the microcentrifuge tube on a magnet (Invitrogen Dynal magnet) for 2 mins and discard the supernatant. Re-suspend the streptavidin magnetic beads in 200 µL of 0.1% BSA in phosphate buffer (pH 7.4).
4. Repeat (step 3) 2 more times to ensure the excess storage solution is removed from streptavidin MBs. Once supernatant is discarded from the third wash, resuspend MBs in 80 µL of 0.1% BSA in phosphate buffer (pH

7.4), 40 µL (0.02-1 mg/mL) of desired concentration of antibody (Ab_2), and 80 µL of biotinylated-HRP (2.5 mg/mL), all into the microcentrifuge tube.

5. Incubate the microcentrifuge tube with its contents (streptavidin-MB-biotin-Ab_2-biotin-HRP) at 37^{o}C for 25 mins with slow tilt rotation (Invitrogen Dynabeads MX mixer).
6. Place HRP-MB-Ab_2 bioconjugates on a magnet (Invitrogen Dynal magnet) for 2 mins and discard the supernatant. Resuspend the HRP-MB-Ab_2 bioconjugate in 200 µL 0.1% BSA in phosphate buffer (pH 7.4).
7. Repeat (step 6) 3 times to remove any excess unbound Ab_2 and HRPs. Once sufficiently washed resuspend the HRP-MB-Ab_2 bioconjugates in 200 µL 0.1% BSA in phosphate buffer (pH 7.4). Place the conjugates at 4^{o}C until further use. The HRP-MB-Ab_2 can be used for 2 weeks without noticeable degradation in performance.[15]

5.5 Characterization of magnetic bead bioconjugates

To establish control of MB bioconjugate preparation, the conjugates need to be characterized in order to determine the amount of both the antibodies as well as signal generating enzyme labels. For measuring HRP activity and amount, we recommend the the use of 2,2′-Azino-bis(3-ethylbenzothiazoline-6-sulfonic acid) (ABTS) enzymatic assay. The Bicinchoninic acid (BCA) protein assay can be used to determine the total number of active HRP and Ab_2 bound to MBs respectively. Since BSA is an interfering agent in BCA assay, the last washing step in the bead preparation protocol should be performed using PBS

buffer and not 0.1% BSA, prior to characterization to avoid measuring residual bound BSA.

5.5.1 2,2'-Azino-bis(3-ethylbenzothiazoline-6-sulfonic acid) (ABTS) Enzymatic Assay

The ABTS or (2,2'-azino-bis(3-ethylbenzthiasoline-6-sulfonic acid) assay is a colorimetric assay based on the ABTS cation radical formation.[23, 24] The radical formation is catalyzed by the reduction of horseradish peroxidase in the presence of hydrogen peroxide (Figure 5.4). The ABTS cation radical exhibits a change of color from slightly yellow to an intensely turquoise colored solution with an absorbance of 405 nm. Employing this assay, we are able to determine the number of active signal generating HRP labels present on the MB bioconjugates.

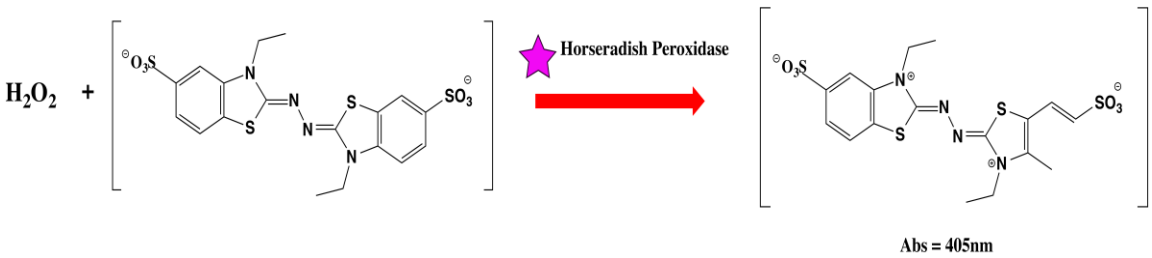

Figure 5.4: Formation of the 2,2'-azino-bis(3-ethylbenzthiasoline-6-sulfonic acid (ABTS) radical catalyzed by horseradish peroxidase in the presence of hydrogen peroxide.

1. Prepare tosyl-activated and streptavidin-coated bead conjugate (HRP-MB-Ab_2) as outline above and also a set of the tosyl-activated bead conjugate

without HRP (MB-Ab_2). The last washing step should be performed using 20 mM phosphate buffer.

2. Prepare 100 mM potassium phosphate buffer in deionized water at pH 5.0 at room temperature.
3. Prepare 9.1 mM 2,2′-Azino-bis(3-ethylbenzothiazoline-6-sulfonic acid) substrate solution (ABTS) (Sigma-Aldrich, product no. A9941) in potassium phosphate buffer ph 5.0 (step 2).
4. Prepare 0.3% (w/w) hydrogen peroxide solution in deionized water.
5. Set spectrophotometer to kinetic mode sampling at 405 nm calculating initial rate every second from 5-120 sec.
6. Blank the spectrophotometer with potassium phosphate buffer (step 2).
7. Immediately mix the reagents as indicated below by inversion and record the ΔAbsorbance for approximately 2 mins.

Table 5.1 Reagents/Sample Volume for ABTS Assay

Reagents/ Sample	Test	Blank
9.1 mM ABTS solution	2.9 mL	2.9 mL
PBS buffer or MBs in PBS buffer	-	50 µL
MB-Ab_2 (Tosyl-activated beads)	50 µL	-
HRP-MB-Ab_2 (Tosyl and streptavidin beads)	50 µL	-
0.3% H_2O_2	100 µL	100 µL

8. The number of HRPs per MB is determined by performing the calculations below, where 3.05 is the total volume in mL of the assay, d.f is dilution factor (10 - 50x), 36.8 is the mM extinction coefficient of oxidized ABTS at 405 nm and 0.05 is the volume in mL of enzyme used.

$$Units/mL\ Enzyme = \frac{\left[\Delta_{405/\min}\ test\right] - \left[\Delta_{405/\min}\ control\right]\ x\ 3.05\ x\ d.f.}{(36.8)\ (0.05)}$$

Units/ mL enzyme is then converted to the moles of HRP using pyragallol units in HRP, Avagadros number, and molecular weight. The number of HRP per MB is obtained by diving the moles of HRP by beads per mg of the MBs (10^{12} beads/mg for tosyl-activated beads and 10^{8} beads/mg of streptavidin-coated beads).

5.5.2 Bicinchoninic acid (BCA) Protein Assay

Bicinchoninic acid (BCA) assay or Smith assay is a copper-based colorimetric assay for total protein quantification. BCA rely on the formation of a Cu^{2+}-protein complex in a basic environment, followed by reduction of the Cu^{2+} to Cu^{+}.[25] The amount of Cu^{2+} that is reduced is proportional to the amount of protein present in solution. Basically, two molecules of bicinchoninic acid chelate to each Cu^{+} ion causing a change of color of the sample solution from green to purple that exhibits a strong absorbance at 562 nm (Figure 5.5). The bicinchoninic Cu^{+} complex is influenced by both the number of peptide bonds, as well as the presence of amino acids cysteine, cystine, tyrosine, and tryptophan side

chains.[26] Elevated temperatures increase exposure of amino acids and minimize the differences caused by unequal amino acid composition in different protein samples. Therefore, to increase assay sensitivity the assay should be performed at an elevated temperature of 60°C.

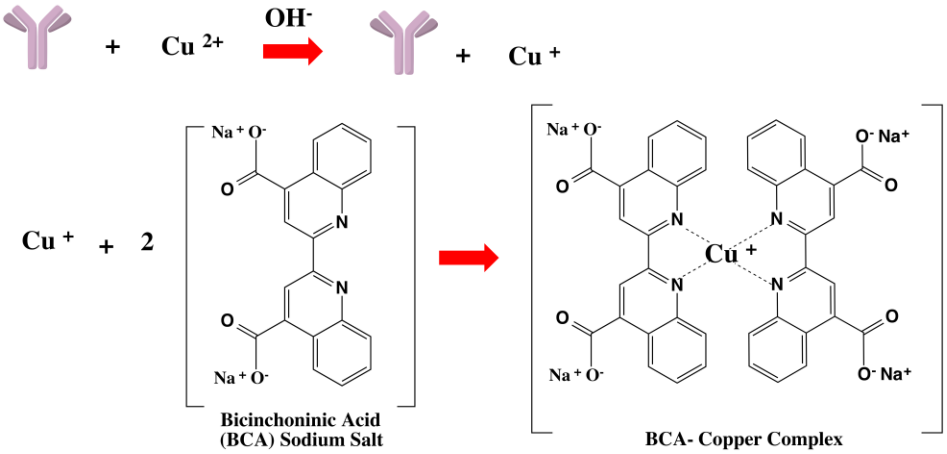

Figure 5.5: The formation of the Bicinchoninic acid (BCA)-copper complex for the BCA total protein assay. This assay proceeds in two steps; the first being the reduction of Cu^{2+} by antibodies in a basic environment and the second step involves the reduced Cu^{+} chelating with two molecules of bicinchoninic acid.

1. Prepare standard concentrations of detection antibody (Ab_2) with concentrations ranging from 1.25-20 µg/mL.
2. Formulate dilutions of MB-Ab_2 for tosyl-activated beads and HRP-MB-Ab_2 for tosyl-activated and streptavidin-coated beads (5-20 dilution factors).
3. Mix a stock solution of the BCA reagents, Pierce™ BCA Protein Assay Kit product number 23225 (25 parts of reagent MA + 24 parts of reagent MB + 1 part reagent MC).

4. Add 500 µL of the samples in step 1 & 2 and PBS buffer or MBs as blank to 500 µL of the stock solution of BCA in step 3.
5. Incubate the samples in step 4 at 60 ˚C for 1 hour for the complex formation.
6. Cool all the samples to room temperature.
7. Measure the absorbance of all the samples at 562 nm within 10 minutes.

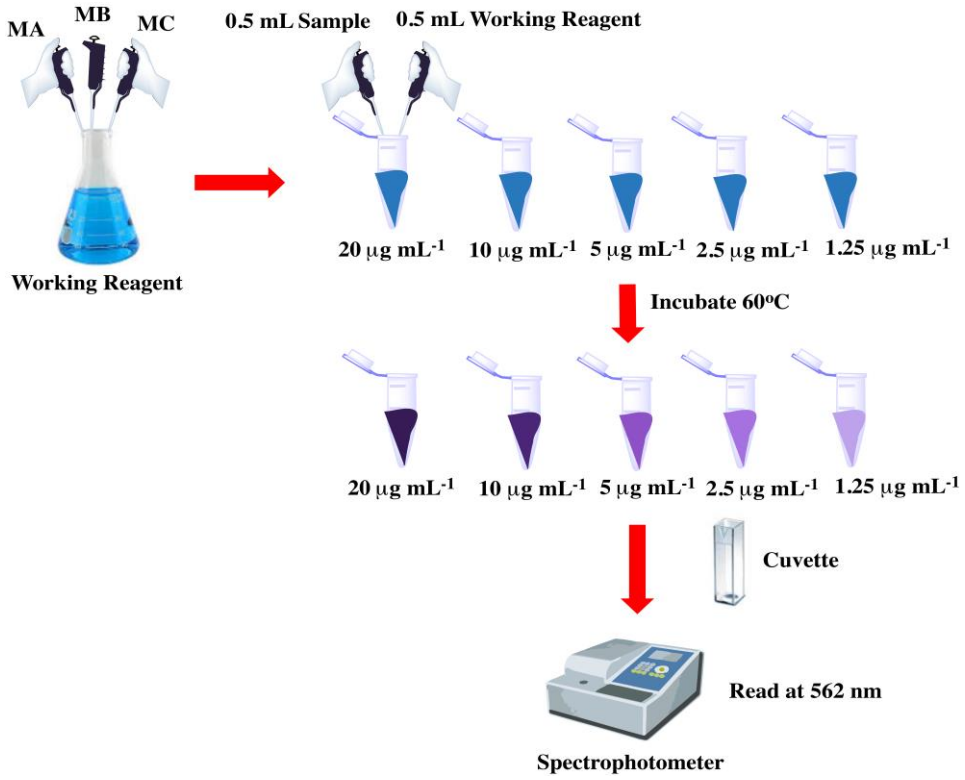

Figure 5.6: The workflow for the Bicinchoninic acid (BCA) total protein assay including the formation of the working reagent, and the development of a standard curve from a range of antibody concentrations.

8. By subtracting absorbance of MB from that of MB-Ab_2 and HRP-MB-Ab_2, the unknown concentration of antibodies on the MB can be found from the

calibration plot of antibody standards obtained with the BCA kit (Figure 7). The number of antibodies on MP surface is obtained by dividing the number of antibodies in the dispersion by the number of particles in the dispersion ((10^{12} beads/mg for tosyl-activated beads and 10^{8} beads/mg of streptavidin-coated beads).

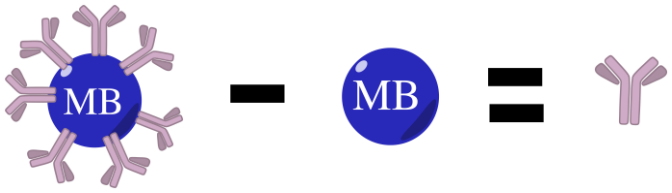

Figure 5.7: Calculating the total antibody concentration from subtracting the absorbance of the magnetic beads from that of the magnetic beads containing the antibody.

5.6 Integration of magnetic beads into Immunoassay

Sensitive and selective immunoassays rely on the ability to fish out a protein analyte of interest from an ocean containing thousands of other proteins. MBs conjugated with highly selective antibodies as well as other protein capture agents provide a simple and effective way to achieve this goal. Typically, the dual labeled magnetic beads are added to a fluid sample, the sample is then mixed in order for proteins to be selectively captured by antibodies that are present on the MBs. Once protein analytes are captured any interfering biomolecules present on the bead surface are removed through washing protocols involving magnetic separation that is either manual[13-15] or automated.[17, 18] Labels present on the

bead surface such as HRPs are then detected to measure the selected protein analyte of interest.

A major factor influencing the selectivity and sensitivity of immunoassays is non-specific binding (NSB). NSB occurs when MB bioconjugates binds to non-antigen sites on the sensor during immunoassay fabrication. Generally, MB bioconjugates generate a signal even if it is bound to sites other than the analyte protein-capture antibody complex. Therefore, signals arising from NSB cannot be differentiated from those originating from antigen-antibody binding, and are not proportional to the analyte concentrations. As a result, NSB raises the detection limit and greatly decreases the sensitivity of the assay. Solving this problem involves creating a sensor surface that inhibits any other binding other than that of the protein antigen with its antibodies. Bovine serum albumin (BSA) or casein with small quantity of detergent such as T-20 in wash buffers are commonly employed to minimize NSB in assays. However, there is no universal blocking agent for NSB in any protein detection system, therefore a thorough characterization of the amplifying formulation is needed to avoid NSB in any amplification strategy. Employing 2% BSA in PBS-T20 on the sensors and 0.1% BSA in PBS-T20 on MB bioconjugates have greatly inhibited NSB in our assays enabling ultralow detection limits to be achieved.[14, 15, 17, 18]

In order to achieve the ultralow detection limits in immunoassays, the concentration of antibodies should be optimized on the MB bioconjugates (HRPMB- Ab_2). Usually, MB bioconjugates are prepared with a wide range of

concentrations for detection antibody (Ab_2) and tested for their immunoassay performance. Keeping the concentration of capture antibody (Ab_1) on the detection platform constant, a blank and a standard sample are tested with different MB-bioconjugates with varying concentrations of Ab_2. The MB bioconjugates with the highest difference between the blank and the sample is then chosen for immunoassay applications.[18] The Ab_1 on the detection platform is optimized as well by varying the concentration of Ab_1 and keeping the concentration of Ab_2 on the MB bioconjugates constant. The key factors that play a role in the MB-bioconjugate with optimal concentration of antibodies are orientation and binding capacity.

Integrating these MB-based immunoassays in microfluidic systems adds to many key advantages in development of a high performance assay as these systems can reproducibly deliver these MB bioconjugates to desired locations in a simple and rapid manner. However, MBs may adsorb to microfluidic device surfaces due to these micrometer-dimensioned channels and micron tube diameters, leading to clogged channels, and an increase in flow resistance.[27] In order to minimize the risk of clogging and decreased assay performance it is recommended that microfluidic tubing be changed every few months and device systems be thoroughly washed with detergents after each use. We also recommend the use of 4–5 times diluted MB bioconjugate (HRP-MB-Ab_2) in immunoassays.

The development of MB bioconjugates for protein capture, manipulation, transport, and labeling has enabled the detection of a library of known cancer biomarker proteins. These proteins are detected at clinically relevant serum levels and have clearly demonstrated their utility in both manual and automated capture systems. There is no doubt that these magnetic bead based technologies are/ will be important tools for future protein detection systems. Interfacing these relatively simple protocols with microfluidic or other automated sample handling technologies will further propel MB protein detection systems into the clinical setting.

5.7 References

1. Konry, T.; Bale, S. S.; Bhushan, A.; Shen, K.; Seker, E.; Polyak, B.; Yarmush, M., Particles and microfluidics merged: perspectives of highly sensitive diagnostic detection. *Mikrochimica acta* **2012,** *176*, 251-269.
2. Rusling, J. F.; Bishop, G. W.; Doan, N.; Papadimitrakopoulos, F., Nanomaterials and biomaterials in electrochemical arrays for protein detection. *J. Materials Chem. B.* **2014,** *2*, 12–30.
3. Chikkaveeraiah, B. V.; Bhirde, A. A.; Morgan, N. Y.; Eden, H. S.; Chen, X., Electrochemical immunosensors for detection of cancer protein biomarkers. *ACS nano* **2012,** *6*, 6546-61.
4. Tekin, H. C.; Gijs, M. A., Ultrasensitive protein detection: a case for microfluidic magnetic bead-based assays. *Lab chip* **2013,** *13*, 4711-39.

5. Sapsford, K. E.; Algar, W. R.; Berti, L.; Gemmill, K. B.; Casey, B. J.; Oh, E.; Stewart, M. H.; Medintz, I. L., Functionalizing nanoparticles with biological molecules: developing chemistries that facilitate nanotechnology. *Chemical Rev.* **2013,** *113*, 1904-2074.
6. Mani, V.; Chikkaveeraiah, B. V.; Rusling, J. F., Magnetic particles in ultrasensitive biomarker protein measurements for cancer detection and monitoring. *Expert Opin. Med. Diagn.* **2011,** *5*, 381-391.
7. Llandro, J.; Palfreyman, J. J.; Ionescu, A.; Barnes, C. H., Magnetic biosensor technologies for medical applications: a review. *Med. Biol. Eng. Comput.* **2010,** *48*, 977-98.
8. Rusling, J. F., Multiplexed electrochemical protein detection and translation to personalized cancer diagnostics. *Anal. Chem* **2013,** *85*, 5304-10.
9. Kadimisetty, K.; Malla, S.; Sardesai, N. P.; Joshi, A. A.; Faria, R. C.; Lee, N. H.; Rusling, J. F., Automated multiplexed ECL Immunoarrays for cancer biomarker proteins. *Anal. Chem* **2015,** *87*, 4472-8.
10. Sardesai, N. P.; Kadimisetty, K.; Faria, R.; Rusling, J. F., A microfluidic electrochemiluminescent device for detecting cancer biomarker proteins. *Anal. Bioanal. Chem.***2013,** *405*, 3831-8.
11. Joshi, A. A.; Peczuh, M. W.; Kumar, C. V.; Rusling, J. F., Ultrasensitive carbohydrate-peptide SPR imaging microarray for diagnosing IgE mediated peanut allergy. *Analyst* **2014,** *139*, 5728-33.

12. Krishnan, S.; Mani, V.; Wasalathanthri, D.; Kumar, C. V.; Rusling, J. F., Attomolar detection of a cancer biomarker protein in serum by surface plasmon resonance using superparamagnetic particle labels. *Angew Chem. Int. Ed. Engl.* **2011,** *50*, 1175-8.
13. Chikkaveeraiah, B. V.; Mani, V.; Patel, V.; Gutkind, J. S.; Rusling, J. F., Microfluidic electrochemical immunoarray for ultrasensitive detection of two cancer biomarker proteins in serum. *Biosens Bioelectron.* **2011,** *26*, 4477-83.
14. Krause, C. E.; Otieno, B. A.; Latus, A.; Faria, R. C.; Patel, V.; Gutkind, J. S.; Rusling, J. F., Rapid microfluidic immunoassays of cancer biomarker proteins using disposable inkjet-printed gold nanoparticle arrays. *ChemistryOpen* **2013,** *2*, 141-5.
15. Malhotra, R.; Patel, V.; Chikkaveeraiah, B. V.; Munge, B. S.; Cheong, S. C.; Zain, R. B.; Abraham, M. T.; Dey, D. K.; Gutkind, J. S.; Rusling, J. F., Ultrasensitive detection of cancer biomarkers in the clinic by use of a nanostructured microfluidic array. *Anal. Chem.* **2012,** *84*, 6249-55.
16. Mani, V.; Chikkaveeraiah, B. V.; Patel, V.; Gutkind, J. S.; Rusling, J. F., Ultrasensitive immunosensor for cancer biomarker proteins using gold nanoparticle film electrodes and multienzyme-particle amplification. *ACS nano* **2009,** *3*, 585-94.
17. Otieno, B. A.; Krause, C. E.; Latus, A.; Chikkaveeraiah, B. V.; Faria, R. C.; Rusling, J. F., On-line protein capture on magnetic beads for ultrasensitive

microfluidic immunoassays of cancer biomarkers. *Biosens. Bioelectron.* **2014,** *53*, 268-74.

18. Krause, C. E.; Otieno, B. A.; Bishop, G. W.; Phadke, G.; Choquette, L.; Lalla, R. V.; Peterson, D. E.; Rusling, J. F., Ultrasensitive microfluidic array for serum pro-inflammatory cytokines and C-reactive protein to assess oral mucositis risk in cancer patients. *Anal. Bioanal. Chem.***2015,** *407*, 7239-43.
19. Jensen, G. C.; Yu, X.; Gong, J. D.; Munge, B.; Bhirde, A.; Kim, S. N.; Papadimitrakopoulos, F.; Rusling, J. F., Characterization of multienzymeantibody- carbon nanotube bioconjugates for immunosensors. *J. Nanosci. Nanotechnol.* **2009,** *9*, 249-55.
20. Mani, V.; Wasalathanthri, D. P.; Joshi, A. A.; Kumar, C. V.; Rusling, J. F., Highly efficient binding of paramagnetic beads bioconjugated with 100,000 or more antibodies to protein-coated surfaces. *Anal. Chem.* **2012,** *84*, 10485 91.
21. Lei, J.; Ju, H., Signal amplification using functional nanomaterials for biosensing. *Chem. Soc. Rev.* **2012,** *41*, 2122-2134.
22. Howarth, M.; Chinnapen, D. J.; Gerrow, K.; Dorrestein, P. C.; Grandy, M. R.; Kelleher, N. L.; El-Husseini, A.; Ting, A. Y., A monovalent streptavidin with a single femtomolar biotin binding site. *Nat. Methods* **2006,** *3*, 267-73.
23. Pütter, J.; Becker, R., *Methods of Enzymatic Analysis* (Bergmeyer, H.U., ed.) **1983,** 3rd ed., Vol III, pp. 286-293, Verlug Chemie, Deerfield Beach, FL.

24. Keesey, J., *Biochemical Information* (1st Ed) **1987**, pp. 58, Boehringer Mannheim Biochemicals, Indianapolis, IN.
25. Smith, P. K.; Krohn, R. I.; Hermanson, G. T.; Mallia, A. K.; Gartner, F. H.; Provenzano, M. D.; Fujimoto, E. K.; Goeke, N. M.; Olson, B. J.; Klenk, D. C., Measurement of protein using bicinchoninic acid. *Anal Biochem.* **1985,** *150*, 76-85.
26. Wiechelman, K. J.; Braun, R. D.; Fitzpatrick, J. D., Investigation of the bicinchoninic acid protein assay: identification of the groups responsible for color formation. *Anal. Biochem.* **1988,** *175*, 231-7.
27. Ng, A. H.; Uddayasankar, U.; Wheeler, A. R., Immunoassays in microfluidic systems. *Anal Bioanal Chem.* **2010,** *397*, 991-1007.